Aus dem
Charité Centrum für Orthopädie und Unfallchirurgie
Julius Wolff Institut für Biomechanik und Muskuloskeletale Regeneration
Berlin Institute of Health at Charité
Charité – Universitätsmedizin Berlin
Prof. Dr.-Ing. Georg N. Duda

Habilitationsschrift

Thema

Die Reibung im Hüftgelenkersatz
- der ‚un'bekannte in-vivo-Belastungsparameter -

Zur Erlangung der Lehrbefähigung für
das Fach experimentelle Orthopädie

vorgelegt dem Fakultätsrat der Medizinischen Fakultät
Charité – Universitätsmedizin Berlin

von
Dr.-Ing. Philipp Damm
aus Zschopau

Eingereicht: 19. Juni 2023
Dekan: Prof. Dr. med. Axel R. Pries

1. Gutachter/in: Prof. Dr. Michael M. Morlock, Hamburg
2. Gutachter/in: Prof. Dr. J. Philippe Kretzer, Heidelberg

Inhalt

1. Einleitung

Die Implantation eines künstlichen Hüftgelenks wird als eine der erfolgreichsten Operation des letzten Jahrhunderts bezeichnet (Learmonth, Young, and Rorabeck 2007). Sie ist zwar mit einer durchschnittlichen 10-Jahres-Revisionsrate von 5% außerordentlich erfolgreich für Patienten zwischen 65 – 79 Jahren, bei jüngeren Patienten (30 – 39 Jahren) liegt die Revisionsrate jedoch bis zu dreifach höher (Lee E. Bayliss et al. 2017a; Garellick et al. 2011; Kuijpers et al. 2020; Sean S. Rajaee et al. 2018; Swedish Hip Arthroplasty Register 2019a; United Kingdom National Joint Registry 2019a). Als primärer Grund für diese erhöhten Versagensraten werden insbesondere deren höheren Aktivitätslevel diskutiert (Gandhi et al. 2010; Johnsen 2006; Koenen et al. 2014; C. A. Mancuso et al. 2009; Scott et al. 2012; Wright, Rudicel, and Feinstein 1994). Unterschiedliche Studien zeigten bereits, dass die heutigen Patienten deutlich aktiver sind als typische Patienten, die in den 1980er bis 1990er Jahren mit einem Gelenkersatz versorgt wurden (Bohannon 2007; Hoorntje et al. 2018; Naal et al. 2007; Schmidutz et al. 2012). Sie kehren postoperativ häufiger und auch früher an den Arbeitsplatz zurück, sind im Alltag aktiver und treiben wieder bzw. auch häufiger Sport (Abe et al. 2014; Bonnin et al. 2018; Lefevre et al. 2013). Ihr Anspruch den gewohnten Freizeitsport beizubehalten bzw. die Aufnahme neuer sportlicher Aktivitäten, spielt für die individuelle Lebensqualität dieser Patienten eine immer größer werdende Rolle (B. W. L. Healy et al. 2008; Koenen et al. 2014; C. A. Mancuso et al. 2009; Wright et al. 1994). Sie haben somit deutlich höhere Erwartungen an die Belastbarkeit und das langfristige Überleben ihres Gelenkersatzes (Cutler, Deaton, and Lleras-Muney 2006; Gandhi et al. 2010; Roser 2019; Scott et al. 2012). Infolgedessen steigen auch die biomechanischen Belastungen, aber auch die damit einhergehende in vivo wirkende Gelenkreibung. Demgegenüber sind die in vivo wirkenden Gelenkbelastungen und die daraus resultierenden Reibbelastungen im Gelenkersatz, insbesondere bei höher belastenden und sportlichen Aktivitäten, völlig unbekannt und somit ein potentieller Risikofaktor für die Lebensdauer und mechanische Stabilität des Gelenkersatzes. Nach Bayliss (2017). beträgt das berechnete Revisionsrisiko für Patienten mit einem Alter von im Mittel 60 Jahren bei der Primäroperation bis zu 35 % (Lee E Bayliss et al. 2017), wohingegen noch jüngere Patienten ein deutlich höheres Revisionsrisiko aufweisen (Lübbeke et al. 2007). Patienten, welche jedoch bei der Primärimplantation 70 Jahre oder älter waren, haben

hingegen ein deutlich geringes Risiko von nur 1-6 %, sich nochmals einer Revisionsoperation unterziehen lassen zu müssen (Lee E Bayliss et al. 2017).

Ungeachtet dessen bleiben die Revisionszahlen trotz erheblicher Verbesserungen auf dem Gebiet der Endoprothetik, insbesondere aufgrund von Abrieb und aseptischer Lockerung auf bemerkenswert konstant hohem Niveau (Urjit Chatterji et al. 2004; Huch et al. 2005) und haben während der letzten zwei Dekaden zu keiner signifikanten Verringerung der Revisionsraten geführt. Die Lebensdauer und Standfestigkeiten vor allem der acetabulären Komponenten stellen hierbei immer noch ein signifikantes klinisches Problem dar. So zeigen Analysen des schwedischen Prothesenregisters, dass bei bis zu 70% aller Primär-Revisionen und bei bis zu 48% aller multiplen Revisionen nur das Inlay oder nur Inlay und Pfanne gewechselt werden mussten (Garllik et al. 2012). Offensichtlich ist somit die in vivo auftretende Reibung nach wie vor der Hauptrisikofaktor für den Gelenkflächen-Abrieb und Lockerung und damit für das langfristige ‚Überleben' des Gelenkersatzes (Australian Orthopaedic Association National Joint Replacement Registry (AOANJRR) 2019; Bergen 2019; CJRR 2008; Grimberg et al. 2020; Leif I Havelin et al. 2009; Huch et al. 2005; NJR Editorial Board NJRSC 2019).

Wenn Faktoren wie das individuelle Aktivitätsniveau, die Arbeitsjahre nach der Operation und die individuelle Lebenserwartung weiter zunehmen, ist zu erwarten, dass das individuelle Lebenszeitrisiko für eine notwendige Revisionsoperation bei jüngeren Patienten sogar noch weiter zunimmt und so die absolute Zahl von Gelenk-Revisionen deutlich ansteigen wird. Speziell der in vivo auftretenden Gleitflächenverschleiß an Inlay und/oder Pfanne, und die damit verbundene aseptische Prothesenlockerung ist immer noch ein ungelöstes Problem in der Hüft-Endoprothetik (Australian Orthopaedic Association National Joint Replacement Registry (AOANJRR) 2019; Bergen 2010, 2019; CJRR 2008; Grimberg et al. 2020; L. I. Havelin et al. 2009; NJR Editorial Board NJRSC 2019). Zur Minimierung dieses Verschleißproblems bedarf es umfangreicher Materialforschung. Hierzu werden wiederum realistische Belastungsdaten in Form der in vivo wirkenden Gelenkbelastung und Gelenkreibung bei alltäglichen, aber insbesondere auch bei höher belastenden Aktivitäten für analytische als auch experimentelle Studien benötigt. Obwohl die Gelenkreibung als ein wesentlicher Risikofaktor für die Standzeit

einer Hüftendoprothese bekannt ist, ist erstaunlich wenig über die tatsächlich in vivo auftretende Reibung und deren in vivo vorherrschenden Einflussparameter bekannt.

Reibung

Die Reibung wird in der Tribologie als Teilgebiet der Mechanik beschrieben als eine Wechselwirkung zwischen zwei sich berührenden Kontaktflächen. Man unterscheidet hierbei im Wesentlichen zwischen der Haftreibung, die auftritt wenn die Kontaktflächen keine Relativbewegung zueinander ausführen, bzw. der Gleitreibung, wenn zwischen den Kontaktflächen eine Relativbewegung stattfindet. In beiden Fällen wirken die auftretenden Reibungskräfte einer potentiellen Bewegung bzw. dem Start einer Bewegung entgegen. Der dabei auftretende Reibungswiderstand ist dabei abhängig vom Material der in Kontakt stehenden Gleitflächen, als auch von der vorherrschenden Gleitflächenschmierung sowie der spezifischen dynamischen Interaktion der artikulierenden Flächen miteinander (Bart, Gucciardi, and Cavallaro 2013). Diese Zusammenhänge wurden bereits im 17. Jahrhundert von Charles Augustin Coloumb (1736-1806) postuliert. So konnte dieser zeigen, dass die auftretende Gleitreibung im ungeschmierten bzw. im trockenen Zustand abhängig von der wirkenden Kontaktkraft ist, jedoch unabhängig von der Größe der interagierenden Kontaktflächen und Gleitgeschwindigkeit. Für eine Charakterisierung der so wirkenden Coloumb´schen Reibung wird in der Tribologie daher der Reibungskoeffizient μ verwendet, welcher sich aus dem Verhältnis von Normalkraft F_N (relativ zur Kontaktfläche) und der vorherrschenden Reibkraft F_R (in Gleitrichtung) ergibt (Abbildung 1).

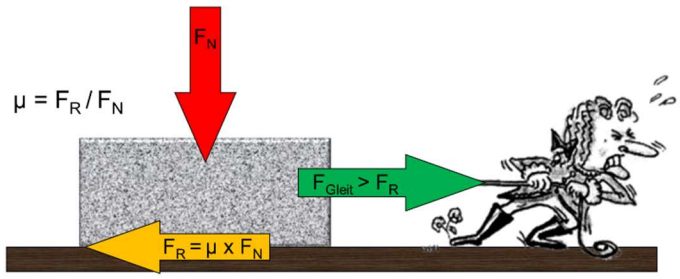

Abbildung 1: Coloumb´sches Gleitreibungsmodell; Reibungskoeffizient μ, Normalkraft F_N, Reibkraft F_R und Gleitkraft F_G

Der Reibungskoeffizient nach Coloumb ($\mu = F_R/F_N$) ist somit primär abhängig von den Materialen der in Kontakt stehenden Gleitflächen, bzw. deren Oberflächenrauigkeiten und ist somit für die jeweilige Gleitpaarung zunächst als konstant anzusehen. In der

Realität wird dieser Zusammenhang jedoch durch Veränderungen der mechanischen, chemischen und physikalischen Eigenschaften der Kontaktflächen beeinflusst, welche wiederum von der Materialpaarung, dem elasto-plastischem Verhalten der Gleitpartner, den Oberflächeneigenschaften und insbesondere auch der vorherrschenden Schmierung zwischen den Gleitpartnern abhängen. Neben der Trockenreibung bzw. Festkörperreibung, bei der keinerlei Schmierung der Gleitpartner erfolgt, unterscheidet man in der Tribologie daher prinzipiell zwischen drei weiteren Reibungs- bzw. Schmierzuständen (Wang and Wang 2013; Wäsche and Woydt 2014), welche bereits im frühen 20. Jahrhundert durch Richard Stribeck (1902) beschrieben wurden (Abbildung 2).

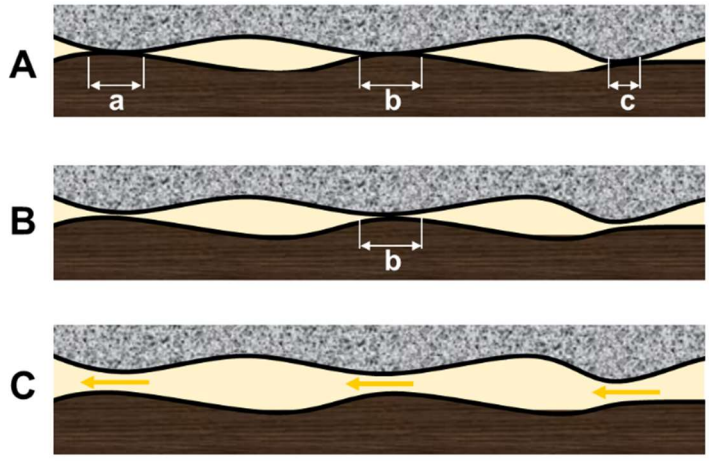

Abbildung 2: Schmierzustände nach Stribeck; (A) Grenzreibung; (B) Mischreibung; (C) Schmierfilmreibung; a, b und c – Kontaktzonen der Gleitpartner

So tritt Grenzreibung auf, wenn beide Gleitpartner bei kleinen Gleitgeschwindigkeiten und hohen Kontaktkräften gegeneinander gleiten, ohne dass der vorhandene Schmierstoff die beiden Kontaktflächen voneinander trennt (Abbildung 2A). Wenn sich mit weiter zunehmender Gleitgeschwindigkeit bzw. bei abnehmender Kontaktkraft ein dünner Schmierfilm ausbildet, welcher die Kontaktflächen während der Bewegung jedoch noch nicht vollständig voneinander trennt, herrscht Mischreibung vor (Abbildung 2B). Dies hat zur Folge, dass der Reibwiderstand und der wirkende Reibkoeffizient bzw. die Reibkraft im Vergleich zum Grenzreibungszustand abnimmt. Nach Stribeck tritt hingegen Schmierfilmreibung auf, wenn die beiden Gleitpartner bei weiter ansteigender Gleitgeschwindigkeit durch den entstehenden hydrodynamischen Druck des Schmiermittels vollständig voneinander getrennt werden und somit keinerlei

Festkörperkontakt mehr auftritt (Abbildung 2C). Dabei nimmt die wirkende Reibkraft und daraus folgend der wirkenden Reibungskoeffizient weiter ab (Jin et al. 2006). Der auftretende Reibungswiderstand ergibt sich dann hauptsächlich aus den inneren Spannungszuständen des Schmierstoffes, infolge der auftretenden geschwindigkeitsabhängigen inneren Scherwiderstände des Fluides, welche der Bewegungsrichtung entgegenwirken. Mit noch weiter steigender Gleitgeschwindigkeit nimmt der Reibungskoeffizient dann jedoch wieder zu (Abbildung 3), da immer mehr ‚Schichten' des Schmierstoffes aufeinander abgleiten, was dann zu einer Zunahme der ‚inneren' Scherspannung im Fluid führt. Von ‚außen' kann dies als eine Zunahme des Widerstandes gegen die Bewegung detektiert werden und somit wieder zu einem Anstieg des auftretenden Reibungskoeffizienten führen (Jin et al. 2006).

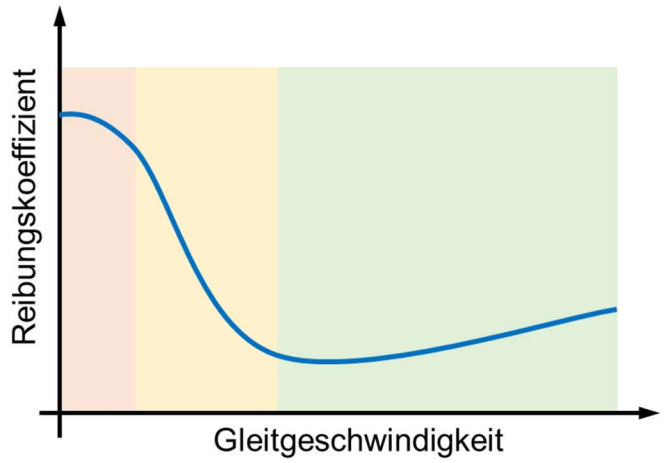

Abbildung 3: Zusammenhang zwischen dem wirkenden Reibungskoeffizienten und der vorherrschenden Gleitgeschwindigkeit; Bereiche: orange - Grenzreibung, gelb – Mischreibung, grün – Schmierfilmreibung

Gelenkschmierung

Die gezeigten Zusammenhänge zwischen der Gleitgeschwindigkeit und dem auftretenden Reibungskoeffizienten gelten jedoch nur unter der Voraussetzung, solang das verwendete Fluid einen linearen Zusammenhang zwischen der von außen einwirkenden Schergeschwindigkeit und der daraus im Fluid resultierenden Scherspannung aufweist (Abbildung 4), es sich also um ein Newton Fluid handelt, wie z.B. Wasser oder Öl. Nicht-Newtonsche Fluide zeigen demgegenüber kein lineares Verhalten relativ zur der auf sie wirkenden Schergeschwindigkeit, wie beispielsweise Mehl-Wasser-Emulsion, Blut oder Synovia.

Zur Charakterisierung der sich ergebenden Fließfähigkeit des Fluides in Abhängigkeit der auf das Fluid wirkenden Scherbelastung wird der Begriff der Viskosität (Zähigkeit) genutzt. Je höher die Viskosität eines Fluides, umso zähflüssiger, also weniger fließfähig ist das beschriebene Fluid. Bei den nicht-Newtonschen Fluiden wird darüber hinaus auch noch zwischen strukturviskosen, also scherverdünnenden und dilatanten, also scherverdickenden Fluiden unterschieden (Abbildung 4). Strukturviskose Fluide reagieren bei einer Zunahme der auf sie wirkenden Scherbelastung somit mit einer Abnahme der Fluid-Viskosität und dilatante Fluide entsprechend mit einer Zunahme der Fluid-Viskosität, also einer Abnahme der relativen Fließfähigkeit.

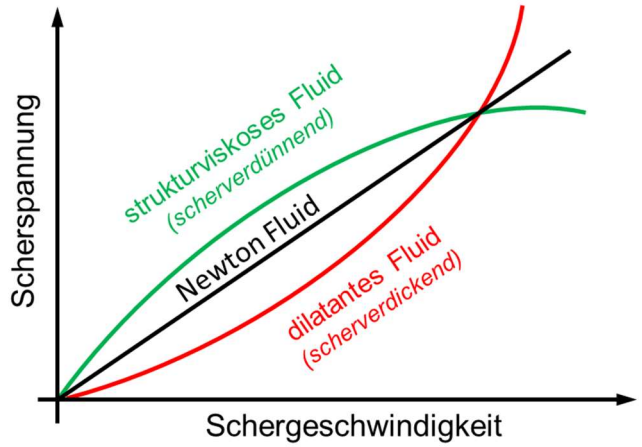

Abbildung 4: Schematische Darstellung des Viskositätsverhaltens unterschiedlicher Fluidtypen in Abhängigkeit der auf sie wirkenden Schergeschwindigkeit

Ein typisches Beispiel für ein strukturviskoses Fluid ist die (gesunde) Synovia. Mit zunehmender Gleitgeschwindigkeit im Gelenk nimmt ihre Viskosität ab, sie wird also dünnflüssiger und ihre Fließfähigkeit nimmt zu (Fam, Bryant, and Kontopoulou 2007; Mazzucco et al. 2002). Sie wird in der Membrana synovialis gebildet und ist ein Konglomerat aus unterschiedlichen Proteinen und Hyaluronsäure. Analysen unterschiedlicher Synovialfluide konnten bereits zeigen, dass der Hyaluronsäure Gehalt in arthrotischen Gelenken um den Faktor 2 niedriger ist als in gesunden Gelenken und insbesondere aber auch, das die Viskosität der Synovia maßgeblich von degenerativ bedingten Veränderungen im Gelenk beeinflusst wird (Fam et al. 2007). Während sich die gesunde Synovia bei hohen Scherraten wie ein nicht-Newtonsches Fluid verhält (Abbildung 5A), kann hingegen bei einer rheumatischen Synovia von einem Newtonschen Verhalten ausgegangen werden, dessen Viskosität nicht von der

Scherrate abhängt. Eine arthrotische Synovia weist hingegen nur eine leicht geringere Abhängigkeit von der Scherrate im Vergleich zur gesunde Synovia (Fam et al. 2007; Gao, Fisher, and Jin 2011) auf. Neben dem Hyaluronsäure Gehalt ist aber auch der Proteinanteil in der Synovia für deren spezifische Schmiereigenschaften bestimmend und es konnte bereits gezeigt werden, dass dieser in arthrotischen Gelenken deutlich erhöht ist (Chikama 1985). Des Weiteren ist bereits bekannt, dass die Synovia auch altersbedingten Änderungen unterworfen ist, wobei dessen Viskosität mit steigendem Alter abnimmt (Jebens and Monk-Jones 1959) (Abbildung 5B).

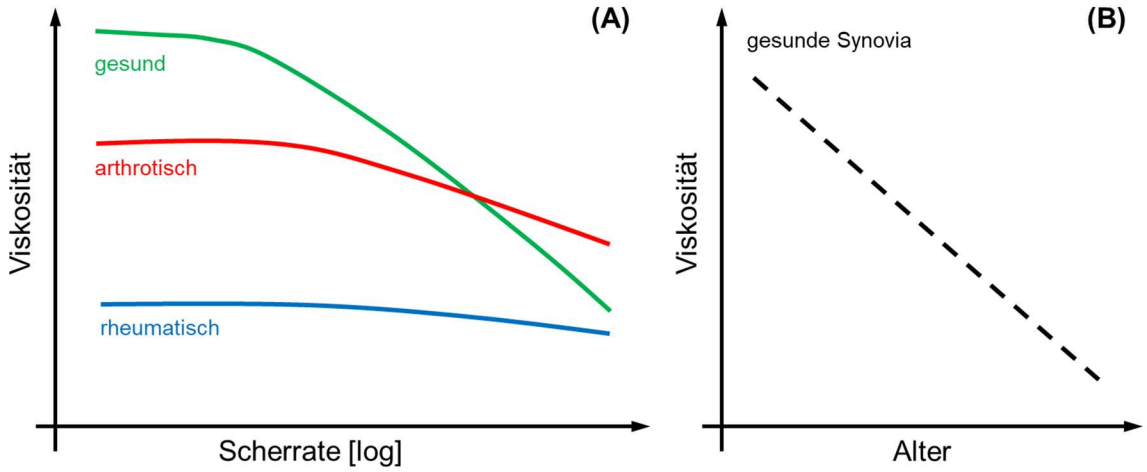

Abbildung 5: (A) Schematischer Zusammenhang zwischen Scherrate und Viskosität für gesunde (grün), arthrotische (rot) und rheumatische (blau) Synovia, nach (Fam et al., 2007); (B) Schematische Darstellung der altersbedingte Viskositätsänderungen gesunder Synovia, nach (Jebens and Monk-Jones 1959)

Die sich aus diesen in-vitro-Analysen ergebenden Reib- und Schmierbedingungen wurden in der Vergangenheit bereits genutzt, um mittels verschiedener in-vitro-Simulationsversuchen und unterschiedlichen Computersimulationen die in vivo wirkende Gelenkreibung systematisch zu quantifizieren. So konnte unter anderem gezeigt werden, dass aufgrund der numerisch bestimmten Schmierfilmdicke im Gelenkersatz, insbesondere beim Gehen während der Einbein-Standphase am Rand der lasttragenden Kontaktfläche primär Festkörperreibung vorherrscht, wohingegen im Zentrum potentiell Schmierfilmreibung auftritt (Gao et al. 2011). Darüber hinaus zeigten diese Simulationen, dass während der anschließenden Schwungphase die resultierende Schmierfilmdicke zwar wieder ansteigt, dieser Aufbau jedoch wesentlich von der untersuchten Materialpaarung der Gleitpartner abhängt. So deuteten die

Ergebnisse darauf hin, dass bei typischen hart-hart-Paarungen (z.B.: Keramik versus Keramik) in vivo nur bei ca. 10% des Gang-/Lastzyklus Flüssigkeitsreibung vorherrscht, wohingegen beim Fahrradfahren bei ca. 90% des Lastzyklus Flüssigkeitsreibung auftreten kann. Bei typischen hart-weich-Paarungen (z.B. Keramik versus Polyethylen) wird jedoch bisher davon ausgegangen, dass aufgrund der höheren Rauigkeit des weichen Gleitpartners ausschließlich Grenz- bzw. Mischreibung auftritt. Aufgrund der unterschiedlichen Modell- und Viskositätsannahmen unterscheiden sich die Ergebnisse quantitativ jedoch stark (Gao et al. 2011; Jalali-Vahid et al. 2001; Jin et al. 2006; Meyer and Tichy 2003a; Wang et al. 2008).

Die sich aus diesen Faktoren ergebende Gelenkreibung ist heute bereits als ein wesentlicher Einflussfaktor für das Überleben der Gleitpartner anerkannt (Australian Orthopaedic Association National Joint Replacement Registry (AOANJRR) 2019; Bergen 2019; CJRR 2008; Hall and Unsworth 1997; L. I. Havelin et al. 2009; Kennedy et al. 1998; Korduba et al. 2014; NJR Editorial Board NJRSC 2019; Schäfer, Soltész, and Bernard 1998; Scholes and Unsworth 2000; Scholes, Unsworth, and Goldsmith 2000). Neben den sich daraus ergebenden mechanischen Abriebpartikeln der Gleitpartner, die an sich bereits ein relevantes biologisches Problem sind (Abu-Amer, Darwech, and Clohisy 2007; Kadoya, Kobayashi, and Ohashi 1998; Marshall, Ries, and Paprosky 2008), wirkt das resultierende Reibmoment auch als Torsionsbelastung am Pfanne/Becken-Interface und führt so zu einer weiteren mechanischen Belastung der knöchernen Verankerung (Curtis et al. 1992; Mjöberg, Hansson, and Selvik 1984). Bisher ist diese in vivo auftretende Beanspruchung jedoch weitestgehend unbekannt, da nicht die Möglichkeit bestand, die Reibung und das individuelle Reibverhalten direkt in vivo zu ermitteln.

Als weitere potentielle Versagensgründe werden auch Fehlpositionierungen der Implantat-Komponenten diskutiert (Kennedy et al. 1998; Korduba et al. 2014; Nevelos et al. 2001; Wan, Boutary, and Dorr 2008). Aus technischer Perspektive ist die Reibung, wie bereits beschrieben, zwischen zwei Gleitpartnern zum einen abhängig von den verwendeten Materialien (z. B. Metall, Keramik, Polyethylen) und den auf das Implantat wirkenden Belastung, zum anderen aber auch von der lasttragenden Kontaktfläche, also der individuellen Gelenküberdachung und somit von der individuellen Implantat-Orientierung (Kennedy et al. 1998; Korduba et al. 2014). Eine

intraoperative Positionierung der Gelenk-Komponenten innerhalb einer „Safe Zone“ soll eine optimale Gelenküberdachung im Alltag gewährleisten (lasttragende Kontaktfläche) und so das Revisionsrisiko reduzieren (Kennedy et al. 1998; Korduba et al. 2014; Lewinnek et al. 1978; Nevelos et al. 2001; Wan et al. 2008). Als „korrekt“ wird bisher eine „Safe Zone“ angesehen, wenn eine im Hinblick auf einen optimierten ‚Range of Motion‘ definierte Zielzone bei der Implantat-Positionierung eingehalten wird. Am bekanntesten ist die von Lewinnek postulierte „Safe Zone“ (Lewinnek et al. 1978): Diese geht davon aus, dass die Implantation der Pfanne immer in der gleichen Orientierung erfolgen sollte, um eine optimale Gelenküberdachung insbesondere hinsichtlich Lastübertragung und Torsionsstabilität sicherzustellen, und empfiehlt daher eine Positionierung in 40° (±10°) Inklination und 15° (±10°) Anteversion. Allerdings zeigten retrospektive Versagensanalysen keinen Unterschied zwischen den Revisionsraten von Pfannen, die innerhalb bzw. außerhalb dieser „Safe Zone“ implantiert wurden (Abdel et al. 2016; Parratte et al. 2016). Daraus lässt sich schließen, dass eine individuell optimale Pfannenorientierung und die daraus resultierende Gelenküberdachung für einige Patienten außerhalb der „Safe Zone“ liegen kann. Ein potentieller Erklärungsansatz für die beobachteten Abweichungen könnten die individuellen postoperativen Beckenkippungen darstellen (Philippot et al. 2009; Zhu, Wan, and Dorr 2010), welche direkt die funktionelle Orientierung der Hüftpfanne und so die resultierende postoperative Gelenküberdachung beeinflussen (Babisch, Layher, and Amiot 2008; Pierrepont et al. 2016; Zhu et al. 2010). Verschiedene Studien konnten darüber hinaus zeigen, dass der reibungsinduzierte Abrieb im künstlichen Gelenkersatz wiederum direkt durch die individuelle Gelenküberdachung beeinflusst werden kann (Nevelos et al. 2001; Wan et al. 2008). Die Ermittlung von realistischen Belastungsdaten, aber insbesondere auch die Ermittlung der tatsächlich in vivo wirkenden Reibbedingungen ist somit für die zukünftige Weiterentwicklung der Prothesen unabdingbar. Eine weitere biomechanische und insbesondere auch tribologische Optimierung dieser Gelenkversorgung ist aber auch durch die steigende Anzahl junger (Nemes et al. 2020; Pabinger and Geissler 2014) und besonders aktiverer Patienten (U. Chatterji et al. 2004; W. L. Healy et al. 2008; Huch et al. 2005; B. C. A. Mancuso et al. 2009), die mit einem Hüftgelenkersatz versorgt werden, nach wie vor hoch relevant und notwendig.

Ziel meiner wissenschaftlichen Arbeiten war es daher, im Rahmen einer longitudinal angelegten Studie, die im totalen Hüftgelenkersatz auftretenden Kontaktkräfte und

Reibmomente bei besonders aktiven Patienten erstmals direkt in vivo zu messen und systematisch zu analysieren, um so spezifische Einflussparameter der individuell wirkenden Gelenkreibung zu identifizieren.

Für die Durchführung der geplanten Studie zur in-vivo-Messung der wirkenden Gelenkbelastungen und insbesondere für die Messung der in vivo wirkenden Gelenkreibung, wurde zunächst ein spezielles instrumentiertes Hüftimplantat entwickelt. Als besondere Anforderung wurde hierfür eine 6-Komponenten-Messung definiert, um die wirkenden Kontaktkräfte in drei Raumrichtungen, als auch die auftretenden Reibmomente um die drei Raumachsen direkt in vivo messen zu können. Darüber hinaus durfte das instrumentierte Implantat kein höheres Risiko für den Patienten im Vergleich zum Standardimplantat mit sich bringen und musste für eine Anwendung im Rahmen einer klinischen Studie zugelassen sein.

Instrumentierte Hüftendoprothese zur direkten Messung der in vivo wirkenden Gelenkreibung

Als Basis für die Instrumentierung wurde ein seit Jahrzehnten klinisch erfolgreicher Implantatschaft, welcher auf dem Sportorno Design basiert (CTW Classic - Merete Medical GmbH) und zementfrei implantiert wird, ausgewählt. Es wurden zwei unterschiedliche Schaftgrößen (10 und 12,5) im Halsbereich so modifiziert, dass die für die in-vivo-Belastungsmessungen benötigte Messelektronik dort eingebracht werden konnte (Abbildung 6).

Die modifizierten Implantate unterscheiden sich vom Standartimplantat somit nur in der Halsgeometrie (alt 12/14 Konus, neu 14/16 Konus). Nach Einbringung der Mess-Telemetrie und von sechs Dehnungsmessstreifen (DMS) in den aufgebohrten Implantathals wurde dieser mit einem Deckel (inkl. Antennen-Durchleitung) verschlossen und mit dem Elekronenstrahl-Schweißverfahren unter Vakuum verschweißt. So wird gewährleistet, dass es zu keinem direkten Kontakt zwischen Telemetrie und Körpergewebe kommen kann. Alle darüber hinaus mit dem Körpergewebe in Berührung kommenden Materialien sind klinisch bewährt, körperverträglich und es besteht kein erhöhtes Risiko gegenüber klinisch üblichen Endoprothesen und deren medizinischen Funktionen.

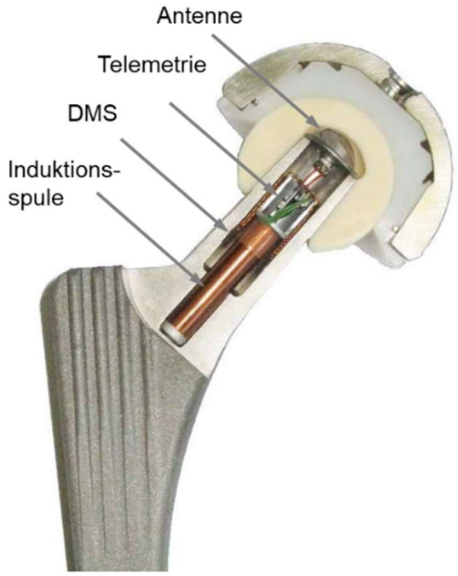

Abbildung 6: Schnittbild der instrumentierten Hüftendoprothese mit Telemetrie, 6 Dehnungsmessstreifen (DMS), Induktionsspule und interner Antenne zur drahtlosen Datenübertragung

Die Energieversorgung der internen Telemetrie erfolgt induktiv über ein elektromagnetisches Wechselfeld (4 kHz), welches über eine externe Spule induziert wird. Auf eine Batterie im Inneren des Implantates, welche die Energieversorgung der Telemetrie nur über einen eng begrenzten Zeitraum ermöglicht, kann somit verzichtet werden und es sind zeitlich unbegrenzte Messungen möglich. Sobald das externe elektromagnetische Wechselfeld ausgeschaltet ist, wird die interne Telemetrie nicht mehr mit Spannung versorgt, ist passiv und es werden keine Messdaten erhoben.

Die mechanische Stabilität der instrumentierten Implantate (Damm et al. 2010a) wurde durch Dauerfestigkeitsprüfungen nach DIN ISO 7206 getestet. Darüber hinaus wurde eine Prüfung auf Sterilität, sowie ein quantitativer Nachweis von Endotoxin in Flüssigkeiten und Eluaten mittels LAL-Test entsprechend EN ISO 10993-11, SOP 09-010 durch die Abteilung Mikrobiologie und Validierung der Firma Vanguard AG durchgeführt. Die Prüfung der technischen Unbedenklichkeit wurde anschließend durch eine unabhängige Prüfstelle (BerlinCERT, Prüf- und Zertifizierstelle für Medizinprodukte GmbH an der Technischen Universität Berlin) nach der Richtlinie 90/385/EWG der „Active Implantable Medical Devices Directive“ (AIMDD) sowie dem Medizinproduktgesetz geprüft. Es wurde bestätigt, dass die instrumentierte Hüftendoprothesen bei bestimmungsmäßiger Verwendung technisch unbedenklich im Sinne der AIMDD sowie des Medizinproduktgesetzes sind und somit im Rahmen einer

klinischen Studie verwendet werden dürfen (Berlin CERT Zertifikat-Register-Nr.: Z-08-470-MP).

Im Anschluss an die Zertifizierung wurden insgesamt 20 instrumentierte Schäfte mit zwei unterschiedlichen Schaftgrößen hergestellt (10x Schaft 10; 10x Schaft 12,5) und mit zwei unterschiedlichen Kugelkopfgrößen (M, L) kalibriert und einem Genauigkeitstest unterzogen (Bergmann et al. 2008).

In-vivo-Studie und Patientenrekrutierung

Für die Durchführung der geplanten Studie wurde ein Ethikantrag gemäß §20 MPG mit dem Titel „Hüftmessprothese: Belastungsmessung bei Patienten mittels einer instrumentierten Endoprothese“ bei der Ethikkommission der Charité – Universitätsmedizin Berlin gestellt, beraten und genehmigt (EA2/057/09), sowie anschließend beim Deutschen Register für klinische Studien registriert (DRKS00000563).

Die Studienteilnehmer wurden im Rahmen der klinischen üblichen Patientenaufklärung durch die beteiligten Studienärzte, an den teilnehmenden Studienzentren (Charité - Centrum für Muskuloskeletale Chirurgie und Sana Kliniken Sommerfeld), auf die Möglichkeit der Studienteilnahme hingewiesen und über Inhalt und Risiken der Studie aufgeklärt. Alter und Geschlecht der Studienteilnehmer richtete sich dabei nach der typischen Population, die unabhängig von der Messprothese für eine Hüftendoprothesen-Implantation indiziert waren. Es wurde jedoch angestrebt, aus dieser Patientengruppe jüngere und besonders aktive Patienten zu rekrutieren.

Im Zeitraum von April 2010 bis Januar 2013 konnten so 10 jüngere und besonders aktive Patienten als Studienteilnehmer eingeschlossen werden (Tabelle 1). Im Zuge der Implantation wurden diese dann jeweils mit einem instrumentierten Hüftschaft in Kombination mit einem Al_2O_3-Keramik-Kopf (BIOLOX forte, CeramTec GmbH, Plochingen, Deutschland) und einem XPE-Inlay (Durasul, Zimmer GmbH, Winterthur, Schweiz) mit zementfreier Titan-Pfanne (Allofit, Zimmer GmbH, Winterthur, Schweiz) versorgt.

Tabelle 1: Studienteilnehmer

Patient	Alter	Geschlecht	BMI [kg/m²]	Implantation
H1L	55	M	24	Apr. 2010
H2R	61	M	27	Aug. 2010
H3L	59	M	31	Nov. 2010
H4L	50	M	25	Jan. 2011
H5L	62	W	31	Apr. 2011
H6R	68	M	27	Nov. 2011
H7R	52	M	28	Nov. 2011
H8L	55	M	25	Apr. 2012
H9L	54	M	34	Sep. 2012
H10R	53	W	37	Jan. 2013

Die Studienpatienten (Abbildung 7) haben neben der schriftlichen Einwilligung zur Studienteilnahme, außerdem schriftlich zugestimmt, dass pseudonymisiert aufgezeichneten Messdaten, insbesondere auch Bilder und Videos auf denen sie persönlich erkennbar sind, in wissenschaftlichen Zeitschriften, auf Tagungen und in einer öffentlich zugänglichen Datenbank (http://OrthoLoad.com) gezeigt werden dürfen.

Abbildung 7: Patienten mit instrumentiertem Hüftimplantat

2. Eigene Arbeiten

2.1. Die in vivo wirkende Gelenkreibung beim Gehen

Erste in-vivo-Belastungsmessungen wurden mit allen Studienpatienten bereits in der frühen postoperativen Phase im Rahmen der Rehabilitation in der Klinik durchgeführt. Die hierbei in vivo auftretenden Gelenkbelastungen wurden im Rahmen verschiedener wissenschaftlicher Publikationen veröffentlicht (Damm, Schwachmeyer, et al. 2013; Schwachmeyer et al. 2013). Um die in vivo wirkende Gelenkreibung erstmals systematisch analysieren zu können, wurden mit allen Patienten drei Monate postoperativ streng kontrollierte Belastungsmessungen beim kontinuierlichen Gehen durchgeführt. Die anschließenden Analysen zeigten große interindividuelle Unterschiede der in-vivo-Gelenkkontaktkraft und resultierenden Gelenkreibung. Es konnte außerdem gezeigt werden, dass die Reibbedingungen in vivo nicht konstant sind, sondern sich im Verlauf des Gangzyklus ändern. Für eine objektive Beurteilung der Reibbedingungen wurde daher ein dreidimensionaler Ansatz zur Bestimmung des Reibungskoeffizienten entwickelt. So konnte u. a. gezeigt werden, dass die in der Literatur berichteten in-vitro-Versuche die in-vivo-Situation nur ungenügend abbilden. Beim Übergang zur Flexionsphase kommt es z.B. in vivo zu einem bisher unbekannten starken Anstieg des Reibungskoeffizienten (μ_{max} = 0.14 im Mittel). Ein solch hoher Reibungskoeffizient wird in der Literatur für den trockenen Reibungszustand angegeben (Xiong and Ge 2001). Dies kann darauf hindeuten, dass sich die Schmierbedingungen im Gelenkspalt im Verlauf des Gangzyklus ändern und lässt somit den Schluss zu, dass viele Simulatorstudien die in-vivo-Bedingungen unrealistischabbilden. Der nachfolgende Text entspricht dem Abstract der Arbeit „Friction in Total Hip Joint Prosthesis Measured In Vivo during Walking", welche im Journal PLoS ONE 2013 veröffentlicht wurde:

„Friction-induced moments and subsequent cup loosening can be the reason for total hip joint replacement failure. The aim of this study was to measure the in vivo contact forces and friction moments during walking. Instrumented hip implants with Al_2O_3 ceramic head and an XPE inlay were used. In vivo measurements were taken 3 months post operatively in 8 subjects. The coefficient of friction was calculated in 3D throughout the whole gait cycle, and average values of the friction-induced power dissipation in the joint were determined.

On average, peak contact forces of 248% of the bodyweight and peak friction moments of 0.26% bodyweight times meter were determined. However, contact forces and friction moments varied greatly between individuals. The friction moment increased during the extension phase of the joint. The average coefficient of friction also increased during this period, from 0.04 (0.03 to 0.06) at contralateral toe off to 0.06 (0.04 to 0.08) at contralateral heel strike. During the flexion phase, the coefficient of friction increased further to 0.14 (0.09 to 0.23) at toe off. The average friction-induced power throughout the whole gait cycle was 2.3 W (1.4 W to 3.8 W).

Although more parameters than only the synovia determine the friction, the wide ranges of friction coefficients and power dissipation indicate that the lubricating properties of synovia are individually very different. However, such differences may also exist in natural joints and may influence the progression of arthrosis. Furthermore, subjects with very high power dissipation may be at risk of thermally induced implant loosening. The large increase of the friction coefficient during each step could be caused by the synovia being squeezed out under load."

Publikation: Friction in Total Hip Joint Prosthesis Measured In Vivo during Walking

Damm P., Dymke J., Ackermann A., Bender A., Graichen G., Bergmann G.
PLoS ONE 8(11): 2013; https://doi.org/10.1371/journal.pone.0174788

OPEN ACCESS Freely available online

PLOS ONE

Friction in Total Hip Joint Prosthesis Measured *In Vivo* during Walking

Philipp Damm[1]*, Joern Dymke[1], Robert Ackermann[1], Alwina Bender[1], Friedmar Graichen[1], Andreas Halder[2], Alexander Beier[2], Georg Bergmann[1]

1 Julius Wolff Institute, Charité – Universitaetsmedizin Berlin, Berlin, Germany, **2** Klinik für Endoprothetik, Sana Kliniken Sommerfeld, Sommerfeld, Germany

Abstract

Friction-induced moments and subsequent cup loosening can be the reason for total hip joint replacement failure. The aim of this study was to measure the *in vivo* contact forces and friction moments during walking. Instrumented hip implants with Al_2O_3 ceramic head and an XPE inlay were used. *In vivo* measurements were taken 3 months post operatively in 8 subjects. The coefficient of friction was calculated in 3D throughout the whole gait cycle, and average values of the friction-induced power dissipation in the joint were determined. On average, peak contact forces of 248% of the bodyweight and peak friction moments of 0.26% bodyweight times meter were determined. However, contact forces and friction moments varied greatly between individuals. The friction moment increased during the extension phase of the joint. The average coefficient of friction also increased during this period, from 0.04 (0.03 to 0.06) at contralateral toe off to 0.06 (0.04 to 0.08) at contralateral heel strike. During the flexion phase, the coefficient of friction increased further to 0.14 (0.09 to 0.23) at toe off. The average friction-induced power throughout the whole gait cycle was 2.3 W (1.4 W to 3.8 W). Although more parameters than only the synovia determine the friction, the wide ranges of friction coefficients and power dissipation indicate that the lubricating properties of synovia are individually very different. However, such differences may also exist in natural joints and may influence the progression of arthrosis. Furthermore, subjects with very high power dissipation may be at risk of thermally induced implant loosening. The large increase of the friction coefficient during each step could be caused by the synovia being squeezed out under load.

Citation: Damm P, Dymke J, Ackermann R, Bender A, Graichen F, et al. (2013) Friction in Total Hip Joint Prosthesis Measured *In Vivo* during Walking. PLoS ONE 8(11): e78373. doi:10.1371/journal.pone.0078373

Editor: Amir A. Zadpoor, Delft University of Technology (TUDelft), The Netherlands

Received May 21, 2013; **Accepted** September 20, 2013; **Published** November 8, 2013

Funding: Funding provided by the German Research Society (SFB760 and BE 804/19-1), http://www.dfg.de, and Deutsche Arthrose-Hilfe e. V., http://www.arthrose.de. The funders had no role in study design, data collection and analysis, decision to publish, or preparation of the manuscript.

Competing Interests: The authors have declared that no competing interests exist.

* E-mail: Philipp.Damm@charite.de

Introduction

In 20% to 40% of all cases [1], polyethylene wear and aseptic loosening are the most frequent reasons for revisions of total hip joint replacements (THR). Both factors are related to friction in the joint. Cup loosening has been reported to be the only cause in 30% to 62% of revisions [2,3]. Subjects, who obtained a THR are becoming increasingly younger and are, therefore, more active and athletic [4,5]. However, higher activity levels produce more wear and more strenuous activities cause higher friction moments. This will increase the risk of implant loosening [6,7]. These facts indicate that reduction of friction between head and cup is critical for further improvement of THR.

Several *in vivo* studies have been performed to investigate the loads acting in hip implants during different activities [8,9]. These studies have shown that the contact force during normal walking falls in a range between 240 and 480% of the bodyweight (BW). However, *in vivo* measurements of friction in hip endoprostheses have not been reported previously.

One *in vivo* study *indirectly* assessed friction in the joint by measuring the implant temperature during an hour of walking [10,11]. Its increase is mainly related to the friction-induced power generated in the implant. A peak temperature of 43.1°C was measured in 1 subject, a level at which bone tissue may already be impaired [12], especially when this temperature occurs repeatedly. Therefore, it cannot be excluded that friction and increased implant temperatures may be underestimated risk factors for the long-term stability of THR.

To determine the friction in total hip joint prosthesis, *in vitro* simulator studies were performed [13,14]. To evaluate the friction between two sliding partners, the coefficient of friction μ was used. For the tribological pairing Al_2O_3/UHMWPE μ ranges depended on the lubricant [13], ranging from 0.044 (distilled water), to 0.054 (bovine serum), and 0.089 (saline). The coefficient increased dramatically up to values of 0.14 when the conditions changed from lubricated to dry [15].

However, most of the simulator tests load the joint only in the flexion-extension plane and use load patterns which may not be realistic [16]. Newer studies investigated friction under more realistic conditions, simulating *in vivo* measured gait data [17]. Varying parameters for friction were investigated, for example, different material combinations for implant head and cup [18], and various lubricant regimes [17,19–22]. These simulator studies were performed under very different test conditions, such as deviating patterns of joint loading and movement or by using different lubricants. Nevertheless, it was shown that friction in THR is mainly influenced by the material of the sliding partners and the lubrication regime.

Table 1. Patients investigated.

Patient	Age	Gender	Body weight	Gait Velocity	Mean Gliding Speed Extension | Flexion
	[years]		[N]	[m/s]	[m/s]
H1	56	m	754	1.0	0.02 | 0.04
H2	62	m	755	1.0	0.03 | 0.05
H3	60	m	880	0.8	0.02 | 0.06
H4	50	m	783	1.0	0.03 | 0.06
H5	62	f	853	0.9	0.02 | 0.08
H6	69	m	832	1.1	0.03 | 0.05
H7	53	m	899	1.1	0.03 | 0.06
H8	56	m	779	1.1	0.03 | 0.06
Average	*59*	-	*821*	*1.0*	*0.03 | 0.06*

doi:10.1371/journal.pone.0078373.t001

The aim of our study was to determine the *in vivo* contact forces in hip implants during walking, plus the moments caused by friction, and derive the coefficient of friction from these data. These data will help to understand the *in vivo* lubrication conditions and allow validating, potentially improving the conditions applied in joint simulators.

Methods

Ethic statement

The study was approved by the Charité Ethics committee (EA2/057/09) and registered at the 'German Clinical Trials Register' (DRKS00000563). All patients gave written informed consent prior to participating in this study.

Subjects and measurements

Eight subjects with instrumented hip joint prostheses (Table 1) participate in this study. Measurements were taken 3 months postoperatively (pOP) during level walking at a self-selected walking speed. Selected trials of each investigated subject are also shown and can be downloaded at the public data base www.OrthoLoad.com.

Measuring equipment

Joint forces and friction moments were measured *in vivo* with instrumented hip implants. The prosthesis (CTW, Merete Medical, Berlin, Germany) has a titanium stem, a 32 mm Al_2O_3 ceramic head (BIOLOX forte, CeramTec GmbH, Plochingen, Germany) and an XPE inlay (Durasul, Zimmer GmbH, Winterthur, Switzerland). A telemetry circuit, 6 strain gauges, and a secondary induction coil are placed in the hollow neck, which is closed by welding. A detailed description of the instrumented implant was published previously [23]. A coil around the hip joint inductively powers the inner electronics. The strain gauge signals are transferred via an antenna in the implant head to the external receiver. These signals and the subject's movements are recorded simultaneously on videotape. The external measurement system has previously been described in detail [24,25].

From the 6 strain gauge signals, the 3 force and 3 moment components acting on the implant head are calculated [26] with an accuracy of 1–2%. The femur-based coordinate system [27] is fixed in the center of the head of a right sided implant, but is defined relative to the bone. Data from left implants were mirrored to the right side. The positive force components F_x, F_y, and F_z act in lateral, anterior, and superior directions, respectively (Figure 1A). From the 3 force components the resultant contact force F_{res} is calculated. The measured friction moments M_x, M_y, and M_z, act clockwise around the positive axes. The 3 moment components deliver the resultant friction moment M_{res}. Positive/negative moments M_x are caused by extension/flexion of the joint. Positive/negative moments M_y act during abduction/adduction. Positive/negative moments M_z are caused by external/internal rotation.

Data evaluation

All forces are reported as percent of bodyweight (% BW) and the friction moments as % BWm. Average force-time patterns

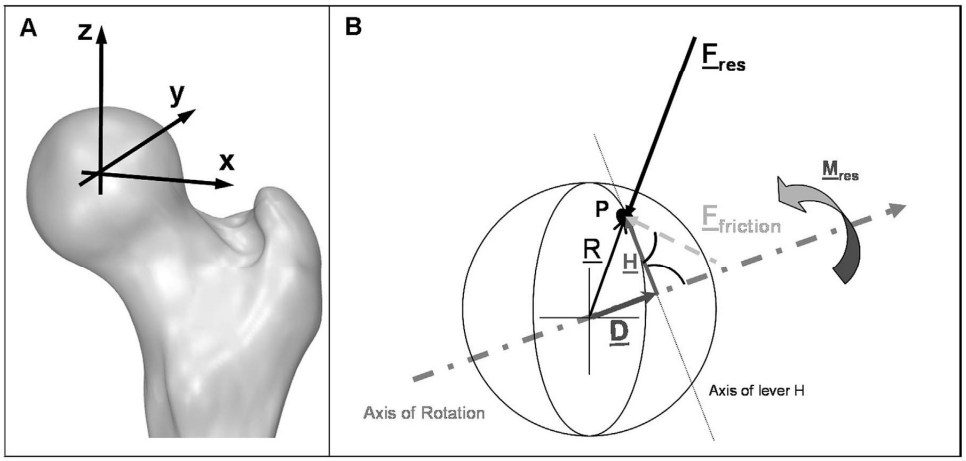

Figure 1. Coordinate system and vectors for calculation of the coefficient of friction μ. Right joint, posterior view.
doi:10.1371/journal.pone.0078373.g001

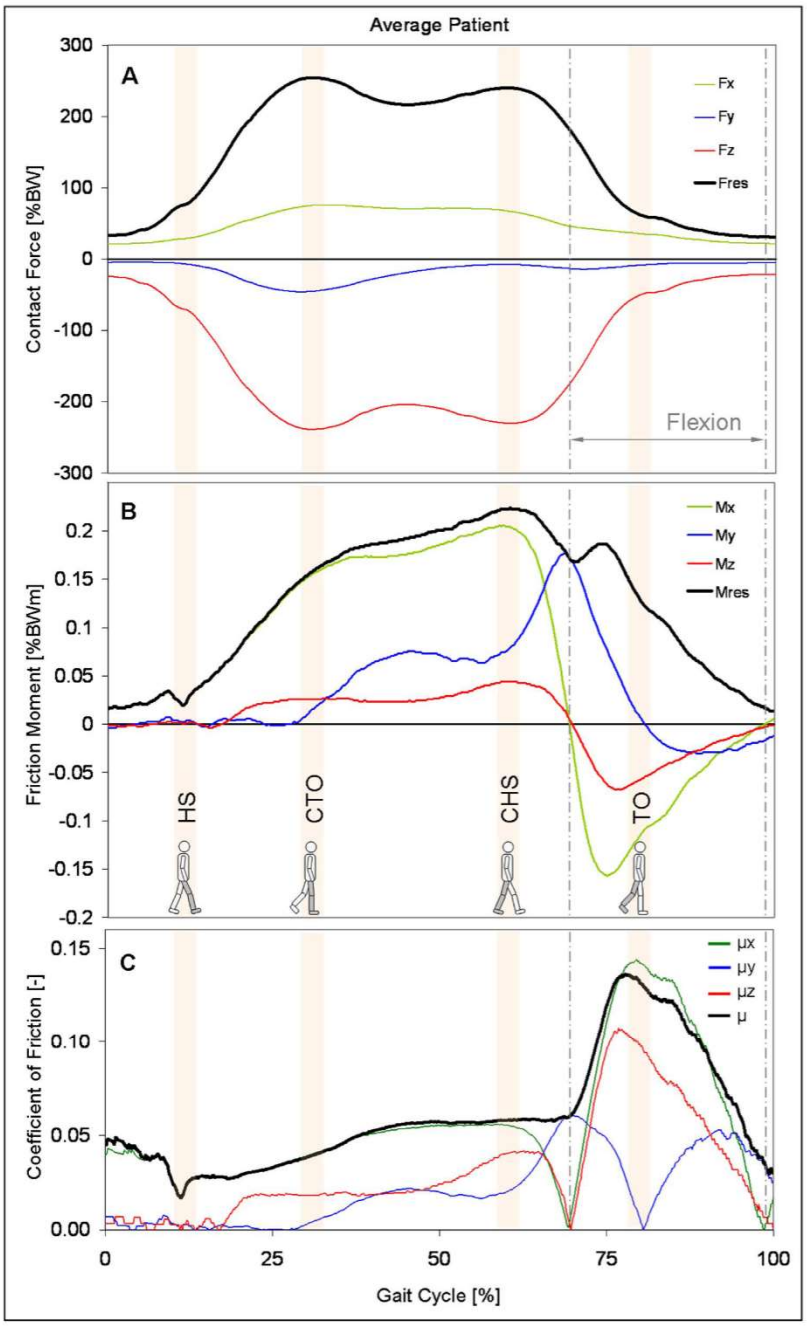

Figure 2. Time courses of contact force, friction moment, and coefficient of friction. Top: contact force F_{res} and its components. Middle: friction moment M_{res} and its components. Bottom: coefficients of friction.μ from 3D calculation; μ_x (sagittal plane), μ_y (frontal plane), and μ_z (horizontal plane) from simplified 2D calculations. The data presented are for an average subject during level walking at approximately 1 m/s. Vertical lines: borders of the flexion phase. The diagram starts before heel strike.
doi:10.1371/journal.pone.0078373.g002

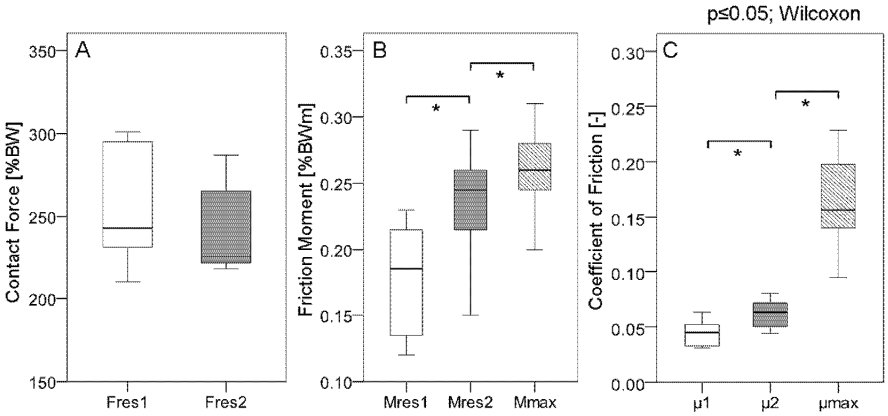

Figure 3. Peak values of contact force, friction moment and coefficient of friction. A: contact force F_{res}, B: friction moment M_{res}, C: coefficient of friction μ. Individual numerical mean values and ranges from 8 subjects. $M_{res1}|M_{res2}$, $\mu_1|\mu_2$ = values at the instant of the force maxima $F_{res1}|F_{res2}$ (see Figure 2). M_{max}, μ_{max} = absolute maxima during a whole walking cycle.
doi:10.1371/journal.pone.0078373.g003

from 32–96 steps were calculated for each subject. The employed 'time warping' method [28] weighted the congruency of high forces more than that of lower ones. First the period times of all the included steps are normalized. The single time scales were then distorted in such a way that the squared differences between all deformed curves, summed over the whole cycle time, were smallest. Finally, an arithmetically averaged load-time pattern was calculated from all the deformed curves. Using these algorithms, an average time course was first calculated from the time patterns of the resultant joint forces F_{res}. The obtained time deformations of the single trials were then transferred to the corresponding force and moment components before averaging them, too. The resultant friction moment M_{res} was calculated from an average of its components.

This procedure was first applied on all trials of the single subjects, leading to 'individual' averages. These averages from all subjects were then combined to a 'general' average, which describes the loads acting in an 'average' subject.

In some cases, peak values were not taken from the averaged time courses, but instead, the numerical peak values of the *single* trials were averaged, first individually and then inter-individually. Extreme values of the averaged load-time patterns can slightly deviate from these numerically averaged numbers. These values of the average subject were statistically analysed ($p \leq 0.05$; Wilcoxon).

Coefficient of friction

The coefficient of friction μ between the head and the cup was calculated by a 3D approach (Figure 1B). Joint movement takes place in a plane perpendicular to the axis of the vector $\underline{M}_{res}$. This axis is not perpendicular to the axis of vector $\underline{F}_{res}$. The vector of the friction force $\underline{F}_{friction}$ acts perpendicular to $\underline{F}_{res}$ at point P on the head. $\underline{H}$ is the vector of the lever arm between $\underline{F}_{Friction}$ and the axis of $\underline{M}_{res}$ and is perpendicular to both. $\underline{D}$ is a vector in direction of $\underline{M}_{res}$. $\underline{R}$ = 16 mm is the radius vector to point P.

Assuming a Coulomb friction between the head and the cup, the friction force acting on the head is

$$F_{friction} = \mu * F_{res} \quad (1)$$

The moment determined by the force $\underline{F}_{friction}$ and its lever arm $\underline{H}$ has to counteract $\underline{M}_{res}$. Because $\underline{F}_{friction}$ and $\underline{H}$ are perpendicular to each other, this delivers the scalar equation

$$H * F_{friction} = M_{res} \quad (2)$$

From the combination of (1) and (2), the following equation can be derived:

$$\mu = M_{res}/(H * F_{res}) \quad (3)$$

$\underline{R}$ is the radius of the head. R points to P and has the direction opposite to $\underline{F}_{res}$:

$$\underline{R} = -R * \underline{F}_{res}/F_{res} \quad (4)$$

$\underline{H}$ can be substituted by

$$\underline{H} = \underline{R} - \underline{D} \quad (5)$$

With $\underline{D}$ being the orthogonal projection of $\underline{R}$ on $\underline{M}_{res}$:

$$\underline{D} = R * \cos(\underline{R},\underline{M}_{res}) * \underline{M}_{res}/M_{res} \quad (6)$$

The angle between $\underline{R}$ and $\underline{M}_{res}$ can be derived from their scalar product:

$$\cos(\underline{R},\underline{M}_{res}) = (\underline{R} * \underline{M}_{res})/(R * M_{res}) \quad (7)$$

Applying (4), (6), (7), equation (5) becomes

$$\underline{H} = R * (\underline{F}_{res}/F_{res}) * [(\underline{M}_{res}/M_{res})^2 - 1] \quad (8)$$

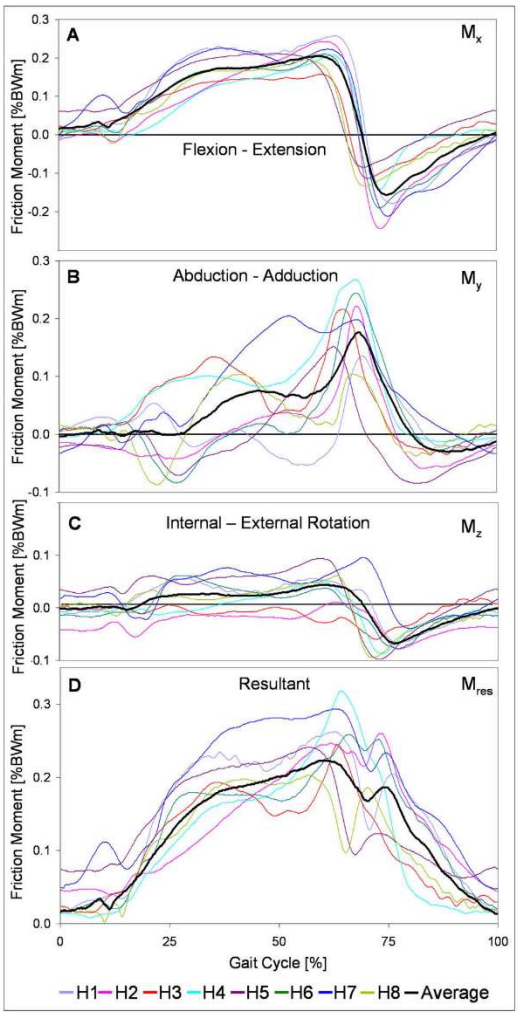

Figure 4. Components of friction moment. Components M_x, M_y, M_z around x, y, z axes (see Figure 1). Individually averaged patterns of subjects H1 to H8 (color), and average patterns of all subjects (black). doi:10.1371/journal.pone.0078373.g004

The friction coefficient μ is determined from (3), using the measured load vectors $\underline{F}_{res}$ and $\underline{M}_{res}$, the known head radius R, and the lever arm H, which is calculated by (8). Due to measuring errors, μ will be inaccurate if $\underline{F}_{res}$ or $\underline{M}_{res}$ is very small. Therefore, μ was only determined for $F_{res} \geq 20\%$ BW *and* $M_{res} \geq 0.02\%$ BWm.

In previous simulator tests, μ has mostly been determined in the sagittal plane. To compare our 3D-derived values with this data, we additionally calculated μ from the forces and moments measured in the sagittal, frontal, and horizontal planes as follows:

$$\mu_x = M_x/(F_{yz} * R) \quad (9a)$$

$$\mu_y = M_y/(F_{xz} * R) \quad (9b)$$

$$\mu_z = M_z/(F_{xy} * R) \quad (9c)$$

F_{yz}, F_{xz} and F_{xy} are the forces in the sagittal, frontal, and horizontal planes, respectively.

Friction-induced power

In addition to the measured joint loads and the calculated friction coefficient μ, we determined the friction-induced power Q in the joint, which is caused by the friction force $F_{friction}$. With v being the gliding speed between head and cup, Q is given by the simplified equation

$$Q = F_{friction} * v = F_{res} * \mu * v \quad (10)$$

Average values of Q were calculated separately for the extension and flexion phases of the gait cycle:

$$Q_{ext} = F_{ext} * \mu_{ext} * v_{ext} \quad (11a)$$

$$Q_{flex} = F_{flex} * \mu_{flex} * v_{flex} \quad (11b)$$

The average power Q_{aver} over the *whole* gait cycle was then determined from

$$Q_{aver} = (Q_{ext} * T_{ext} + Q_{flex} * T_{flex})/(T_{ext} + T_{flex}) \quad (11c)$$

Calculations were based on the intra-individually averaged load-time patterns of the single subjects. Before F_{ext}, μ_{ext}, F_{flex}, and μ_{flex} were inserted in (11a, b), their time-dependent values were averaged arithmetically over the corresponding time periods T_{ext} and T_{flex}. The speed v was determined from the flexion/extension range of the shank in the sagittal plane, the times of flexion and extension, and the radius of the prosthetic head. The data of 4–7 steps per subject were averaged. Because no gait analyses had been performed, the shank movement had to be determined from the patient videos. The Intra-observer variation of v and therefore Q was on average 1%, the inter-observer variability of four investigators was on average 2%.

Results

Unless stated otherwise, the values reported here were taken from the time patterns of the average subject. The notation "X|Y" indicates a value of X at the instant of the first peak F_{res1} of the resultant force and a value of Y at the second peak F_{res2}.

Joint contact forces

Figure 2A shows the time patterns of F_{res} and its components for the average subject during one walking cycle. F_{res} was nearly identical with $-F_z$; the latter acts distally along the z-axis of the femur and compresses the hip joint. F_{res} had 2 peak values $F_{res1}|F_{res2}$. F_{res1} acted at about the time of contralateral toe off (CTO) and F_{res2} close to contralateral heel strike (CHS).

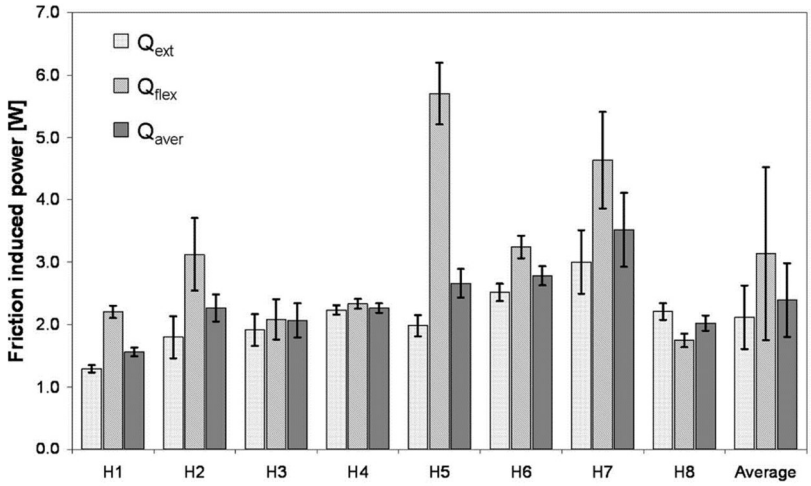

Figure 5. Average friction-induced power Q during flexion and extension phases and whole walking cycle. Q_{ext} = Q during extension phase; Q_{flex} = Q during flexion phase; Q_{aver} = Q during whole step; Individual values of subjects H1 to H8 and averages (right columns).
doi:10.1371/journal.pone.0078373.g005

Figure 3A contains individual numerical averages of the 8 subjects. For $F_{res1}|F_{res2}$ peak values of 248|233% BW at 31|57% of the gait cycle were determined. However, these peak forces varied widely inter-individually. F_{res1} ranged from 210% BW (subject H3) to 301% BW (H8), and F_{res2} from 218% BW (H3) to 287% BW (H8). In 6 subjects F_{res1} was higher than F_{res2}, but in H2 and H3 F_{res1} was lower than F_{res2}. The peak forces during the repeated trials of the same subject had standard deviations in the ranges of 7–14% BW (F_{res1}) and 5–14% BW (F_{res2}).

Friction moments

Figure 2B shows the time courses of M_{res} and its components. M_{res} increased from heel strike (HS) to CHS and reached values of $M_{res1}|M_{res2}$ = 0.16|0.21% BWm. The maximum M_{max} = 0.22% BWm acted slightly later than the force maximum F_{res2}. M_{res} climbed to a second, smaller peak of 0.19% BWm, which acted 15% of the cycle time after CHS, but before toe off of the ipsilateral leg (TO). During the intermediate minimum between CHS and TO, the joint rotation changed from extension to flexion. From HS to CHS, M_{res} was predominantly determined by component M_x, which acts in the sagittal plane of movement. After that and until the end of the stance phase the absolute values of M_y in the frontal plane exceeded those of M_x.

The patterns and magnitudes of M_x were relatively uniform for all 8 subjects (Figure 4A). On average the maximum of M_y had nearly the same magnitude as that of M_x (Figure 4B). The individual maxima of M_y (second peak value in subject H7) acted at very similar times. However, the variation of the individual maxima was much larger compared to M_x. Especially during the first half of the stance phase the time courses of M_y individually varied greatly. On average the peak value of the moment M_z was about ¼ of that of M_x or M_y (Figure 4C). The individual time courses of M_z were similar, but the magnitudes varied considerably.

Figure 3B shows the averages and ranges of the peak values of M_{res} at the times of $F_{res1}|F_{res2}$. $M_{res1}|M_{res2}$ individually varied extremely with inter-trial standard deviations of 0.01 to 0.03% BW for both peak moments M_{res1} and M_{res2}. M_{res1} ranged from 0.12% BWm (H2) to 0.23% BWm (H1), while M_{res2} lay between 0.15% BWm (H3) and 0.29% BWm (H7). In 7 subjects M_{res} increased between the times of F_{res1} and F_{res2} (Figure 4D), with peak values of M_{max} between 0.2% BWm (H8) and 0.32% BWm (H4); it decreased only in H3, but increased again after the time of F_{res2}. In 5 subjects M_{max} occurred with a time delay after F_{res2} between 6% (H4) and 16% (H2) of the gait cycle; in 1 patient M_{max} occurred 2% before F_{res2} (H7), and in 2 subjects, no time delay was observed (H5 and H8). The individual inter-trial standard deviations of M_{max} lay between 0.01 and 0.03% BWm.

Friction coefficients

At HS μ was the lowest with an average value of $\mu = 0.02$ (Figure 2C) and then increased nearly linearly. The values at the times of $F_{res1}|F_{res2}$ were $\mu_1|\mu_2 = 0.04|0.06$. After the instant when the joint rotation changed from extension to flexion, μ rose dramatically and reached its maximum μ_{max} = 0.14, shortly before TO.

The individual numerical values of μ at the instants of $F_{res1}|F_{res2}$ varied by a factor of 2 (Figure 3B); μ_1 had values between 0.03 (lowest in H2, H4, H8) and 0.06 (highest in H3); μ_2 varied between 0.04 (H3, H8) and 0.08 (H7). The maxima μ_{max}, which occurred shortly before TO, varied more, with values between 0.09 (H8) and 0.23 (H2).

The average patterns of the coefficients μ_x, μ_y, μ_z, calculated by the two-dimensional approaches, changed throughout the whole gait cycle (Figure 2C). μ_x in the main plane of movement corresponded well to μ (3D) throughout most of the loading cycle. However, shortly before and after joint rotation changed from extension to flexion, μ_x fell to zero. During the flexion phase, especially at its end, μ_x also deviated from μ. A temporary decline similar to μ_x was also observed for μ_z in the plane of femur rotation, when joint movement changed from extension to flexion. At the same time μ_y in the abduction-adduction plane reached a maximum.

Friction-induced power

With Q_{flex} = 5.0 W, the highest friction-induced power was observed in subjects H5 and H7 during the flexion phase (Figure 5),

although F_{res} and M_{res} were very small (Figure 2A) during most of this period. In 7 of the 8 subjects, Q_{flex} was higher than Q_{ext}, which was mainly due to the higher values of μ and v during flexion (equation 11a, b). The individual differences between Q_{flex} and Q_{ext} varied considerably (Figure 5). The greatest difference was calculated for H5, in which Q_{Flex} was 2.9 times higher than Q_{ext}. The smallest difference was 4%, observed in H4. In H8, Q_{flex} was 21% lower than Q_{ext}. The inter-individual average power throughout the whole cycle was $Q_{aver} = 2.3$ W, with a range between 1.4 W (H1) and 3.8 W (H7). The average sliding speed during flexion was 2.2 times higher than during extension (Table 1), with individual values between 1.5 (H8) and 4.5 (H5).

Discussion

This study reports for the first time on the assessment of *in vivo* friction in artificial hip joints during walking. The *in vivo* measured friction moment, at 3 month post-operative, increased during every gait cycle and as a consequence the coefficient of friction.

Forces and friction moments

Different *in vitro* test conditions were applied by others when investigating friction in hip joint prostheses. Several studies investigated friction by moving the joint in one plane like a pendulum [18,19,29,30], simulating flexion/extension, and neglected movement around the other 2 axes. Our results show that these test conditions may be much too simplified. In reality the abduction-adduction moment M_y rises to nearly the same peak value (0.18% BWm) as the flexion-extension moment M_x (0.2% BWm). Additionally, the joint contact force is not sinusoidal. It may affect the re-formation of a lubricating film during the swing phase when applying a sinus-load.

The resultant moment M_{res} shows a different time-course than the resultant force F_{res} (Figure 2A, B). Although the second force maximum is slightly lower than the first one, the moment is much higher at the instant of the second force peak. This is because friction continuously increases during the extension phase of walking (Figure 2C). The additional peak in the moment curve, shortly before TO, is caused by the sharp increase of the moments M_x and M_z when the hip begins to flex (see below). This finding stands in contrast to *in vitro* findings [18,30], which are based on movements in only one plane. In these studies, the moment showed a plateau phase.

Micro-separation during the swing phase, as reported by others [31,32], can alter the lubrication conditions in the joint. This effect was never observed in our subjects, investigated now and in the past. Otherwise fast changes in the directions of F_{res} or one of its components would have been observed.

Coefficient of friction

The coefficient μ increases by 46% from HS to the instant when the joint starts to flex (Figure 2C). Directly after the change of joint movement from extension to flexion, μ rose sharply in all subjects and reached its maximum at about TO, when the resultant force has markedly been fallen already. This effect has not been described previously in such detail.

It must be assumed that the synovia is squeezed out by the high forces during the extension. *In vitro* studies reported that μ increases when the sliding properties change from lubricated to dry [17,21,22,35]. Furthermore numerical studies with hard/hard pairings have shown that the thickness of the fluid film changes in relation to the joint loading during the gait cycle [30,34]. It was shown that the fluid film thickness decreases at the end of the swing phase, and therefore μ and wear rise, if the swing phase load is increased [30]. A higher swing phase load prevents or restrains the re-formation of the lubrication film, required for good lubrication during the subsequent stance phase. If this explanation also holds true for the investigated ceramic/polyethylene combination of head/cup, a higher swing phase load would let μ decrease less sharply after TO and thus raise the level at which μ starts at the next HS.

Moreover, the strong increase of μ when the joint starts to flex could possibly be caused by a breakdown of the fluid film at the temporary stop of the relative joint movement, similar to the *in vitro* observation during the first step after a rest [33].

Another factor influencing the time pattern of μ may be a changing size of the load bearing area between head and cup, perpendicular to the resultant force vector. This could be especially true if μ were dependent on the pressure magnitude. Both factors could not be investigated in this study.

In contrast to previous *in vitro* studies, the *in vivo* coefficient of friction was now determined for the 3D case. The obtained pattern of μ differs from the pattern of μ_x in the main movement plane of the femur. Both coefficients are nearly identical from HS to CHS and deviate by no more than 5%. However, during the flexion phase, the difference between both coefficients increased up to 9% at TO.

Studies with a simple pendulum test determined values of μ_x between 0.04 and 0.09 for a lubricated regime [18,36,37]. This compares well with our finding of $\mu_1 = 0.04$ and $\mu_2 = 0.06$ during the extension phase. However, $\mu_{max} = 0.14$ at the instant of toe off was much higher in our study.

The peak values of F_{res} individually varied by 39%, but the peak values of μ differed by 246% (Figure 3C). The variance of μ is most likely due to individually different lubrication properties of the synovia fluid.

Friction-induced power

The friction-induced temperature rise in ceramic/PE implants has been measured *in vivo* previously [10]. An estimated average friction-induced power of 0.79 W during walking was reported, which is much less than the average of 2.3 W determined in the current study. It may be that heat convection by the blood flow has been underestimated in the previous study. Other reasons for this discrepancy may be differences between the subjects investigated, and the small sizes of both cohorts. This assumption is supported by another result of the cited study, namely that the temperature increase, measured after 1 hour of walking, individually varied by a factor of nearly 3 after the body weight of all subjects had been standardized. A similarly large factor of 2.7 was observed for the friction-induced power Q_{aver}, which decreased to 2.3 after normalizing the body weight.

The large individual differences of Q_{aver} are most likely caused by varying synovia properties, as already indicated by the variations of μ. Additionally, different running-in effects of the gliding partners may affect the friction-induced power. This running-in effect and the expected decrease of μ and Q_{aver} with increased postoperative time will be investigated in a future study.

In conclusion it was shown: The friction moment in the hip joint mainly occurred in the frontal and sagittal plane during walking. The resultant coefficient of friction increased nearly linearly during extension and increased drastically in the beginning of flexion with the maximum value approximately the ipsilateral toe off. This suggests that the synovia is squeezed out of the intra-articular joint space. Furthermore, the peak values of the coefficient of friction were always determined during the flexion phase. This indicates that the lubrication regime certainly changed into a dry phase at every step.

Limitations of the study

There are some limitations to this study: the number of investigated subjects was small; they were younger than the majority of hip-replacement patients; and only one implant type was investigated at only one speed of walking and one time after implantation. However, the large individual variations of friction coefficient and generated power, as well as the changes of the friction coefficient throughout the gait cycle will probably not be much influenced qualitatively by age or materials. The effects of walking speed and postoperative time is currently investigated an additional study.

Acknowledgments

The authors gratefully acknowledge the voluntary collaboration of all subjects.

Author Contributions

Conceived and designed the experiments: PD GB. Performed the experiments: PD JD. Analyzed the data: PD RA. Contributed reagents/materials/analysis tools: PD AB FG AH AB. Wrote the paper: PD GB.

References

1. CJRR (2013) CJRR annual report: Hip and knee replacements in Canada. Canadian Institute for Health Information.
2. Havelin LI, Fenstad AM, Salomonsson R, Mehnert F, Furnes O, et al. (2009) The Nordic Arthroplasty Register Association: a unique collaboration between 3 national hip arthroplasty registries with 280,201 THRs. Acta orthopaedica 80: 393 401. doi:10.3109/17453670903039544.
3. AOA (2007) Australian Orthopaedic Association National Joint Replacement Registry. Annual Report 2007.
4. Huch K, Müller KAC, Stürmer T, Brenner H, Puhl W, et al. (2005) Sports activities 5 years after total knee or hip arthroplasty: the Ulm Osteoarthritis Study. Annals of the Rheumatic Diseases 64: 1715 1720. doi:10.1136/ard.2004.033266.
5. Chatterji U, Ashworth MJ, Lewis PL, Dobson PJ (2004) Effect of total hip arthroplasty on recreational and sporting activity. ANZ journal of surgery 74: 446 449.
6. Flugsrud GB, Nordsletten L, Espehaug B, Havelin LI, Meyer HE (2007) The effect of middle-age body weight and physical activity on the risk of early revision hip arthroplasty. Acta Orthopaedica 78: 99 107. doi:10.1080/17453670610013493.
7. Malchau H, Herberts P, Söderman P, Odén A (2000) Prognosis of Total Hip Replacement. The swedish national hip arthroplasty registry.
8. Bergmann G, Deuretzbacher G, Heller M, Graichen F, Rohlmann A, et al. (2001) Hip contact forces and gait patterns from routine activities. Journal of biomechanics 34: 859 871.
9. Bergmann G, Graichen F, Rohlmann A (1993) Hip joint loading during walking and running, measured in two patients. Journal of biomechanics 26: 969 990.
10. Bergmann G, Graichen F, Rohlmann A, Verdonschot N, Van Lenthe GH (2001) Frictional heating of total hip implants. Part 2: finite element study. Journal of biomechanics 34: 429 435.
11. Bergmann G, Graichen F, Rohlmann A, Verdonschot N, Van Lenthe GH (2001) Frictional heating of total hip implants. Part 2: finite element study. Journal of biomechanics 34: 429 435.
12. Li S, Chien S, Branemark P-I (1999) Heat shock-induced necrosis and apoptosis in osteoblasts. Journal of orthopaedic research 17: 891 899. doi:10.1002/jor.1100170614.
13. Hall RM, Unsworth A (1997) Review Friction in hip prostheses. Biomaterials 18: 1017 1026.
14. Mattei L, Di Puccio F, Piccigallo B, Ciulli E (2011) Lubrication and wear modelling of artificial hip joints: A review. Tribology International 44: 532 549. doi:10.1016/j.triboint.2010.06.010.
15. Xiong D, Ge S (2001) Friction and wear properties of UHMWPE/Al2O3 ceramic under different lubricating conditions. 250: 242 245.
16. Bergmann G, Graichen F, Rohlmann A, Bender A, Heinlein B, et al. (2010) Realistic loads for testing hip implants. Bio-medical materials and engineering 20: 65 75. doi:10.3233/BME-2010-0616.
17. Bishop NE, Hothan A, Morlock MM (2012) High Friction Moments in Large Hard-on-Hard Hip Replacement Bearings in Conditions of Poor Lubrication. Journal of Orthopaedic Research: 1 7. doi:10.1002/jor.22255.
18. Brockett C, Williams S, Jin Z, Isaac G, Fisher J (2006) Friction of Total Hip Replacements With Different Bearings and Loading Conditions. Journal of Biomedical Materials Research: 508 515. doi:10.1002/jbmb.
19. Scholes SC, Unsworth A, Goldsmith AAJ (2000) A frictional study of total hip joint replacements. Physics in medicine and biology 45: 3721 3735.
20. Scholes SC, Unsworth A, Hall RM, Scott R (2000) The effects of material combination and lubricant on the friction of total hip prostheses. Wear 241: 209 213. doi:10.1016/S0043-1648(00)00377-X.
21. Unsworth A (1978) The effects of lubrication in hip joint prostheses. Physics in medicine and biology 23: 253 268.
22. Scholes SC, Unsworth A (2000) Comparison of friction and lubrication of different hip prostheses. Proceedings of the Institution of Mechanical Engineers Part H Journal of engineering in medicine 214: 49 57.
23. Damm P, Graichen F, Rohlmann, Bender A, Bergmann G (2010) Total hip joint prosthesis for in vivo measurement of forces and moments. Medical Engineering & Physics 32: 95 100.
24. Graichen F, Arnold R, Rohlmann, Bergmann G (2007) Implantable 9-channel telemetry system for in vivo load measurements with orthopedic implants. IEEE transactions on bio-medical engineering 54: 253 261. doi:10.1109/TBME.2006.886857.
25. Graichen F, Bergmann G, Rohlmann (1994) Telemetric transmission system for in vivo measurement of the stress load of an internal spinal fixator. Biomedizinische Technik Biomedical engineering 39: 251 258.
26. Bergmann G, Graichen F, Rohlmann A, Westerhoff P, Heinlein B, et al. (2008) Design and calibration of load sensing orthopaedic implants. Journal of biomechanical engineering 130: 021009. doi:10.1115/1.2898831.
27. Wu G, Siegler S, Allard P, Kirtley C, Leardini A, et al. (2002) ISB recommendation on definitions of joint coordinate system of various joints for the reporting of human motion part I: ankle, hip, and spine. Journal of Biomechanics 35: 543 548. doi:10.1016/j.pathophys.2011.08.001.
28. Bender A, Bergmann G (2011) Determination of Typical Patterns from Strongly Varying Signals. Computer Methods in Biomechanics and Biomedical Engineering iFirst: 1 9. doi:10.1080/10255842.2011.560841.
29. Saikko V (1992) A simulator study of friction in total replacement hip joints. Proceedings of the Institution of Mechanical Engineers Part H Journal of engineering in medicine 206: 201 211.
30. Williams S, Jalali-Vahid D, Brockett C, Jin Z, Stone MH, et al. (2006) Effect of swing phase load on metal-on-metal hip lubrication, friction and wear. Journal of biomechanics 39: 2274 2281. doi:10.1016/j.jbiomech.2005.07.011.
31. Blumenfeld TJ, Glaser DA, Bargar WL, Langston GD, Mahfouz MR, et al. (2011) In vivo assessment of total hip femoral head seperation from the acetabular cup during 4 common daily activities. Orthopedics 34: e127 e132. doi:10.3928/01477447-20110427-06.
32. Dennis D, Komistek RD, Northcut EJ, Ochoa J, Ritchie A (2001) In vivo determination of hip joint separation and the forces generated due to impact loading conditions. Journal of biomechanics 34: 623 629.
33. Morlock M, Nassutt R, Wimmer M, Schneider E (2000) Influence of Resting Periods on Friction in Artificial Hip Joint Articulations. Bone: 6 16.
34. Meyer DM, Tichy JA (2003) 3-D Model of a Total Hip Replacement In Vivo Providing Hydrodynamic Pressure and Film Thickness for Walking and Bicycling. Journal of Biomechanical Engineering 125: 777. doi:10.1115/1.1631585.
35. Hall RM, Unsworth A, Wroblewski BM, Siney P, Powell NJ (1997) The friction of explanted hip prostheses. British journal of rheumatology 36: 20 26.
36. Hall RM, Unsworth A (1997) Friction in hip prostheses. Biomaterials 18: 1017 1026.
37. Jin Z, Stone M, Ingham E, Fisher J (2006) (v) Biotribology. Current Orthopaedics 20: 32 40. doi:10.1016/j.cuor.2005.09.005.

2.2. Änderung der Gelenkreibung im postoperativen Verlauf

Die drei Monate postoperativ in vivo gemessenen Gelenkbelastungen beim Gehen haben gezeigt, dass insbesondere die Gelenkreibung interindividuell bereits in der frühen postoperativen Phase stark variiert. Darüber hinaus konnte gezeigt werden, dass die Gelenkreibung beim Gehen während der Extensionsphase in vivo zwar vergleichbar ist, sich aber während der Flexionsphase deutlich von in vitro ermittelten Reibdaten unterscheidet (Affatato et al. 2008; Brockett et al. 2006; Fialho et al. 2007; Hall and Unsworth 1997; Liao 2003; Mattei et al. 2011; Saikko 1992; Scholes, Unsworth, Hall, et al. 2000; Scholes and Unsworth 2000, 2006; Unsworth 1978; Williams et al. 2006). Aufgrund dessen stellten wir die Hypothese auf, dass die Gelenkreibung in vivo zum einen durch individuelle und aktivitätsabhängige ‚Einlauf-Effekte', aber auch durch die individuellen Schmiereigenschaften der Synovia bedingt wird (Balazs 1974; Fam et al. 2007; Hall and Unsworth 1997; Scholes and Unsworth 2000). Im Verlauf von drei zu 12 Monaten postoperativ wurden daher weitere in-vivo-Belastungsmessungen beim Gehen mit den Studienpatienten durchgeführt. Primäres Ziel dieser Messungen war es, potenzielle postoperative Änderungen der Gelenkkontaktkräfte und resultierenden Gelenkreibung beim kontinuierlichen Gehen systematisch zu untersuchen. Es konnte gezeigt werden, dass sich die Gelenkkontaktkraft im weiteren postoperativen Verlauf nicht signifikant verändert. Im Vergleich dazu wurde jedoch eine signifikante Reduktion des in vivo wirkenden Reibmomentes beobachtet, jedoch wiederum mit großen interindividuellen Unterschieden. Der nachfolgende Text entspricht dem Abstract der Arbeit *„Postoperative changes in in vivo measured friction in total hip joint prosthesis during walking"*, welche im Journal PLoS ONE 2015 veröffentlicht wurde:

"Loosening of the artificial cup and inlay is the most common reasons for total hip replacement failures. Polyethylene wear and aseptic loosening are frequent reasons. Furthermore, over the past few decades, the population of patients receiving total hip replacements has become younger and more active. Hence, a higher level of activity may include an increased risk of implant loosening as a result of friction-induced wear.

In this study, an instrumented hip implant was used to measure the contact forces and friction moments in vivo during walking. Subsequently, the three-dimensional coefficient of friction in vivo was calculated over the whole gait cycle. Measurements

were collected from ten subjects at several time points between three and twelve months postoperative.

No significant change in the average resultant contact force was observed between three and twelve months postoperative. In contrast, a significant decrease of up to 47% was observed in the friction moment. The coefficient of friction also decreased over postoperative time on average. These changes may be caused by ‘running-in’ effects of the gliding components or by the improved lubricating properties of the synovia. Because the walking velocity and contact forces were found to be nearly constant during the observed period, the decrease in friction moment suggests an increase in fluid viscosity.

The peak values of the contact force individually varied by 32%-44%. The friction moment individually differed much more, by 110%-129% at three and up to 451% at twelve months postoperative. The maximum coefficient of friction showed the highest individual variability, about 100% at three and up to 914% at twelve months after surgery. These individual variations in the friction parameters were most likely due to different ‘running-in’ effects that were influenced by the individual activity levels and synovia properties.”

Publikation: Postoperative changes in in vivo measured friction in total hip joint prosthesis during walking

Damm P., Bender A. Bergmann G.

PLoS ONE. 2015; 10(3): e0120438.; https://doi.org/10.1371/journal.pone.0120438

PLOS | ONE

RESEARCH ARTICLE

Postoperative Changes in *In Vivo* Measured Friction in Total Hip Joint Prosthesis during Walking

Philipp Damm*, Alwina Bender, Georg Bergmann

Julius Wolff Institute, Charité—Universitaetsmedizin Berlin, Berlin, Germany

* Philipp.Damm@charite.de

OPEN ACCESS

Citation: Damm P, Bender A, Bergmann G (2015) Postoperative Changes in *In Vivo* Measured Friction in Total Hip Joint Prosthesis during Walking. PLoS ONE 10(3): e0120438. doi:10.1371/journal.pone.0120438

Academic Editor: Amitava Mukherjee, VIT University, INDIA

Received: August 25, 2014

Accepted: January 22, 2015

Published: March 25, 2015

Data Availability Statement: Data are available from the Orthoload database: http://www.orthoload.com/database/. To view the data, input the following search terms: Implant: Hip Joint III; Activity: Walking; Level Walking; Parameter: none; Patient: all. Relevant video and numerical data files are named as follows: H1L_130710_1_110; H1L_151110_1_51; H2R_151110_1_184; H2R_160211_2_67; H2R_14_03_11_1_186; H3L_040211_1_83; H3L_140311_1_126; H3L_260811_1_87; H4L_250311_2_12; H4L_290411_1_149; H4L_240611_1_170; H4L_111111_2_60; H5L_040711_2_54; H5L_020911_2_8;

Abstract

Loosening of the artificial cup and inlay is the most common reasons for total hip replacement failures. Polyethylene wear and aseptic loosening are frequent reasons. Furthermore, over the past few decades, the population of patients receiving total hip replacements has become younger and more active. Hence, a higher level of activity may include an increased risk of implant loosening as a result of friction-induced wear. In this study, an instrumented hip implant was used to measure the contact forces and friction moments *in vivo* during walking. Subsequently, the three-dimensional coefficient of friction *in vivo* was calculated over the whole gait cycle. Measurements were collected from ten subjects at several time points between three and twelve months postoperative. No significant change in the average resultant contact force was observed between three and twelve months postoperative. In contrast, a significant decrease of up to 47% was observed in the friction moment. The coefficient of friction also decreased over postoperative time on average. These changes may be caused by 'running-in' effects of the gliding components or by the improved lubricating properties of the synovia. Because the walking velocity and contact forces were found to be nearly constant during the observed period, the decrease in friction moment suggests an increase in fluid viscosity. The peak values of the contact force individually varied by 32%-44%. The friction moment individually differed much more, by 110%-129% at three and up to 451% at twelve months postoperative. The maximum coefficient of friction showed the highest individual variability, about 100% at three and up to 914% at twelve months after surgery. These individual variations in the friction parameters were most likely due to different 'running-in' effects that were influenced by the individual activity levels and synovia properties.

Introduction

Loosening of the artificial cup and inlay is the most common reason for the failure of total hip replacements [1–3]. Polyethylene (PE) wear and aseptic loosening are frequent reasons for revisions of total hip joint prostheses (THP), account for 26% and 48% of all revisions,

H5L_060212_2_53; H6R_220212_1_42; H6R_200412_1_126; H6R_280912_1_89; H7R_210212_1_36; H7R_170412_1_109; H7R_130712_1_128; H8L_260712_1_57; H8L_130912_1_153; H9L_191212_1_38; H9L_180213_1_89; H10R_260413_1_81; H10R_260613_1_158; H10R_250913_1_130. Additional relevant data may be found using the following search terms: Implant: Hip Joint III; Activity: Gaitanalysis; Walking; Level Walking; Parameter: none; Patient: all. Relevant files are named as follows: H1L_060511_1_50; H2R_150811_2_98; H3L_141111_1_28; H4L_270112_2_80; H5L_050412_1_75; H6R_201112_2_107; H7R_191112_1_47; H8L_270213_2_55; H8L_240413_1_42; H9L_301013_1_62; H10R_300114_1_82.

Funding: Support was provided by the German Research Society (SFB760 and BE 804/19-1) [http://www.dfg.de] and Deutsche Arthrose-Hilfe e.V. [http://www.arthrose.de]. The funders had no role in study design, data collection and analysis, decision to publish, or preparation of the manuscript.

Competing Interests: The authors have declared that no competing interests exist.

respectively [1,4]. One study has indicated that 30% to 40% of all THP revisions require a change of cup or inlay [5], thus making friction in the joint one of the main parameters affecting the life span of total hip prostheses. THP patients have become younger and more active over the past few decades [6,7]. This higher level of activity has resulted in increased wear rates and, consequently, requires earlier revision of THP [8,9].

To determine the parameters of friction in THP, several *in vitro* studies under different test conditions have been published, using new or explanted prostheses and different head diameters and lubricants [10–21]. In most studies, the coefficient of friction (μ) was determined by a simple pendulum test, which showed that the friction in the THP was primarily influenced by the material of the sliding partners and the lubrication regime.

Previous studies with instrumented implants measured the contact forces in THP *in vivo* [22–26]. However, in these studies, it was not possible to determine the friction within the implant, with the exception of one study that reported the friction-induced temperature increase during walking [27]. In that publication, it was postulated that the temperature in the THP was mainly caused by the friction parameters between the sliding partners and the lubricating properties of the synovia. Peak temperatures up to 43°C were measured after one hour of walking. Because bone tissues may already be damaged at temperatures exceeding 43°C [28], it can be assumed that repeated high implant temperatures are a risk factor for the long-term stability of the THP.

Using a newly developed instrumented hip implant [29], we were able to measure the joint friction *in vivo* for the first time. Initial results were reported for three months postoperatively (pOP) [30], and it was shown that the *in vivo* coefficient of friction is similar to the *in vitro* value obtained during the extension phase of the hip joint. However, during the flexion phase, μ strongly differs from the *in vitro* data. The maximum *in vivo* values of μ, calculated from the contact forces and friction moments, suggest a 'dry' friction during the hip flexion phase of walking.

The aim of this study was to measure the changes of contact forces, friction moments and coefficients of friction between three and twelve months pOP. We hypothesized that μ would decline due to 'running-in' effects and that both, friction moments and μ, would show great individual variability, depending on the synovial properties.

Methods

Variables

F_{res} Resultant hip joint contact force
$\underline{F}_{res}$ Vector of F_{res}
M_{res} Resultant friction moment
$\underline{M}_{res}$ Vector of M_{res}
$F_{Friction}$ Friction force
$\underline{F}_{Friction}$ Vector of $F_{Friction}$
R Radius of implant head (16 mm)
$\underline{R}$ Vector from origin of coordinates to contact point P
$\underline{D}$ Vector from origin of coordinates to vector H
$\underline{H}$ Vector vertical to $\underline{M}_{res}$, pointing to P
μ Coefficient of friction
HS Ipsilateral heel strike
CTO Contralateral toe off
CHS Contralateral heel strike
TO Ipsilateral toe off
XPE Cross-linked polyethylene

Measurement equipment

Joint forces and friction moments were measured *in vivo* using instrumented hip implants. The prosthesis (CTW, Merete Medical, Berlin, Germany) is based on a clinically successful implant with a titanium stem, a 32 mm Al_2O_3 ceramic head and a XPE inlay. A telemetry circuit, six-strain gauges and an induction coil are arranged in the hollow neck. The implant is powered inductively by a coil around the hip joint. The strain gauge signals are transferred to the external receiver at radio frequency via an antenna inside of the implant head [31]. The telemetric load signals and the patient movements are recorded simultaneously on video. Detailed descriptions of the implant [29] and the external measurement system [31,32] have previously been published.

Using the six strain gauge signals, the three force and three moment components acting on the implant head are calculated with an accuracy of 1–2%. The femur-based coordinate system [33] is located in the head center of a right-sided implant; data from left-sided implants are mirrored. Positive forces F_x, F_y, and F_z act in the lateral, anterior, and superior directions; the measured friction moments (M_x, M_y and M_z) turn right around the positive coordinate axes. The resultant contact force F_{res} and the resultant friction moment M_{res} are calculated from their three components. Because the force component in direction of the femoral axis always acts downwards, F_{res} points toward the center of the implant head.

Patients and measurements

The study was approved by the ethical committee (EA2/057/09) and registered with the 'German Clinical Trials Register' (DRKS00000563). Ten patients (8m/2f) with hip osteoarthritis gave written informed consent to participate in the study and have their images published (Table 1).

Measurements were taken during level walking at several time points (Table 2) between three and thirteen months pOP. Selected trials of each investigated subject are also shown and can be downloaded at the public data base www.OrthoLoad.com.

Data evaluation

All forces and moments are reported as a percentage of patient bodyweight (%BW and %BWm, respectively). Average force- and moment-time patterns were calculated separately for

Table 1. Patient data and walking speeds.

Subject pOP	Age [years]	Sex	Bodyweight [N]	Gait Velocity [m/s]	
	12 months pOP		12 months pOP	3 months pOP	12 months pOP
H1L	56	male	760	1.0	1.1
H2R	62	male	767	1.0	1.1
H3L	60	male	983	0.8	1.0
H4L	51	male	796	1.0	1.0
H5L	63	female	855	0.9	1.2
H6R	69	male	815	1.1	1.1
H7R	53	male	916	1.1	1.3
H8L	56	male	836	1.1	1.1
H9L	55	male	1197	1.1	1.2
H10R	54	female	995	0.9	1.2
Average	58	-	892	1.0	1.1

doi:10.1371/journal.pone.0120438.t001

Table 2. Number of averaged steps at postoperative months 1 to 13.

Patient	Month pOP												
	1	2	3	4	5	6	7	8	9	10	11	12	13
H1L	-	-	67	-	-	-	71	-	-	56	-	-	67
H2R	-	32	49	-	-	65	88	-	-	-	86	52	-
H3L	-	32	82	72	-	-	-	-	45	-	-	105	-
H4L	30	98	53	-	51	-	48	-	-	36	-	63	-
H5L	-	41	69	-	58	-	-	-	-	69	-	41	-
H6R	-	54	71	-	65	-	51	-	-	83	-	44	-
H7R	-	93	96	-	60	46	-	66	-	77	-	45	-
H8L	-	31	50	-	59	-	-	-	-	58	-	53	-
H9L	43	85	84	-	43	60	-	-	-	-	-	-	83
H10R	-	104	30	-	91	-	-	39	-	-	-	28	-
≈ Months pOP	"3" (3)			"6" (5 to 6)			"9" (8 to 10)				"12" (12 to 13)		
Average	10 Subjects			9 Subjects			8 Subjects				10 Subjects		

All available data were used to calculate postoperative trends in single subjects.

doi:10.1371/journal.pone.0120438.t002

each subject and measurement day using a 'time warping' method [34]. This averaging procedure was first performed on repeated trials of the single subjects. The obtained load patterns of all subjects were then averaged again, leading to data which are typical for an 'average' subject. All data were analyzed for the time points of three, six, nine and twelve months pOP (Table 2).

Unless stated otherwise, all presented data refers to the obtained 'average' subject. Because errors between the single trials were minimized over all loading cycles, the peak values of the average curves can slightly deviate from the averaged numerical values at the 1st and 2nd peak.

Changes of the measured peak values over the pOP time were analyzed for each subject separately and for the 'average' subject (Tables 3 and 4). The changes over time were analyzed individually using the Mann-Whitney-U test and across all subjects using the Wilcoxon test. Furthermore a regression analysis was performed, for each subject separately and for the average subject, to determine the correlation between the measured peak values of F_{res}, M_{res} and μ (y) and the pOP time in months (m), using the logarithmic relationship

$$y = a + b * \ln(m) \quad (1)$$

Table 3. Mean values at 3 and 12 months post operative of the 'average' subject.

value	unit	3 months		12 months	
		Mean	STD	Mean	STD
Fres1	%BW	*255*	*10*	*252*	*12*
Fres2	%BW	*238*	*9*	*245*	*8*
Mres1	%BWm	*0.174*	*0.019*	*0.107*	*0.017*
Mres2	%BWm	*0.234*	*0.020*	*0.174*	*0.020*
μ1	-	*0.045*	*0.005*	*0.028*	*0.004*
μ2	-	*0.062*	*0.005*	*0.047*	*0.005*
μmax	-	*0.175*	*0.020*	*0.179*	*0.036*

Arithmetic means and standard deviation (STD) of the contact force (F_{res}), friction moment (M_{res}) and coefficient of friction (μ).

doi:10.1371/journal.pone.0120438.t003

Table 4. Load and friction changes.

Subject	F_{res1}	$p(F_{res1})$	F_{res2}	$p(F_{res2})$	M_{res1}	$p(M_{res1})$	M_{res2}	$p(M_{res2})$	μ_1	$p(\mu_1)$	μ_2	$p(\mu_2)$	μ_{max}	$p(\mu_{max})$
H1L	6	<0.001	4	<0.001	-37	<0.001	-9	<0.001	-41	<0.001	-14	<0.001	-13	<0.001
H2R	1	0.306	8	<0.001	-72	<0.001	-36	<0.001	-72	<0.001	-44	<0.001	-15	0.029
H3L	-4	<0.001	2	<0.001	-51	<0.001	-2	<0.001	-48	<0.001	-6	<0.001	22	<0.001
H4L	4	<0.001	3	<0.001	-44	<0.001	-52	<0.001	-46	<0.001	-53	<0.001	-26	<0.001
H5L	-1	0.467	3	<0.001	-45	<0.001	-34	<0.001	-44	<0.001	-34	<0.001	-17	<0.001
H6R	5	<0.001	13	<0.001	-35	<0.001	-34	<0.001	-38	<0.001	-42	<0.001	-27	<0.001
H7R	0	0.903	6	<0.001	-38	<0.001	-28	<0.001	-36	<0.001	-32	<0.001	57	<0.001
H8L	-13	<0.001	-2	0.039	-67	<0.001	-60	<0.001	-56	<0.001	-59	<0.001	-12	<0.001
H9L	-3	<0.001	-1	0.083	-33	<0.001	-49	<0.001	-37	<0.001	-48	<0.001	-42	<0.001
H10R	-1	0.083	-8	<0.001	13	<0.001	30	<0.001	18	<0.001	48	<0.001	101	<0.001
AverageSubject H	-1	0.863	4	0.730	-47	0.004	-34	0.003	-46	0.002	-37	0.004	-8	0.605

Individual and average change [%] of peak joint contact forces, friction moments and coefficients of friction from 3 to 12 months postoperative. Arithmetic mean values were calculated without the data from subject H10R. Tests: Mann-Whitney-U. (individual subjects) respectively Wilcoxon test ('average' subject).

doi:10.1371/journal.pone.0120438.t004

The coefficient of correlation (R^2) and the residual-standard-error (RSE) were calculated and statistically analyzed with a t-test. For all statistical calculations a type-I-error level was defined with $\alpha = 0.05$.

Coefficient of friction

In the following equations, the underlined symbols are vectors; all others are scalar values. In the Coulomb approach, the friction force $F_{Friction}$ between the cup and ball is determined using the resultant contact force F_{res} and the coefficient of friction μ (Fig. 1):

$$F_{Friction} = \mu * F_{res} \quad (2)$$

The ball turns around the axis of $\underline{M}_{res}$. $\underline{H}$ is the lever arm between $\underline{F}_{Friction}$ and the axis of $\underline{M}_{res}$. Because $F_{Friction}$ counteracts the moment M_{res}, we obtain

$$M_{res} = H * F_{Friction} \quad (3)$$

(2) and (3) deliver

$$\mu = M_{res} / (H * F_{res}) \quad (4)$$

$\underline{R}$ is the radius of the ball and points in direction of $\underline{F}_{res}$:

$$\underline{R} = R * \underline{F}_{res}/F_{res} \quad (5)$$

H can be substituted by

$$\underline{H} = \underline{R} - \underline{D} \quad (6)$$

with $\underline{D}$ being the orthogonal projection of $\underline{R}$ on $\underline{M}_{res}$:

$$\underline{D} = R * \cos(\underline{R}, \underline{M}_{res}) * \underline{M}_{res}/M_{res} \quad (7)$$

Applying (5) and (7), equation (6) becomes

$$\underline{H} = R * [\underline{F}_{res}/F_{res} - \cos(\underline{R}, M_{res}) * (\underline{M}_{res}/M_{res})] \quad (8)$$

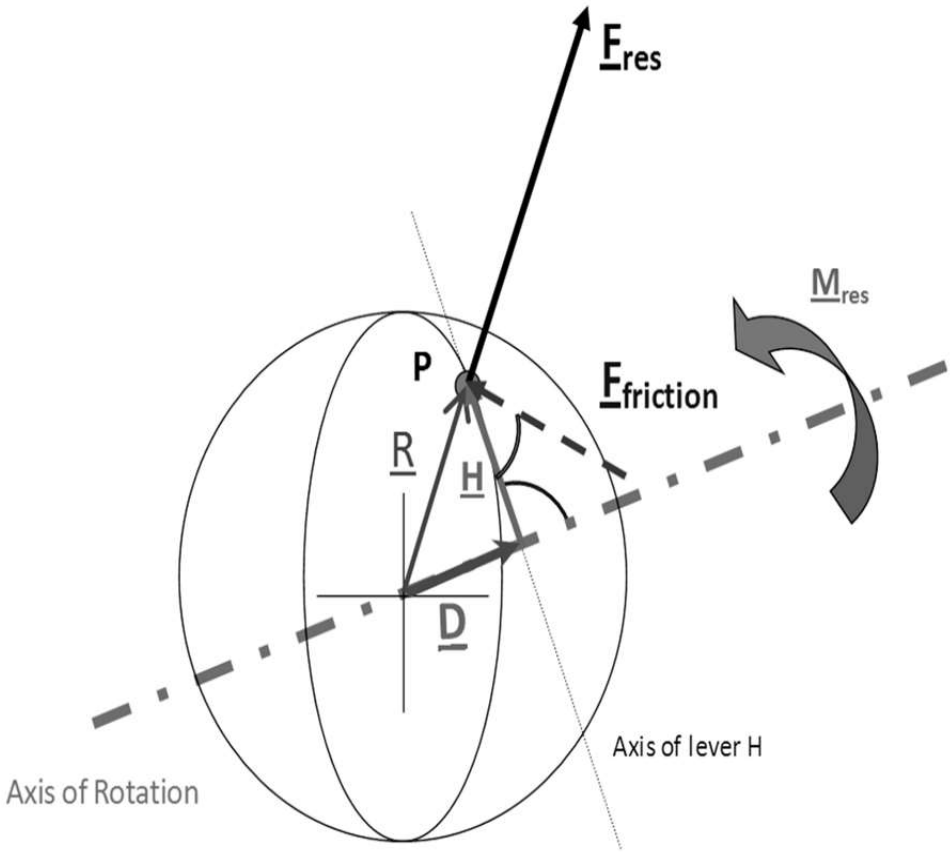

Fig 1. Model for calculating the 3D coefficient of friction μ. In reality, the component F_z is measured negatively, and the direction of F_{res} is thus towards the ball surface

doi:10.1371/journal.pone.0120438.g001

with

$$\cos(\underline{R}, \underline{M}_{res}) = \cos(\underline{F}_{res}, \underline{M}_{res}) = < \underline{F}_{res}, \underline{M}_{res} > / (F_{res} * M_{res}) \quad (9)$$

because equation (5) holds true.

To obtain μ with an accuracy of 5%, only joint forces $F_{res} \geq 25\%BW$ and moments $M_{res} \geq 0.02\%BWm$ were included in the analysis.

Gait velocity

The gait velocity was determined individually at three months pOP using the video clips, as described elsewhere [30]. At twelve months pOP, the velocity was determined individually using simultaneously measured 3D gait data (Vicon Nexus, Vicon Motion Systems Ltd., UK). The distance travelled during one walking trial was measured between the first and last HS of the ipsilateral leg for each walking trial separately. It was divided by the elapsed time and the obtained speed was subsequently averaged over all trials.

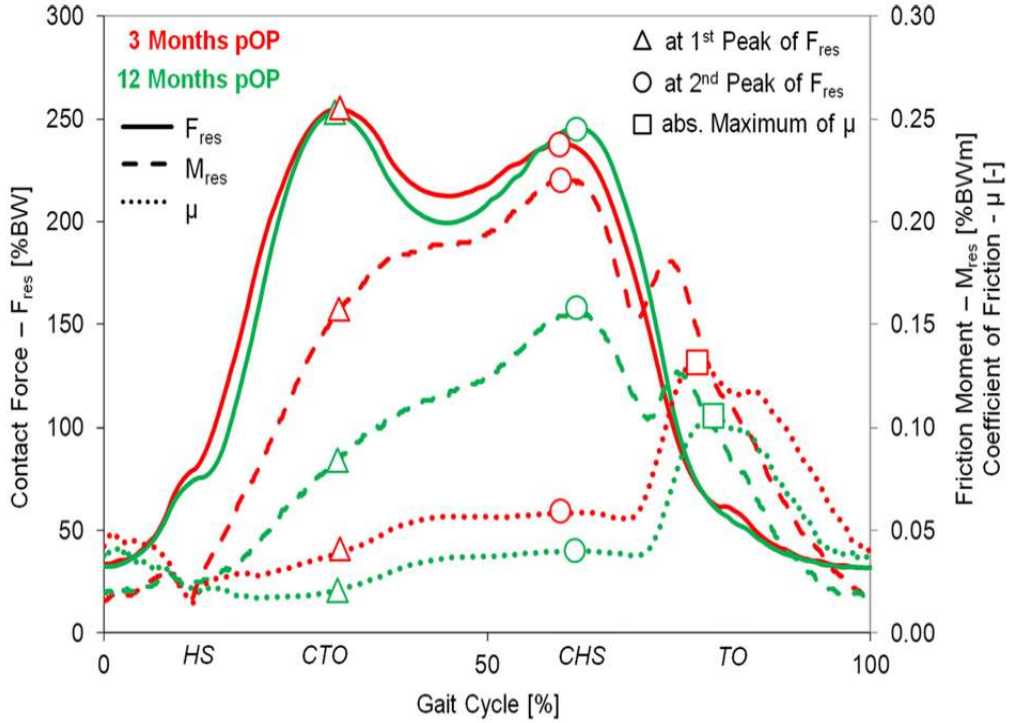

Fig 2. Postoperative changes of loads and friction. Average time courses of F_{res}, M_{res} and μ during one gait cycle at three and twelve months pOP. The indicated values M_{res1}, M_{res2}, μ_1, μ_2 and μ_{max} were determined at the instants of the peak forces F_{res1} and F_{res2}.

doi:10.1371/journal.pone.0120438.g002

Results

During gait, the resultant joint force F_{res} had two extreme values (Fig. 2), labeled F_{res1} and F_{res2}. At the instants of these peak forces the friction moments M_{res1} and M_{res2} were determined. The coefficient of friction μ was calculated throughout the whole gait cycle and the values μ_1 and μ_2 at the instants of F_{res1} and F_{res2} plus the absolute maximum value μ_{max} were analyzed.

Joint contact force

The resultant joint force F_{res} was calculated using the measured force components in lateral, anterior, and superior directions. In Fig. 2, the patterns of F_{res} (bold lines) of the 'average' subject are shown for two different time points, three and twelve months pOP. Both patterns are similar and show two typical peak values. The first maximum (F_{res1}) occurs at the time of contralateral toe off (CTO), and the second maximum (F_{res2}) at the contralateral heel strike (CHS).

At three months pOP, peak values of 255%BW (F_{res1}) and 238%BW (F_{res2}) were determined for the 'average' subject (Figs. 2 and 3, Table 3). The values of F_{res1} individually ranged between 209%BW (H3L) and 301%BW (H8L) (Fig. 4), which is a variation by 44% F_{res2} laid between 217%BW (H9L) and 287 (H8L); it had a variation of 32%.

At twelve months pOP (Figs. 2 and 3, Table 3), peak values of 252%BW (F_{res1}) and 245% BW (F_{res2}) were determined for the 'average' subject. F_{res1} individually varied (Fig. 4) between

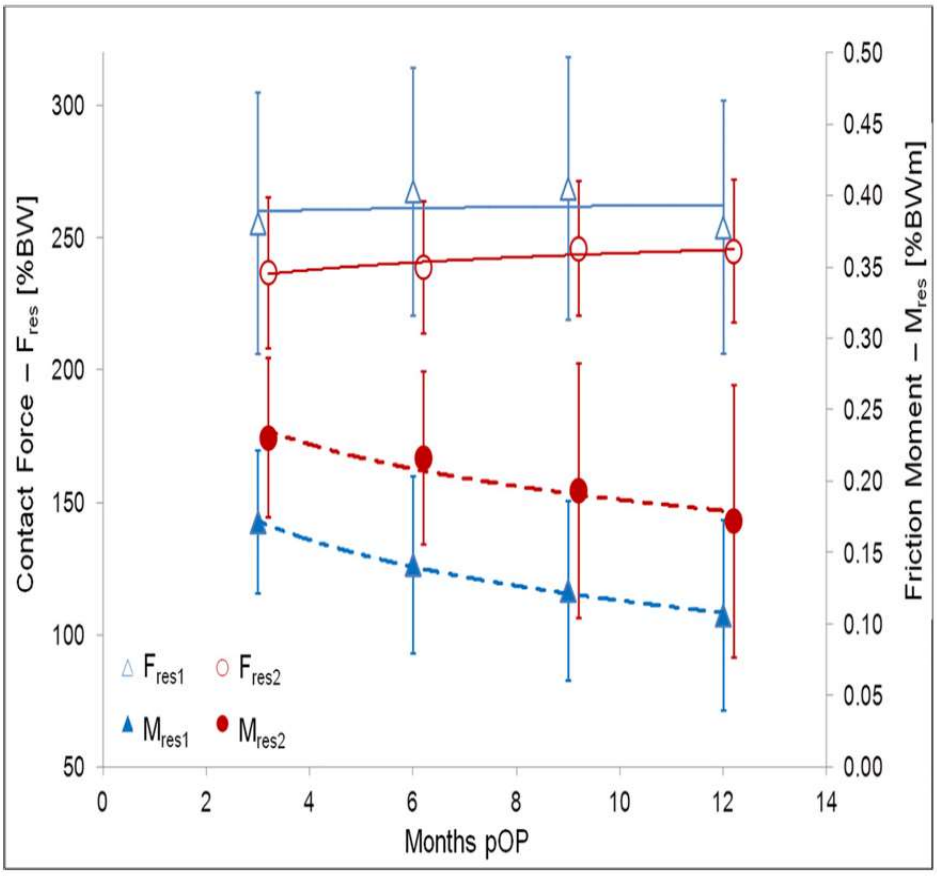

Fig 3. Postoperative changes of contact forces and friction moments. Average and standard deviations.

doi:10.1371/journal.pone.0120438.g003

220%BW (H3L) and 294%BW (H7R) by 34%. F_{res2} ranged between 215%BW (H9L) and 283% BW (H8L) with a variation of 32%.

Over the three- to twelve-month pOP period (Figs. 2, 3 and 4), F_{res1} declined by -1% on average (Table 4). It increased in four subjects, but decreased in five subjects and remained constant in one (H7R). The individual changes laid between +6% (H1L) and -13% (H8L). The change of F_{res2} during the pOP time was +4%. F_{res2} increased in seven and decreased in three subjects (Table 4). The individual changes laid between -8% (H10R) and +13% (H6R). For the 'average' subject a logarithmic correlation was determined between the pOP month and the peak values F_{res1} and F_{res2} (Fig. 3) with $R^2 = 0.03$ and $R^2 = 0.68$ (Table 5).

Friction moment

During walking, M_{res} increased in all patients between heel strike (HS) and CHS (Fig. 2, dashed lines), with a first maximum around CHS. The local minimum of the M_{res} curve between CHS and TO represents the instant when the rotational direction of the joint changes from

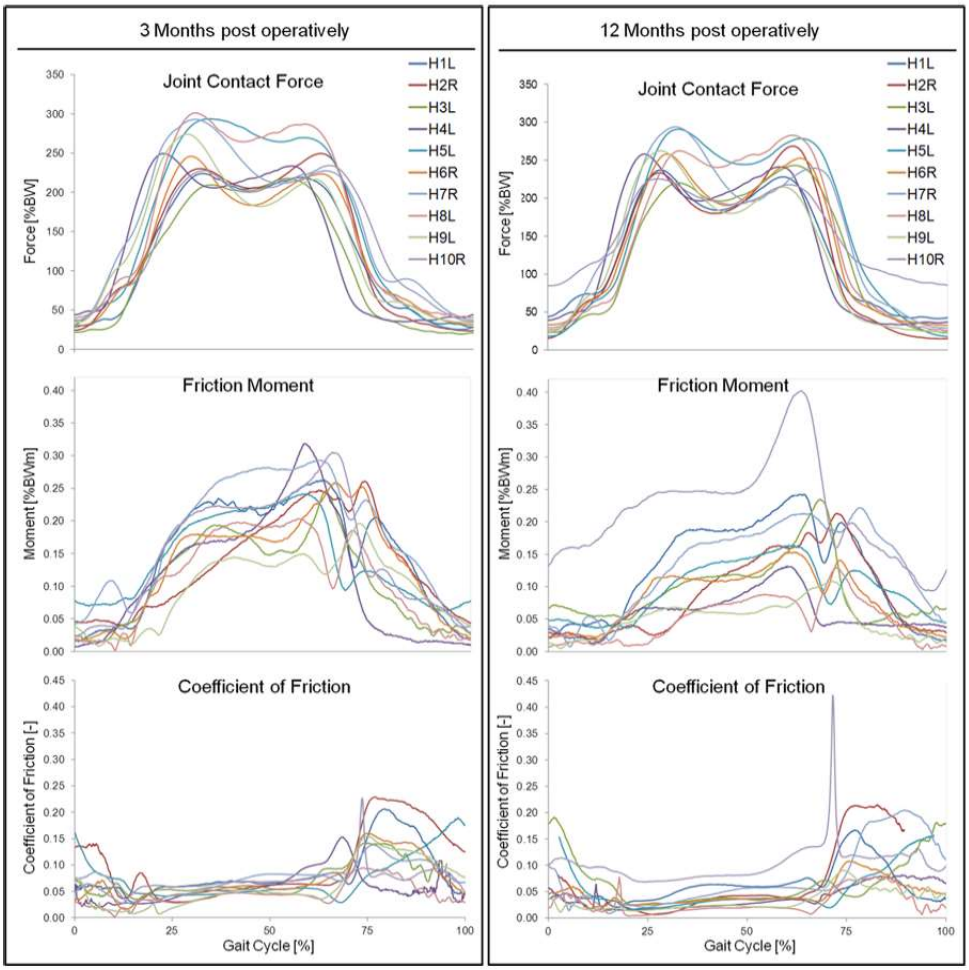

Fig 4. Individual contact forces, friction moments and coefficients of friction. Load pattern during one gait cycle at three (left) and twelve (right) months postoperatively.

doi:10.1371/journal.pone.0120438.g004

extension to flexion. It is followed by a second, smaller maximum during the flexion phase, shortly before TO.

At three months pOP, friction moments of 0.174%BWm (M_{res1}) and 0.234%BWm (M_{res2}) were determined for the 'average' subject (Figs. 2 and 3, Table 3). After the local minimum, a smaller second maximum of 0.186%BWm was determined during the flexion phase of the gait cycle. M_{res1} individually ranged between 0.096%BWm (H9L) and 0.220%BWm (H7R), a variation by 129%. M_{res2} laid between 0.137%BWm (H9L) and 0.301%BWm (H10R) (Fig. 4) and varied by 119%. The smaller second maximum ranged from 0.124%BWm (H5L) to 0.261% BWm (H2R) with a variation of 110%.

At twelve months pOP (Figs. 2 and 3, Table 3), average friction moments of 0.107%BWm (M_{res1}) and 0.174%BWm (M_{res2}) were found. M_{res1} ranged between 0.027%BWm (H2R) and

Table 5. Average postoperative trends of the contact force (F_{res}), friction moment (M_{res}) and coefficient of friction (μ).

Average	R^2	RSE	a	p(a)	b	p(b)
Fres1	*0.023*	*7.657*	*265*	*0.002*	*-1.592*	*0.849*
Fres2	*0.679*	*2.831*	*232*	*0.001*	*5.597*	*0.176*
Mres1	*0.994*	*0.003*	*0.225*	*0.001*	*-0.048*	*0.003*
Mres2	*0.917*	*0.009*	*0.281*	*0.004*	*-0.042*	*0.043*
μ1	*0.992*	*0.001*	*0.059*	*0.001*	*-0.013*	*0.004*
μ2	*0.993*	*0.001*	*0.073*	*<0.001*	*-0.011*	*0.004*
μmax	*0.251*	*0.009*	*0.166*	*0.010*	*0.007*	*0.499*

Logarithmic regression functions y = a + b*ln(m) with m = postoperative month, the residual-standard-error (RSE) and the p-values for the intercept a and the slope b (t-test)

doi:10.1371/journal.pone.0120438.t005

0.143%BWm (H1L); it highly varied by 430% (Fig. 4). M_{res2} laid between 0.069%BWm (H9L) and 0.402%BWm (H10R), which is an even higher variation of 451%. The second smaller maximum had an average of 0.130%BWm. It ranged from 0.045%BWm (H4L) to 0.247%BWm (H10R) and varied by 449%.

From three to twelve months pOP, M_{res1} decreased significant on average by -47% (Table 4). But this change was individually very different, with values between +13% (H10R) and -72% (H2R). M_{res2} sunk on average by -34%, with individual changes between +30% (H10R) and -60% (H8L). The smaller second maximum of M_{res} was decreased by -28%. With exception of H10R, M_{res1} and M_{res2} decreased in all subjects over the first twelve months pOP.

A logarithmic correlation was observed between the pOP month and the peak values M_{res1} and M_{res2} (Fig. 3) with $R^2 = 0.994$ and $R^2 = 0.917$ for the 'average' subject (Table 5). The slope of M_{res} from HS to CTO decreased by approximately -50% during the pOP time.

Coefficient of friction

The coefficient of friction (μ) increased throughout the whole load phase from HS to TO (Fig. 2, dotted lines). This increase was approximately linear during the stance phase between CTO and CHS. Shortly after the CHS, at approximately 70% of the gait cycle, μ increased sharply and always reached its absolute maximum (μ_{max}) shortly before TO.

At three months pOP (Fig. 2, Table 3), values of $\mu_1 = 0.045$, $\mu_2 = 0.062$ and $\mu_{max} = 0.175$ were determined for the 'average' subject. As with F_{res} and M_{res}, the coefficient of friction individually varied much (Fig. 4). μ_1 ranged from 0.032 (H8L) to 0.063 (H1L), and varied by 97%. μ_2 laid between 0.04 (H9L) and 0.081 (H10R), which is a variation by 103%. μ_{max} had values between 0.095 (H8L) and 0.229 (H2R); it varied by 141%.

At twelve months pOP (Fig. 2, Table 3), values of $\mu_1 = 0.028$, $\mu_2 = 0.047$ and $\mu_{max} = 0.179$ were determined for the 'average' subject (Fig. 2). μ_1 varied extremely between 0.007 (H2R) to 0.071 (H10R), which is a variation of 914%. μ_2 was individually less different; it had values between 0.02 (H9L) to 0.116 (H10R) and thus varied by 480%. μ_{max} ranged from 0.079 (H8L) to 0.442 (H10R) with a variation of 459%.

From three to twelve months pOP (Figs. 2, 3 and 4), the coefficient of friction decreased on average (Table 4). The reduction of μ_1 was -34%, with individual changes between +18% (H10R) and -72% (H2R). μ_2 sunk by -46% on average, with individual changes between +48% (H10R) and -59% (H8L). The values of μ_1 and μ_2 decreased in all subjects, with the exception of H10R. μ_{max} decreased by -8% on average; it rose in seven subjects but sunk in three of them. The individual changes laid between +101% (H10R) and -42% (H9L).

A logarithmic correlation between the pOP month and μ was found for the 'average' subject, with $R^2 = 0.992$ (μ_1), $R^2 = 0.993$ (μ_2) and $R^2 = 0.251$ (μ_{max}) (Table 5). Furthermore, the correlation was also calculated for each subject separately. The coefficients of correlation for μ_1 ranged between 0.999 (H2R) and 0.226 (H10R), those for μ_2 between 0.999 (H6R) and 0.745 (H8L) and for μ_{max} between 0.954 (H9L) and 0.007 (H1L), respectively.

Discussion

In this study, it was possible for the first time to simultaneously measure joint contact forces and friction moments *in vivo* during walking. High friction moments may endanger the stability of cup fixation and cause fretting between the prosthesis head and the taper. Loosening moments of acetabular cups depend on the quality of the cup-bone interface, which is influenced, among others, by the fixation technique and the type of coating. For cementless press-fit cups, cyclic loosening moments as low as 8Nm were determine *in vitro* [35]. The maximal measured friction moment (intra-individual average!) was 0.402%BWm in H10R (Fig. 4), which corresponds to 3.99Nm or 50% of the critical value. This shows that the real friction moments, which act during higher demanding activities than walking or when extreme force occur during stumbling [36], may reach dangerous values, especially shortly after implantation.

Joint loads and gliding parameters

Simulator tests on friction and wear in hip implants have been performed under varying conditions. In some cases, the joint was moved in one plane only, using sine wave loads and movements, while the movements around the other joint axes were ignored [11,18,21,37]. However, during walking, the hip joint moves not only around the x-axis (flexion/extension) but also around the y-axis (abduction/adduction) and the z-axis (internal/external rotation). An earlier study [30] showed that friction also depends on the moments around the other two axes. Furthermore, the joint movement is not sinusoidal, and the contact loads typically have two peaks at CTO and CHS. We have shown that the friction moment M_{res} increases *in vivo* between HS and CHS, when it reaches its maximum. This finding is contrary to the *in vitro* situation, where the measured friction moment showed a plateau phase during the loading of the joint [11,21].

In the current *in vivo* study, μ has been calculated in 3D and has been proven not to be constant throughout the gait cycle (Fig. 2). During each step it increased (Table 3, 4) from 0.045 to 0.175 (three months pOP) respectively from 0.028 to 0.179 (twelve months pOP). μ reaches its absolute maximum shortly before TO, when the movement changes from extension to flexion. At that instant, the relative velocity between ball and cup is either zero or very low. Earlier studies reported that μ differed when the lubrication conditions were changed [19,20,38]. The high peak value of μ is probably best explained by the assumption that the synovia is squeezed out under high loads and transported back into the joint when the load is low during the swing phase [21].

Postoperative changes

No significant change of the resultant contact force F_{res} in the 'average' subject was observed between three and twelve months pOP. However, the joint loads during the first three months are not reported here. In an earlier study, F_{res} showed during that time an average increase of 18% (F_{res1}) and 21% (F_{res2}) when walking with crutches [39]. This data was only based on subjects H1L to H7R, who also participated in this study. Future simulations of bone remodeling around hip implants by finite element modeling should simulate increasing contact forces during the first three months while maintaining constant contact force values afterwards.

A significant decrease of the friction moment M_{res} in the postoperative course was observed throughout the whole gait cycle for the 'average' subject. At the instants of the two peaks of

F_{res}, M_{res} decreased significantly by 47% (M_{res1}) and 34% (M_{res2}). These changes may be caused by 'running-in' effects of the gliding components or by improved lubricating properties of the synovia [40]. A fluid with a high viscosity needs more time to flow out of the intra-articular joint space, provided that the contact force and sliding speed are the same. Synovia is a non-Newton fluid [40], and its viscosity therefore depends on contact force, sliding velocity and shear stress [13,19,40,41]. Because the walking velocity and contact forces were found to be nearly constant during the observed period, the decrease in M_{res} suggests an increase in fluid viscosity by about 50%, an effect which had not be investigated in the current study. The logarithmic decrease of the coefficient of friction over the postoperative time suggests a change in synovia viscosity and, possibly, an additional smoothening of the gliding surfaces.

Typical simulator studies, which investigated the friction of soft-on-hard parings as in our study (XPE/Al_2O_3), delivered μ-values between 0.04 and 0.09 [11,13,42] for a lubricated regime and for a 'dry' sliding condition values between 0.13 and 0.14 were determined [43]. The sharp increase of μ between CHS and TO did not change significantly between three and twelve months pOP. This finding suggests that during early flexion, hip joint friction does not depend much on synovial properties. This finding, along with the high absolute peak values μ_{max}, indicates the presence of 'dry' friction [43] in the joint during the early flexion phase. However, several studies have shown that the fluid film thickness in a soft-on-hard pairing is much lower than the roughness of the polyethylene bearing surface [44,45]. This suggests that 'mixed' or 'boundary lubrication' conditions occurring for this tribological pairing [42].

A time-dependent logarithmic trend of μ_{max} was also observed, but only with $R^2 = 0.251$ and a high inter-individual range (0.013 to 0.886). The significance of postoperative changes of μ_{max} in only some of the subjects may be due to different activity levels and therefore different running in effects [46].

Inter-individual differences

The observed peak values of F_{res} varied individually by 44% (three months pOP) and 34% (twelve months pOP). In contrast to these relatively small deviations, M_{res} individually differed by 129% (three months pOP) and even 451% (twelve months pOP). For μ, the individual variation laid between 141% (three months pOP) and 914% (twelve months pOP). These strong individual variations of M_{res} are most likely due to different 'running-in' effects, which are caused by the individual activity levels and synovial properties.

In subject H10R, the peak μ_{max} was extremely high and was greater than that observed in all of other subjects. This observation may possibly be explained if one assumes that in H10R the movement in the joint really fell to zero at the instant when the movement changed from extension to flexion. In the other subjects, however, the joint may still have been slightly rotating in the frontal and horizontal planes. The fluid film may thus have been broken down completely in the joint of H10R only. To clarify this hypothesis, future study will focus on individually different movements in the joint and on deviating areas of load transfer, which will be analyzed using individual gait data and anatomical conditions.

It was shown that the peak values of the *in vivo* acting friction moments during walking were smaller than critical torsion torque at the cup-bone interface [35]. However, higher friction moments can be expected during high demanding activities, which might be critical for the cup fixation, especially shortly after implantation.

This study has reported for the first time post operative changes and the individual differences of the *in vivo* forces and friction moments acting in total hip joint replacements. These in vivo loads can now be used as realistic input data for friction and wear simulator studies.

Examples of the *in vivo* measurements are published at the public data base www.orthoload.com.

Limitations of the study

There are some limitations to this study. The number of investigated subjects was small and only one implant type was investigated only during level walking. The peak values of the friction moment and friction coefficient and their time-dependent changes individually varied extremely. Possible factors, causing these variations, were not evaluated. Such factors as implant orientation, sliding speed and contact area in the joint, as well as friction during other activities are currently investigated in an additional study.

Acknowledgments

We thank all patients for their cooperation.

Author Contributions

Conceived and designed the experiments: PD GB. Performed the experiments: PD. Analyzed the data: PD AB. Contributed reagents/materials/analysis tools: PD AB. Wrote the paper: PD GB.

References

1. Bergen H. Annual Report 2010—Norwegian Arthroplasty Register. 2010.
2. David D, Graves S, Tomkins A. Australien Orthopaedic Association National Joint Replacement Registry. Anual Report. Adelaide:AOA; 2013. 2013.
3. Garellick G, Karrholm J, Rogmark C, Rolfson O, Herberts P. Swedish Hip Arthroplasty Register—Annual Report 2011. 2011.
4. CJRR. CJRR report: Total hip and total knee replacements in Canada. Canadian Institute for Health Information. 2008.
5. Havelin LI, Fenstad AM, Salomonsson R, Mehnert F, Furnes O, Overgaard S, et al. The Nordic Arthroplasty Register Association: a unique collaboration between 3 national hip arthroplasty registries with 280,201 THRs. Acta Orthop. 2009; 80: 393–401. doi: 10.3109/17453670903039544 PMID: 19513887
6. Huch K, Müller KAC, Stürmer T, Brenner H, Puhl W, Günther K- P. Sports activities 5 years after total knee or hip arthroplasty: the Ulm Osteoarthritis Study. Ann Rheum Dis. 2005; 64: 1715–1720. PMID: 15843453
7. Chatterji U, Ashworth MJ, Lewis PL, Dobson PJ. Effect of total hip arthroplasty on recreational and sporting activity. ANZ J Surg. 2004; 74: 446–449. PMID: 15191479
8. Flugsrud GB, Nordsletten L, Espehaug B, Havelin LI, Meyer HE. The effect of middle-age body weight and physical activity on the risk of early revision hip arthroplasty. Acta Orthop. 2007; 78: 99–107. PMID: 17453400
9. Malchau H, Herberts P, Söderman P, Odén A. Prognosis of Total Hip Replacement. swedish Natl hip Arthroplast Regist. 2000;
10. Liao Y. The effect of frictional heating and forced cooling on the serum lubricant and wear of UHMW polyethylene cups against cobalt—chromium and zirconia balls. Biomaterials. 2003; 24: 3047–3059. PMID: 12895577
11. Brockett C, Williams S, Jin Z, Isaac G, Fisher J. Friction of Total Hip Replacements With Different Bearings and Loading Conditions. J Biomed Mater Res. 2006; 508–515.
12. Affatato S, Spinelli M, Zavalloni M, Mazzega-Fabbro C, Viceconti M. Tribology and total hip joint replacement: current concepts in mechanical simulation. Med Eng Phys. 2008; 30: 1305–17. doi: 10.1016/j.medengphy.2008.07.006 PMID: 18774742
13. Hall RM, Unsworth A. Review Friction in hip prostheses. Biomaterials. 1997; 18: 1017–1026. PMID: 9239463
14. Scholes SC, Unsworth A. The effects of proteins on the friction and lubrication of artificial joints. Proc Inst Mech Eng Part H J Eng Med. 2006; 220: 687–693.

15. Scholes SC, Unsworth A, Hall RM, Scott R. The effects of material combination and lubricant on the friction of total hip prostheses. Wear. 2000; 241: 209–213.
16. Fialho JC, Fernandes PR, Eça L, Folgado J. Computational hip joint simulator for wear and heat generation. J Biomech. 2007; 40: 2358–2366. PMID: 17270192
17. Mattei L, Di Puccio F, Piccigallo B, Ciulli E. Lubrication and wear modelling of artificial hip joints: A review. Tribol Int. Elsevier; 2011; 44: 532–549.
18. Saikko V. A simulator study of friction in total replacement hip joints. Proc Inst Mech Eng Part H J Eng Med. 1992; 206: 201–211. PMID: 1300112
19. Scholes SC, Unsworth A. Comparison of friction and lubrication of different hip prostheses. Proc Inst Mech Eng Part H J Eng Med. 2000; 214: 49–57.
20. Unsworth A. The effects of lubrication in hip joint prostheses. Phys Med Biol. 1978; 23: 253–68. PMID: 643921
21. Williams S, Jalali-Vahid D, Brockett C, Jin Z, Stone MH, Ingham E, et al. Effect of swing phase load on metal-on-metal hip lubrication, friction and wear. J Biomech. 2006; 39: 2274–81. PMID: 16143337
22. Bergmann G, Rohlmann, Graichen F. In vivo Messung der Hüftgelenkbelastung 1. Teil: Krankengymnastik. Z Orthop. 1989; 127: 672–679. PMID: 2618148
23. Stansfield B, Nicol AC, Paul JP, Kelly IG, Graichen F, Bergmann G. Direct comparison of calculated hip joint contact forces with those measured using instrumented implants. An evaluation of a three-dimensional mathematical model of the lower limb. J Biomech. 2003; 36: 929–936. PMID: 12757801
24. Brand RA, Crowninshield RD, Pedersen DR. Forces on the femoral head during acitivties of daily living. Iova Orthop J. 1982; 2: 43–49.
25. Paul JP. Force actions transmitted by joints in the human body. Proc R Soc Lond B Biol Sci. 1976; 192: 163–72. PMID: 3785
26. Taylor SJ, Perry JS, Meswania JM, Donaldson N, Walker PS, Cannon SR. Telemetry of forces from proximal femoral replacements and relevance to fixation. J Biomech. 1997; 30: 225–34. PMID: 9119821
27. Bergmann G, Graichen F, Rohlmann A, Verdonschot N, van Lenthe GH. Frictional heating of total hip implants. Part 1: measurements in patients. J Biomech. 2001; 34: 421–8. PMID: 11266664
28. Li S, Chien S, Branemark P- I. Heat shock-induced necrosis and apoptosis in osteoblasts. J Orthop Res. 1999; 17: 891–9. PMID: 10632456
29. Damm P, Graichen F, Rohlmann A, Bender A, Bergmann G. Total hip joint prosthesis for in vivo measurement of forces and moments. Med Eng Phys. 2010; 32: 95–100. doi: 10.1016/j.medengphy.2009.10.003 PMID: 19889565
30. Damm P, Dymke J, Ackermann R, Bender A, Graichen F, Halder A, et al. Friction in total hip joint prosthesis measured in vivo during walking. PLoS One. 2013; 8: e78373. doi: 10.1371/journal.pone.0078373 PMID: 24260114
31. Graichen F, Bergmann G, Rohlmann A. Telemetric transmission system for in vivo measurement of the stress load of an internal spinal fixator. Biomed Tech Biomed Eng. 1994; 39: 251–258. PMID: 7811908
32. Graichen F, Arnold R, Rohlmann A, Bergmann G. Implantable 9-channel telemetry system for in vivo load measurements with orthopedic implants. IEEE Trans Biomed Eng. 2007; 54: 253–61. PMID: 17278582
33. Wu G, Siegler S, Allard P, Kirtley C, Leardini A, Rosenbaum D, et al. ISB recommendation on definitions of joint coordinate system of various joints for the reporting of human motion—part I: ankle, hip, and spine. J Biomech. 2002; 35: 543–548. PMID: 11934426
34. Bender A, Bergmann G. Determination of Typical Patterns from Strongly Varying Signals. Comput Methods Biomech Biomed Engin. 2011;iFirst: 1–9. doi: 10.1080/10255842.2010.483682 PMID: 21905293
35. Curtis MJ, Jinnah RH, Valerie WD, Hungerford DS. The initial stability of uncemented acetabular components. Br Editor Sov Bone Jt Surg. 1992; 74-B: 372–376.
36. Bergmann G, Graichen F, Rohlmann. Hip joint contact forces during stumbling. Langenbeck's Arch Surg. 2004; 389: 53–59.
37. Scholes SC, Unsworth A, Goldsmith AAJ. A frictional study of total hip joint replacements. Phys Med Biol. 2000; 45: 3721–35. PMID: 11131195
38. Hall RM, Unsworth A, Wroblewski BM, Siney P, Powell NJ. The friction of explanted hip prostheses. Br J Rheumatol. 1997; 36: 20–6. PMID: 9117168
39. Damm P, Schwachmeyer V, Dymke J, Bender A, Bergmann G. In vivo hip joint loads during three methods of walking with forearm crutches. Clin Biomech. Elsevier Ltd; 2013; 28: 530–5. doi: 10.1016/j.clinbiomech.2012.12.003 PMID: 23643290

40. Fam H, Bryant JT, Kontopoulou M. Rheological properties of synovial fluids. Biorheology. 2007; 44: 59–74. Available: http://www.ncbi.nlm.nih.gov/pubmed/17538199 PMID: 17538199

41. Balazs EA. The Physical Properties of synovial Fluid and the special role of hyaluronic Acid. Disord Knee. 1974; 63–75.

42. Jin Z, Stone M, Ingham E, Fisher J. (v) Biotribology. Curr Orthop. 2006; 20: 32–40.

43. Xiong D, Ge S. Friction and wear properties of UHMWPE/Al2O3 ceramic under different lubricating conditions. Wear. 2001; 250: 242–245.

44. Jalali-Vahid D, Jagatia M, Jin ZM, Dowson D. Prediction of lubricating film thickness in UHMWPE hip joint replacements. J Biomech. 2001; 34: 261–6. PMID: 11165292

45. Fisher J, Dowson D. Tribology of total artificial joints. Proc Inst Mech Eng H. 1991; 205: 73–9. Available: http://www.ncbi.nlm.nih.gov/pubmed/1840723 PMID: 1840723

46. Unsworth A. Tribology of artifical hip joints. Proc Inst Mech Eng Part J J Eng Tribol. 2006; 220: 711–718.

2.3. Einfluss statischer Belastung auf die Gelenkreibung

Die Lockerung von Pfanne und Inlay ist eine der häufigsten Ursachen für das Versagen eines Hüft-Endoprothesen-Systems (Bergen 2010; David, Graves, and Tomkins 2013; Garellick et al. 2011). In der Literatur wird von Simulator-Reibversuchen berichtet, die zeigen, dass im Vergleich zu zyklischer Bewegung die Gelenkreibung beim Bewegungsbeginn nach statischen Belastungen signifikant erhöht ist (Morlock et al. 2000; Nassutt, Wimmer, and Morlock 2003). Hauptziel der im Rahmen dieser Teilstudie durchgeführten in-vivo-Belastungsmessungen war es zu untersuchen, ob dieser auch aus der Technik bekannte Effekt der Anlaufreibung, in der in-vivo-Situation ebenfalls auftritt, und zu beurteilen, ob die dabei wirkenden Reibbelastungen ein potenzieller Risikofaktor insbesondere für die frühe postoperative Pfannenstabilität sind. Es konnte gezeigt werden, dass schon kurze statische Belastungen, wie sie schon bei kurzen Gehpausen auftreten, zu einer signifikanten Erhöhung der Gelenkreibung in vivo führen. Die Ergebnisse dieser Studie bestätigen somit, dass auch die in vivo wirkenden Spitzenmomente in Hüftimplantaten schon nach einer kurzen Gangpause im Mittel mit bis zu 143% signifikant höher sind als bei kontinuierlichen Bewegungen. Diese deutlich erhöhten Reibbelastungen, welche unter anderem als Torsionsbelastung ins Knochen-Implantat-Interface übertragen werden, sind somit potenzielle Risikofaktoren, insbesondere für mechanisch induzierte Pfannenlockerungen. Dieses Risiko ist bei zementfrei verankerten Pfannen, bei unzureichender Verankerung bzw. in den ersten postoperativen Monaten am höchsten. Der nachfolgende Text entspricht dem Abstract der Arbeit *„In vivo measured joint friction in hip implants during walking after a short rest”*, welche im Journal PLoS ONE 2017 veröffentlicht wurde.

“It has been suspected that friction in hip implants is higher when walking is initiated after a resting period than during continuous movement. It cannot be excluded that such increased initial moments endanger the cup fixation in the acetabulum, overstress the taper connections in the implant or increase wear. To assess these risks, the contact forces, friction moments and friction coefficients in the joint were measured in vivo in ten subjects. Instrumented hip joint implants with telemetric data transmission were used to access the contact loads between the cup and head during the first steps of walking after a short rest.

The analysis demonstrated that the contact force is not increased during the first step. The friction moment in the joint, however, is much higher during the first step than during continuous walking. The moment increases throughout the gait cycle were 32% to 143% on average and up to 621% individually. The high initial moments will probably not increase wear by much in the joint. However, comparisons with literature data on the fixation resistance of the cup against moments made clear that the stability can be endangered. This risk is highest during the first postoperative months for cementless cups with insufficient under-reaming. The high moments after a break can also put taper connections between the head and neck and neck and shaft at a higher risk.

During continuous walking, the friction moments individually were extremely varied by factors of 4 to 10. Much of this difference is presumably caused by the varying lubrication properties of the synovia. These large moment variations can possibly lead to friction-induced temperature increases during walking, which are higher than the 43.1°C which have previously been observed in a group of only five subjects."

Publikation: In vivo measured joint friction in hip implants during walking after a short rest.

Damm P., Bender A., Duda G., Bergmann G.

PLoS ONE 12(3): e0174788.; https://doi.org/10.1371/journal.pone.0174788

PLOS ONE

RESEARCH ARTICLE

In vivo measured joint friction in hip implants during walking after a short rest

Philipp Damm*, Alwina Bender, Georg Duda, Georg Bergmann

Julius Wolff Institute, Charité–Universitätsmedizin Berlin, Berlin, Germany

* philipp.damm@charite.de

OPEN ACCESS

Citation: Damm P, Bender A, Duda G, Bergmann G (2017) *In vivo* measured joint friction in hip implants during walking after a short rest. PLoS ONE 12(3): e0174788. https://doi.org/10.1371/journal.pone.0174788

Editor: Jose Manuel Garcia Aznar, University of Zaragoza, SPAIN

Received: November 16, 2016

Accepted: March 15, 2017

Published: March 28, 2017

Data Availability Statement: Selected trials of each of the investigated subjects are also shown and can be downloaded at the public data base www.orthoload.com.

Funding: This work was supported by Deutsche Forschungsgemeinschaft (Be 804/19-1), the German Federal Ministry of Education and Research (BMBF 01EC1408A; Overload-PrevOP; SP03), Deutsche Arthrose-Hilfe and OrthoLoad Club. The funders had no role in study design, data collection and analysis, decision to publish, or preparation of the manuscript.

Abstract

Introduction

It has been suspected that friction in hip implants is higher when walking is initiated after a resting period than during continuous movement. It cannot be excluded that such increased initial moments endanger the cup fixation in the acetabulum, overstress the taper connections in the implant or increase wear. To assess these risks, the contact forces, friction moments and friction coefficients in the joint were measured *in vivo* in ten subjects. Instrumented hip joint implants with telemetric data transmission were used to access the contact loads between the cup and head during the first steps of walking after a short rest.

Results

The analysis demonstrated that the contact force is not increased during the first step. The friction moment in the joint, however, is much higher during the first step than during continuous walking. The moment increases throughout the gait cycle were 32% to 143% on *average* and up to 621% *individually*. The high initial moments will probably not increase wear by much in the joint. However, comparisons with literature data on the fixation resistance of the cup against moments made clear that the stability can be endangered. This risk is highest during the first postoperative months for cementless cups with insufficient under-reaming. The high moments after a break can also put taper connections between the head and neck and neck and shaft at a higher risk.

Discussion

During *continuous* walking, the friction moments *individually* were extremely varied by factors of 4 to 10. Much of this difference is presumably caused by the varying lubrication properties of the synovia. These large moment variations can possibly lead to friction-induced temperature increases during walking, which are higher than the 43.1˚C which have previously been observed in a group of only five subjects.

Competing interests: The authors have declared that no competing interests exist.

Introduction

Total hip joint replacement is performed more than 200,000 times in Germany alone [1]. During recent decades, the patients became younger and more active. Hence, their demands for functionality and lifetime of the implants have increased. Loosening of the artificial cup and inlay is one of the most common reasons for the failure of total hip replacements [2–4]. Polyethylene wear and aseptic loosening of the cup account for 26% and 48%, respectively, of reoperations [2,5]. Another study demonstrated that 30% to 40% of all revisions require a change of cup or inlay [6].

Wear is caused by friction, and aseptic loosening can be due to moments that stress the fixation in the acetabulum. These moments are not only determined by the patient's activities and, thus, the frequency and magnitude of the contact forces but also by the amount of friction in the joint. *In vitro* studies using different test conditions [7–18] demonstrated that the materials of the implant head and inlay primarily influenced the friction. In several studies, the stability of cup-bone bonding was investigated in cadavers or using plastic bone substitutes. A loosening moment of 8.8 Nm was reported for cementless cups [19], but values as low as 2.2 Nm were reported [20], both with an under-reaming of 1 mm. In comparison, our own *in vivo* load measurements with instrumented hip implants [21] have determined average friction moments during walking between 2.25 ±0.29 Nm (three months postoperatively) and 1.76 ±0.83 Nm (12 months postoperatively) [22,23]. This indicates that already during typical activities of daily living, such as walking, critical friction moments can occur in total hip joint replacements.

Analogous to higher moments in technical joints after movement started, it was suspected that friction in joint implants may also be higher after a short break, during which time the lubrication film breaks down [24,25]. Based on *in vivo* measurements [26] of typical activity times and resting periods in hip patients and using a pin-on-ball test, joint friction was investigated *in vitro* after movement began [24]. Friction after 5 s resting was 30% higher in ceramic-UHMWPE pairings than during the following continuous movement. The increase depended on the tribological pairing of the implant and correlated to the rest time. The results of this study confirmed that the peak moments in hip implants are higher after a rest than during continuous movements and may jeopardize the cup fixation. However, the *in vitro* data cannot directly be applied to *in vivo* situations because the kind of movement, the force amplitudes and the lubricant are different. The lubricating property of the synovia has an especially large influence on friction in the joint, as a difference of up to 451% in the friction moments in a group of ten subjects suggests [23]. Such individual differences of lubrication may also effect the possibly increased moments after a rest.

The main goal of this study was to obtain *in vivo* data on the increases of friction moments and friction coefficients after joint movement began. This enables the estimation of the potential risk of cup loosening due to high moments. For this purpose, contact forces and friction moments in instrumented hip implants of ten subjects were measured during walking, and the friction coefficients were calculated from these data.

Methods

Instrumented hip implant

To measure friction between the head and cup *in vivo*, instrumented hip implants were used [21]. The titanium implant (CTW, Merete Medical, Berlin; Germany) was combined with a 32 mm Al_2O_3 ceramic head and an XPE inlay. The neck of this clinically proven standard implant was modified to house an inductive power supply, six strain gauges, signal amplifiers and

telemetric data transmission [21]. The external measurement system [27,28] supplied the inductive coil around the patient's hip joint. The received signals were recorded simultaneously with the patient's images on video tape.

Joint contact forces and friction moments. The femur-based coordinate system [29] was located in the head center of a right-sided implant [30]. Data from left implants were mirrored to the right side. The **resultant joint contact force F_{res}** was calculated from the three force components in the lateral (F_x), anterior (F_y), and superior (F_z) directions. The **resultant friction moment M_{res}** was determined from the three components M_x, M_y, M_z, rotating positively around the corresponding axes.

Calculation of coefficient of friction

Based on all force and moment components, the magnitude of the three-dimensional **coefficient of friction μ** was calculated [23], assuming Coulomb friction and a head radius R:

$$\mu = M_{res}/(H * F_{res}) \quad (1)$$

The lever arm H is given by the following equation, see also [23]

$$\underline{H} = R * [\underline{F}_{res}/F_{res} - \cos(\underline{R}, \underline{M}_{res}) * (\underline{M}_{res}/M_{res})] \quad (2)$$

The coefficient μ was only determined for $F_{res} \geq 25\%BW$ and $M_{res} \geq 0.02\%BWm$ to ascertain an accuracy of μ better than 5%.

Patients and measurements

Ten patients with instrumented implants participated in the study (Table 1). They gave their informed written consent to participate. The study was approved by the ethical committee of the Charité–Universitätsmedizin Berlin, Germany (EA2/057/09) and was registered in the German Clinical Trials Register (DRKS00000563). The measurements were performed an average of 17 months (12–31 months) postoperatively during 10m of level walking at a self-selected walking speed. Five to eighteen trials per subject were recorded. The subjects stood still on both legs for 12 s, on average, before they started walking with the ipsilateral leg.

Data evaluation

All forces were determined as a percent of the patient's bodyweight (**%BW**); the friction moments in %BW*m. For a subject with a body weight of 100 kg, as an example, the values must be multiplied by a factor of 9.81 to obtain numbers in N or Nm. The continuous time patterns and the numerical peak values of forces and moments were analyzed separately for each of the first four steps after rest. Each complete step started and ended at the instants when F_{res} became a minimum (Figs 1 and 2). The 'Start' phase, preceding the first step, started when the ipsilateral leg started to move after stance and ended when F_{res} became a minimum before heel strike. If not mentioned as being '*individual*', all reported data refer to results from the *average* subject.

Time patterns: First, the durations of the Start phases and the four steps were averaged (Fig 1) from all individual trials (Table 1). Then, the time patterns of all six force and moment components and the results from all trials were averaged, separately for the Start phase and the four steps. For averaging, a dynamic time warping procedure was applied [31], which delivered an output that retains the typical maxima and minima of the included signals. Finally, the obtained *individual* averages were averaged again from all subjects to obtain the load-time

Table 1. Investigated subjects and the measurement parameters.

Subject	Bodyweight	Measurement	Ø Rest	Trials	Gender	Age
	[N]	[months post OP]	[s]			[years]
H1L	760	13	5	6	male	56
H2R	767	12	7	6	male	62
H3L	1.096	12	11	18	male	60
H4L	796	12	7	11	male	51
H5L	863	31	14	10	female	65
H6R	856	24	18	8	male	70
H7R	899	24	21	5	male	54
H8L	874	18	20	10	male	57
H9L	1197	13	5	11	male	55
H10R	995	12	10	9	female	54
Average	**910**	**17**	**12**	**10**	**-**	**58**

https://doi.org/10.1371/journal.pone.0174788.t001

behavior of an *average* subject (Fig 2). The friction coefficient μ throughout each trial was calculated from these *individual* or *average* force and moment components.

Numerical values: For the Start phase (Fig 1), the absolute maxima $\mathbf{F_{start}}$, $\mathbf{M_{start}}$, **and** $\boldsymbol{\mu_{start}}$ of the resultant force, the resultant moment and the friction coefficient were analyzed. During each of the following steps, the curves of the force F_{res} always exhibited two peak values $\mathbf{F_{CTO}}$ and $\mathbf{F_{CHS}}$ (Figs 1 and 2), at approximately the instant of contralateral toe off (CTO) and contralateral heel strike (CHS). One of both peak values was always the absolute maximum of F_{res}. For the moment M_{res}, the two values $\mathbf{M_{CTO}}$ and $\mathbf{M_{CHS}}$ were determined at the same instants as the peak forces. The maximum resultant moment $\mathbf{M_{max}}$ throughout the entire cycle duration mostly acted *very shortly* after M_{CHS} and is about 10% to 15% higher (Table 2). Two numerical

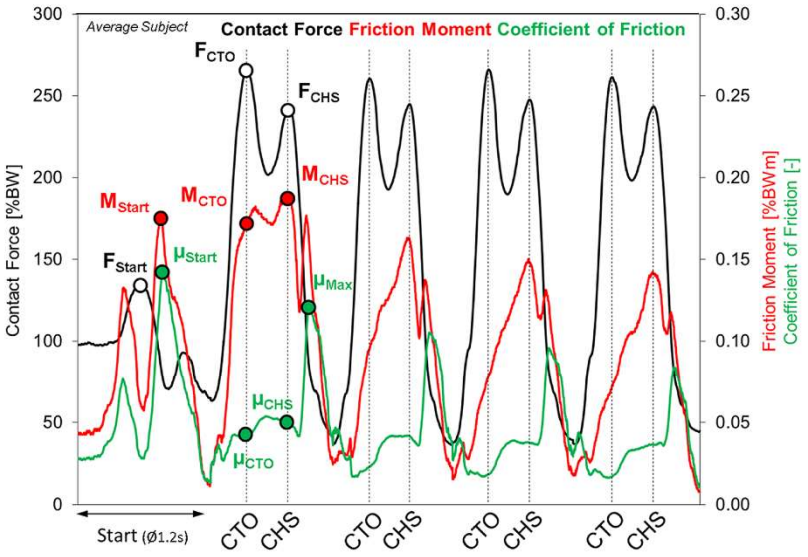

Fig 1. Resultant force F_{res}, resultant friction moment M_{res} and friction coefficient μ before "Start" and during four steps after rest. Data from average subject.

https://doi.org/10.1371/journal.pone.0174788.g001

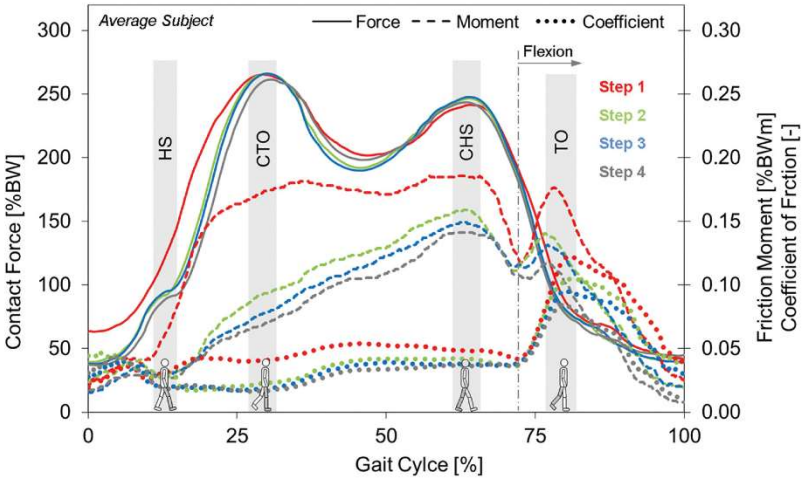

Fig 2. Resultant joint contact force F_{res}, resultant friction moment M_{res} and coefficient of friction μ for steps 1 to 4 after rest. M_{res} and μ are higher during step 1 (red lines) than during the following steps. F_{res} is higher only until CTO. HS = ipsilateral heel strike, CTO = contralateral toe off, CHS = contralateral heel strike, TO = ipsilateral toe off. Data from average subject after average rest time of 12 s.

https://doi.org/10.1371/journal.pone.0174788.g002

values μ_{CTO} and μ_{CHS} of the friction coefficient were also identified at the instants of the two peak forces. The absolute maximum μ_{max} of the friction coefficient was denoted as μ_{max}.

Separately for the Start phase and the four steps, these distinct force, moment and coefficient values were first determined numerically from the time patterns of the single trials and then averaged in the same sequence as the load-time patterns. First, the *individual* averages were calculated and then, based on the obtained numbers, the values for the *average* subject plus the corresponding minima, maxima and standard deviations. Information about the variations of all parameters in the individuals and their average is supplied by the reported standard deviations. The procedure used for averaging the *time patterns* minimized the summed errors between all included patterns throughout the entire measurement time. Therefore, the peak values in the *curves* of the average subject (Fig 2) can slightly deviate from the corresponding, *numerically* averaged peak values (Table 2).

To determine whether the values of the eight F_{res}, M_{res} and μ measurements during the first step were different from the corresponding values during the last step, each measurement from step 1 of the individual and average subjects was compared to the value from step 4. The obtained differences in percent were statistically analyzed (Wilcoxon, $p \leq 0.05$).

Rest times: To investigate whether the duration of the rest time influenced the changes of M_{res} and μ, the individually averaged rest times per trial (Table 1) were correlated to the changes of the corresponding six M_{res} and μ values between steps 1 and 4.

Results

Joint contact forces F_{res}

Time patterns: During the early gait phase until CTO, F_{res} was much higher during step 1 than during steps 2 to 4 (Fig 2). This surplus was 59% when the steps started and 35% at ipsilateral heel strike (HS). After reaching CTO and until the end of the cycles, F_{res} was nearly the same for all four steps.

Table 2. Resultant forces and moments plus coefficient of friction during the first four steps after rest. Data from individual and average subjects at the instants of contralateral toe off (CTO) and contralateral heel strike (CHS) plus maximum values throughout the entire gait cycle. "Start" = maximum values before complete step 1 started. SD = standard deviation. Minima and maxima indicated in bold.

Subject	F_{Start}	M_{Start}	μ_{Start}	F_{CTO}	F_{CHS}	M_{CTO}	M_{CHS}	M_{MAX}	μ_{CTO}	μ_{CHS}	μ_{max}	F_{CTO}	F_{CHS}	M_{CTO}	M_{CHS}	M_{MAX}	μ_{CTO}	μ_{CHS}	μ_{max}
	[%BW]	[%BWm]	[1]	[%BW]	[%BW]	[%BWm]	[%BWm]	[%BWm]	[1]	[1]	[1]	[%BW]	[%BW]	[%BWm]	[%BWm]	[%BWm]	[1]	[1]	[1]
	Start							**Step 1**							**Step 2**				
H1L	**92**	0.195	**0.268**	213	**186**	0.258	0.241	0.263	0.076	0.083	0.204	207	**188**	0.161	0.214	0.222	0.049	0.072	0.187
H2R	121	0.229	0.221	**204**	222	0.137	0.177	0.198	0.042	0.051	0.224	**206**	231	**0.029**	0.141	0.180	**0.009**	0.039	0.233
H3L	128	0.178	0.170	223	233	0.202	0.206	0.299	0.057	0.057	0.189	220	239	0.096	0.158	0.225	0.028	0.042	0.238
H4L	93	**0.091**	**0.117**	224	211	**0.097**	0.168	0.179	0.028	0.051	0.115	228	220	0.057	0.110	**0.111**	0.016	0.032	0.129
H5L	155	0.262	0.130	**389**	276	0.258	0.328	0.353	0.043	0.048	0.263	**400**	282	0.118	0.238	0.286	0.028	0.050	**0.382**
H6R	134	0.208	0.177	252	255	0.122	**0.118**	0.145	0.026	0.036	0.118	252	260	0.097	**0.105**	0.141	0.021	0.030	0.144
H7R	**223**	**0.425**	0.224	349	**289**	0.107	0.140	0.181	0.042	0.075	0.175	359	**288**	0.082	0.107	0.151	0.019	0.054	0.160
H8L	129	0.216	0.138	319	288	0.208	0.211	0.217	0.031	**0.029**	**0.101**	308	282	0.133	0.220	0.229	0.025	0.026	**0.090**
H9L	129	0.154	0.150	243	213	0.105	0.119	**0.136**	**0.021**	0.031	0.127	259	228	0.085	0.107	0.113	0.016	**0.024**	0.096
H10R	166	0.240	0.168	242	235	**0.303**	**0.380**	**0.387**	**0.080**	**0.105**	**0.271**	230	238	**0.264**	**0.416**	**0.428**	**0.073**	**0.115**	0.317
Min	92	0.091	0.117	204	186	0.097	0.118	0.136	0.021	0.029	0.101	206	188	0.029	0.105	0.111	0.009	0.024	0.090
Max	223	0.425	0.268	389	289	0.303	0.380	0.387	0.080	0.105	0.271	400	288	0.264	0.416	0.428	0.073	0.115	0.382
Average	***137***	***0.220***	***0.176***	***266***	***241***	***0.180***	***0.209***	***0.236***	***0.045***	***0.057***	***0.179***	***267***	***246***	***0.112***	***0.182***	***0.209***	***0.029***	***0.048***	***0.197***
SD	38	0.087	0.048	60	33	0.072	0.083	0.082	0.019	0.023	0.059	64	30	0.062	0.092	0.091	0.018	0.026	0.091
								Step 3							**Step 4**				
H1L				**204**	**198**	0.130	0.206	0.217	0.041	0.066	0.181	209	**194**	0.115	0.202	0.219	0.035	0.066	0.172
H2R				210	231	**0.023**	0.149	0.181	**0.007**	0.041	0.224	**202**	232	**0.019**	0.149	0.189	**0.007**	0.041	0.230
H3L				219	241	0.103	0.168	0.232	0.030	0.044	0.216	219	240	0.102	0.171	0.231	0.029	0.045	0.215
H4L				232	215	0.054	0.105	0.108	0.015	0.031	0.148	232	218	0.055	0.102	0.103	0.015	0.030	0.213
H5L				**400**	**293**	0.110	0.188	0.245	0.022	0.049	0.245	**358**	271	0.073	0.148	0.174	0.021	0.049	0.195
H6R				248	263	0.079	0.096	0.132	0.020	0.027	0.118	251	249	0.074	**0.084**	0.115	0.021	0.030	0.104
H7R				350	291	0.085	**0.094**	0.145	0.019	0.040	0.146	357	**289**	0.088	0.092	0.142	0.016	0.036	0.129
H8L				313	277	0.103	0.215	0.216	0.022	0.023	**0.088**	310	285	0.094	0.221	0.225	0.020	0.022	0.091
H9L				250	221	0.078	0.096	**0.101**	0.017	**0.021**	0.093	241	208	0.080	0.095	**0.096**	0.017	**0.021**	**0.083**
H10R				238	234	**0.258**	**0.399**	**0.433**	**0.070**	**0.110**	**0.314**	240	238	**0.257**	**0.398**	**0.418**	**0.069**	**0.111**	**0.361**
Min				204	198	0.023	0.094	0.101	0.007	0.021	0.088	202	194	0.019	0.084	0.096	0.007	0.021	0.083
Max				400	293	0.258	0.399	0.433	0.070	0.110	0.314	358	289	0.257	0.398	0.418	0.069	0.111	0.361
Average				***266***	***246***	***0.102***	***0.172***	***0.201***	***0.026***	***0.045***	***0.177***	***262***	***242***	***0.096***	***0.166***	***0.191***	***0.025***	***0.045***	***0.179***
SD				62	31	0.059	0.088	0.092	0.017	0.025	0.069	55	30	0.059	0.090	0.090	0.016	0.025	0.080

https://doi.org/10.1371/journal.pone.0174788.t002

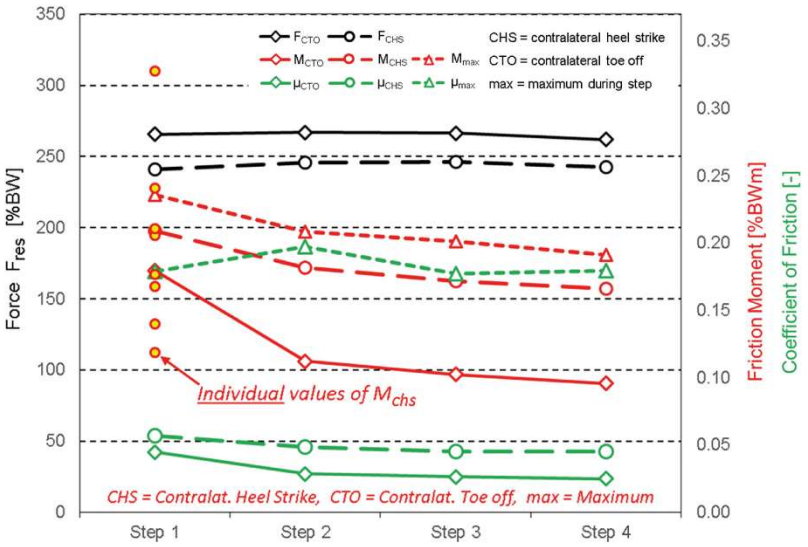

Fig 3. Contact forces F_{res}, friction moments M_{res} and coefficients of friction μ during first four steps after rest. Values at the instant of contralateral toe off (CTO) and contralateral heel strike (CHS) plus maxima (max) during the entire step time. Averages from ten subjects. Small circles = illustration of large individual variation of M_{CHS} during step 1; other variations see Table 2.

https://doi.org/10.1371/journal.pone.0174788.g003

Numerical values: The *individual* variations of the two force peaks $F_{CTO}|F_{CHS}$ were large (Table 2). For each of the four steps the standard deviations were approximately 23|13% of the average values. *From step to step*, both *average* force peaks were nearly unchanged (Table 2, Figs 2 and 3). F_{CTO} during step 1 exceeded the value from step 4 by only 1.3% (Table 3); for F_{CHS} this difference was -0.8%, that is, F_{CHS} was slightly smaller during step 4 than step 1.

Table 3. Increases of forces, moments and coefficient of friction during the first step after walking. Increase in percent of values during step 1 relative to values during step 4. Minima und maxima indicated in bold, p-values: Wilcoxon test.

Subject	F_{CTO} [%]	F_{CHS} [%]	M_{CTO} [%]	M_{CHS} [%]	M_{MAX} [%]	μ_{CTO} [%]	μ_{CHS} [%]	μ_{max} [%]
H1L	1.9	-4.1	124	19	20	116	26	19
H2R	1.0	**-4.3**	**621**	19	5	**542**	23	-3
H3L	1.8	-2.9	98	20	29	94	28	-12
H4L	**-3.4**	-3.2	76	65	74	84	73	**-46**
H5L	**8.7**	1.8	253	**122**	**103**	104	-2	35
H6R	0.4	**2.4**	65	40	26	23	21	14
H7R	-2.2	0.0	22	52	27	160	**105**	36
H8L	2.9	1.1	121	**-5**	-4	57	34	11
H9L	0.8	2.4	31	25	42	25	52	**54**
H10R	0.8	-1.3	**18**	**-5**	**-7**	**16**	**-5**	-25
Min	-3.4	-4.3	18	-5	-7	16	-5	-46
Max	8.7	2.4	621	122	103	542	105	54
Average	***1.3***	***-0.8***	***143.0***	***35.4***	***31.5***	***122.1***	***35.5***	***8.3***
SD	3.1	2.6	172	36	33	147	32	29
p-value	0.201	0.285	0.005	0.013	0.22	0.005	0.014	0.721

https://doi.org/10.1371/journal.pone.0174788.t003

Friction moments M_{res}

Time patterns: The friction moment M_{res} had a different time behavior than F_{res} and revealed only one maximum at or shortly after CHS (Fig 1). During step 1, M_{res} rose sharply after heel strike until CTO, while F_{res} increased, and then changed only a little until CHS (Fig 2). In contrast to this, M_{res} increased nearly linearly between HS and CHS during the following steps. After CHS, M_{res} always fell, approximately until the joint movement changed from extension to flexion. This instant was controlled by the synchronous videos. Then, it rose to an intermediate peak value, most pronounced for step 1, and continuously fell until the step ended. During the entire cycle time, M_{res} was higher during step 1 than later.

Numerical values: In all *subjects*, except H10R, all three moment values, M_{CTO}, M_{CHS} and M_{max} were higher during step 1 than later (Table 2). The *individual* variations of all three moments, were large. For step 1, for example, the standard deviations were 39%, 38% and 33% of the average values. The small red circles shown in Fig 3 illustrate the huge range of *individual* values of M_{CHS} during step 1. During the next three steps the standard deviations were even higher. In the *average* subject, however, uniform step to step changes were observed (Table 2). M_{CTO} fell from step to step (Fig 3) and was most pronounced from step 1 to 2. With 143% ($p = 0.005$), the surplus from step 1 relative to step 4 was very large (Table 3). M_{CHS} was much higher than M_{CTO} and decreased continuously but was less pronounced than M_{CTO} from step 1 to 2. The value during step 1 was only 35% ($p = 0.013$) higher than during step 4. The maximum moment M_{max} only slightly exceeded M_{CHS}. The step to step changes of M_{max} were similar to those of M_{CHS}, with a total surplus during step 1 of 32% relative to step 4. The moment courses in Fig 3 indicate that all three friction moments will probably only slightly decrease further after step 4.

Coefficient of friction μ

Time patterns: The charts of μ from the *average* subject (Figs 1 and 2) show that it was permanently higher during step 1 than during the following steps. During step 1, μ in the *average* subject already rose at HS and stayed at a high level after CTO. The rise during the following three steps only started after CTO. When hip flexion began, μ was nearly the same for all four steps. It then uniformly and sharply increased to the absolute maxima at around ipsilateral toe off (TO), which were more than twice as high than the values during the whole stance phases. After TO, μ continuously decreased during the remaining swing phase.

Numerical values: All three *individual* friction values, μ_{CTO}, μ_{CHS} and μ_{max}, varied a lot, as observed from the ranges and standard deviations in Table 2. In subject H10R, all three friction values were much higher than in all other patients. The *individual* values of $\mu_{CTO}|\mu_{CHS}$ exceeded the *average* ones by up to 176%|239%

In the *average* subject, μ_{CTO} was 122% ($p = 0.005$) higher during the first than during the last step (Table 3, Fig 3). For μ_{CHS}, this surplus was 36% ($p = 0.014$). The extreme *individual* surplus of μ_{CHS} from step 1 to 4 was 105%, observed in subject H7R. The maximum coefficient μ_{max} was on average by only 8% higher during step 1 than step 4. The declines in all three μ values with the step number (Fig 3) was less pronounced than the drops observed for the moments. During step 2, μ_{max} was even larger than during step 1, an effect observed for six of the ten *individual* subjects.

Start phase

During the Start phase, the patterns of F_{res}, M_{res} and μ were different from those during step 1 (Fig 1). The numerical value of F_{start} (Table 2) was on average 48% lower, compared to F_{CTO} during step 1, with individual variations between -60% to -32%. The values $M_{start}|\mu_{start}$,

however, were on average 3%|7% higher, compared to F_{CTO} during step 1. However, these changes again varied a lot, with ranges of -49% to +135% for M_{start} and -51% to +50% for μ_{start}.

Rest times

No or very poor correlations existed between the individually averaged rest times (Table 1) and the six values of M_{res} and μ (Table 3); R^2 was always below 0.23.

Discussion

High friction moments in hip implants increase wear in the joint, especially during the early postoperative weeks, when the fixation stability of cementless implants is lower than later; high friction moments can possibly also endanger the fixation of the cup. It was shown [30] that the peak friction moment during some activities can already reach values that were reported in the literature to jeopardize the cup fixation. [24,25] It has been reported that the *in vitro* friction moments are higher during the first loading cycle after a rest than during continuous movement. This indicated that frequently increased moments after rests might increase the risk for cup loosening or lead to more wear. Because the test conditions in these studies were not realistic, we examined whether the friction moments and the coefficient of friction are higher *in vivo* when walking starts after a rest.

With regard to the reported large individual variations of all load parameters, the average values cannot be generalized. The friction coefficient μ_{CTO}, for example, was by 542% larger during step 1 than step 4 in one subject, but by only 16% in another one. The low significance of the load changes is indicated by the low p-values in Table 2. However, decreases of all moments and friction coefficients except μ_{max} were observed in at least eight of ten subjects. Therefore, the moment and friction increases after a rest prior to walking can be expected for the majority of subjects, but their extend cannot be predicted exactly for a specific individuum. Other limitations to this study are the small number of ten investigated subjects and that only one tribological paring was investigated (Al_2O_3/XPE).

Friction moment and coefficient

During the first step after standing, the friction moment M_{res} at the instant of the first|second force maximum was 143%|35% higher than during step 4. At the same time, the friction coefficient μ from step 1 exceeded that from step 4 by 122%|36%. This means that the decreases of M_{res} and μ throughout the first four steps are approximately proportional.

Figs 1 and 2 show that M_{res} and μ, during the initial step, rise sharply after heel strike, when the contact force F_{res} increases, and stay at increased levels until the CHS, when F_{res} falls again. This behavior is in sharp contrast to the changes of M_{res} and μ during continuous walking (assumed to be represented by step 4), when both measures increase continuously throughout the whole stance phase. The force F_{res} during step 1 is only initially higher than later.

Possible explanations for these observations are as follows: During the initial rest, all or most of the synovia is squeezed out of the joint, leading to a nearly non-lubricated contact between head and cup surfaces. Throughout the first step, until toe off, no synovia can be transported back into the contact zone because this area is pressurized by the high contact force F_{res}. When F_{res} falls after toe off, the joint movement during the swing phase transports synovia back into the joint. The second and all following steps, therefore, start with a sufficient lubricating film. The high contact force then again reduces the lubricating film throughout the stance phase, which leads to the continuous increase of M_{res} and μ. The high values of F_{res} in the beginning of step 1 are probably required for accelerating the body to walking speed.

If these explanations are valid, the friction moments during the one legged stance, when small joint movements cannot be avoided, should also be high. This assumption is confirmed by some exemplary measurements in the public data base OrthoLoad.com (parameters: Implant = 'Hip Joint III' and Activity = 'One Legged Stance'). Such high moments will be the focus of a future study.

With 0.045|0.057, the *average* values of $\mu_{CTO}|\mu_{CHS}$ during step 1 were very close to the maximum of 0.055 found in simulator tests [25]. Only μ_{max}, acting at TO when F_{res} had already fallen to approximately one-third of the two maxima, was three times higher than this literature value. Because all three μ values have fallen to nearly constant levels until step 4; the numbers from this step can be compared to those previously reported for continuous walking [22,23].

All subjects received implants with the same tribological pairing (Al_2O_3/XPE). Nevertheless, the friction moments and the coefficients of friction *individually* varied a lot. Data from step 4, assumed to be representative for continuous walking, demonstrated variations of $M_{CTO}|M_{CHS}|M_{max}$ by factors of 10|5|4. For $\mu_{CTO}|\mu_{CHS}|\mu_{max}$, these factors were nearly identical. Subject H10R especially stands out as the moment and coefficient values were always extremely higher than those in the other subjects. The three values of M_{res} and μ for H10R exceeded the averages from all subjects by up to 167%|239%. Such large variations are probably caused by different individual lubrication conditions, which can be influenced by (i) the lubricating quality of the synovia [14], (ii) the roughness of the gliding surfaces [14,32], (iii) the joint clearance [14,32,33] and (iv) the orientation of the acetabular cup [14,34], which influences the load transmitting area. Data on the impact of other factors, such as the sliding speed or joint contact area, will be investigated in a further study.

Wear

Frequent reasons for revisions of hip joint replacements are still wear and pathological reactions to wear particles [2,5,35]. Simulator studies demonstrated a correlation between the friction between sliding partners and the wear rates [33]. In theory, increased friction moments and coefficients during the first step of walking could, therefore, increase the wear. However, during walking and other repetitive activities, a single starting cycle with high moments is typically followed by many continuous loading cycles with lower moments. Because the wear volume not only depends on the height of the friction moment but also on the number of loading cycles, much increased wear due to increased moments after rest should not be expected.

Cup loosening

The primary and long-term stability of the cup fixation depends, except for the height of the friction moments, on the quality of the cup-bone interface, the fixation technique, the type of porous coating and the bone quality. Simulator studies demonstrated that insufficient under-reaming of the acetabulum decreases the primary fixation stability (Curtis M. J. et al., 1992; Tabata et al., 2015). With an under-reaming of only 1 mm, the loosening moments lay between 2.2 and 8.8 Nm. The *average* maximum moment of M_{res} = 2.15Nm (0.236%BWm, assumed BW = 1000 N), reported here for step 1 just meets the lowest reported value. However, the highest *individual* moment from subject H10L was 4.28 Nm (0.43%BWm, BW = 995 N) and this is much higher than the lowest stability level reported in the literature.

An additional risk factor, not considered in the current study, is the fact that joint friction changes during the first months after replacement (Damm et al. 2015). Three months after surgery, M_{res} was on average by 47% higher than after 12 months. The extreme moment value in H10L would then have further risen to 6.33 Nm. Possible factors for higher postoperative

friction may be a still lacking smoothening of the gliding surfaces and initially insufficient synovia properties. Therefore, even higher values than reported here must be expected shortly after surgery.

The high maximum *in vivo* friction moments and the lowest reported *in vitro* loosening moments together indicate that the higher moments at the beginning of walking can put the cup fixation at risk in subjects with high body weight, inferior lubricating properties of the synovia and cementless cups, which are inserted with too small under-reaming. This risk is highest during the first postoperative months.

Joint temperature

High temperatures in artificial joints could be a potential risk factor for the longevity of the implant system. For the combination of conventional polyethylene and ceramic cups with ceramic and metal heads, friction-induced temperature increases up to 43.1 °C after one hour of walking were reported [36]. These increases varied dramatically and individually, depending on the lubrication properties of the synovia [37] and the tribological materials.

By the same reasons as for the wear a distinct influence of increased moments after breaks on the implant temperature during walking can be excluded. However, the current study again demonstrates that friction moments and coefficients are extremely varied from person to person. The three moment measures individually differed by factors of 4 to 10. A factor of four approximately corresponds to the individual differences of temperature increases measured *in vivo* during walking [36]. The higher factor of ten let us assume that the implant temperature may rise much more in some subjects than observed previously.

Head-stem connection

Friction influences the mechanical stress in the head-neck taper region and, if existent, the neck-stem connection. Up to 143% higher friction moments after a rest, compared to continuous walking, will lead to an increase of these stresses. Therefore, higher friction after a rest can be a potential risk factor for the mechanical stability of suboptimal taper connections. If the mechanical connection becomes loose, micromotion between the components increases and this begins a corrosion cascade [38,39] that can eventually cause implant loosening. Furthermore, increased wear and corrosion products provoke various biological and chemical effects in the surrounding tissues [39,40], which also lead to implant failure.

Conclusion

It was demonstrated that hip joint friction during the first step of walking after a rest is much higher than that during continuous movement. The initial friction moments were raised on *average* by 35% to 143% and *individually* by up to 621% compared to continuous walking.

Wear and cup loosening

The higher moments will probably increase wear in the joint only very slightly, but they can endanger the fixation of the cup in the acetabulum. This risk is highest for cementless cups with insufficient under-reaming and during the first postoperative months.

Head-stem connection

The high moments when walking begins can also put taper connections between the head and neck and between the neck and shaft at a higher risk.

Joint temperature

In five subjects, friction-induced temperature increases up to 43.1°C were observed in hip implants during continuous walking [36]. There was much individual variation, and this was explained by different lubricating properties of the synovia. The measured friction moments during continuous walking, reported here, *individually* varied by factors up to 10, which is more than the differences of the reported temperature increases. Therefore, it seems worthwhile to perform another investigation with a larger group of patients to determine whether even higher implant temperatures during walking may endanger the long-term outcome of the replacement.

Additional data

Selected examples of the *in vivo* measurements, on which this study was based, are published in the public data base www.orthoload.com.

Acknowledgments

This work was supported by Deutsche Forschungsgemeinschaft (Be 804/19-1), the German Federal Ministry of Education and Research (BMBF 01EC1408A; Overload-PrevOP; SPO3), Deutsche Arthrose-Hilfe and OrthoLoad Club.

The funders had no role in study design, data collection and analysis, decision to publish, or preparation of the manuscript.

Author Contributions

Conceptualization: PD GD GB.

Data curation: PD AB GB.

Formal analysis: PD AB.

Funding acquisition: PD GD GB.

Investigation: PD.

Methodology: PD AB GB.

Project administration: PD GD GB.

Resources: PD AB.

Software: AB.

Supervision: PD GD GB.

Validation: PD.

Visualization: PD AB.

Writing – original draft: PD GB.

Writing – review & editing: PD AB GD GB.

References

1. OECD. Health at a Glance 2015 [Internet]. Organisation for Economic Co-operation and Development; 2015.
2. Bergen H. Annual Report 2010—Norwegian Arthroplasty Register. 2010.

3. David D, Graves S, Tomkins A. Australien Orthopaedic Association National Joint Replacement Registry. Anual Report. Adelaide:AOA; 2013. 2013.
4. Garellick G, Karrholm J, Rogmark C, Rolfson O, Herberts P. Swedish Hip Arthroplasty Register—Annual Report 2011. 2011.
5. CJRR. CJRR report: Total hip and total knee replacements in Canada. Canadian Institute for Health Information. 2008.
6. Havelin LI, Fenstad AM, Salomonsson R, Mehnert F, Furnes O, Overgaard S, et al. The Nordic Arthroplasty Register Association: a unique collaboration between 3 national hip arthroplasty registries with 280,201 THRs. Acta Orthop. 2009; 80: 393–401. https://doi.org/10.3109/17453670903039544 PMID: 19513887
7. Liao Y. The effect of frictional heating and forced cooling on the serum lubricant and wear of UHMW polyethylene cups against cobalt—chromium and zirconia balls. Biomaterials. 2003; 24: 3047–3059. PMID: 12895577
8. Brockett C, Williams S, Jin Z, Isaac G, Fisher J. Friction of Total Hip Replacements With Different Bearings and Loading Conditions. J Biomed Mater Res. 2006; 508–515.
9. Affatato S, Spinelli M, Zavalloni M, Mazzega-Fabbro C, Viceconti M. Tribology and total hip joint replacement: current concepts in mechanical simulation. Med Eng Phys. 2008; 30: 1305–17. https://doi.org/10.1016/j.medengphy.2008.07.006 PMID: 18774742
10. Hall RM, Unsworth A. Review Friction in hip prostheses. Biomaterials. 1997; 18: 1017–1026.
11. Scholes SC, Unsworth A. The effects of proteins on the friction and lubrication of artificial joints. Proc Inst Mech Eng Part H J Eng Med. 2006; 220: 687–693.
12. Scholes SC, Unsworth A, Hall RM, Scott R. The effects of material combination and lubricant on the friction of total hip prostheses. Wear. 2000; 241: 209–213.
13. Fialho JC, Fernandes PR, Eça L, Folgado J. Computational hip joint simulator for wear and heat generation. J Biomech. 2007; 40: 2358–2366. https://doi.org/10.1016/j.jbiomech.2006.12.005 PMID: 17270192
14. Mattei L, Di Puccio F, Piccigallo B, Ciulli E. Lubrication and wear modelling of artificial hip joints: A review. Tribol Int. Elsevier; 2011; 44: 532–549.
15. Saikko V. A simulator study of friction in total replacement hip joints. Proc Inst Mech Eng Part H J Eng Med. 1992; 206: 201–211.
16. Scholes SC, Unsworth A. Comparison of friction and lubrication of different hip prostheses. Proc Inst Mech Eng Part H J Eng Med. 2000; 214: 49–57.
17. Unsworth A. The effects of lubrication in hip joint prostheses. Phys Med Biol. 1978; 23: 253–68. PMID: 643921
18. Williams S, Jalali-Vahid D, Brockett C, Jin Z, Stone MH, Ingham E, et al. Effect of swing phase load on metal-on-metal hip lubrication, friction and wear. J Biomech. 2006; 39: 2274–81. https://doi.org/10.1016/j.jbiomech.2005.07.011 PMID: 16143337
19. Curtis MJ, Jinnah RH, Valerie WD, Hungerford DS. The initial stability of uncemented acetabular components. Br Editor Sov Bone Jt Surg. 1992; 74–B: 372–376.
20. Tabata T, Kaku N, Hara K, Tsumura H. Initial stability of cementless acetabular cups: press-fit and screw fixation interaction—an in vitro biomechanical study. Eur J Orthop Surg Traumatol orthopeédie Traumatol. 2015; 25: 497–502.
21. Damm P, Graichen F, Rohlmann A, Bender A, Bergmann G. Total hip joint prosthesis for in vivo measurement of forces and moments. Med Eng Phys. 2010; 32: 95–100. https://doi.org/10.1016/j.medengphy.2009.10.003 PMID: 19889565
22. Damm P, Dymke J, Ackermann R, Bender A, Graichen F, Halder A, et al. Friction in total hip joint prosthesis measured in vivo during walking. PLoS One. 2013; 8: e78373. https://doi.org/10.1371/journal.pone.0078373 PMID: 24260114
23. Damm P, Bender A, Bergmann G. Postoperative changes in in vivo measured friction in total hip joint prosthesis during walking. PLoS One. 2015; 10: e0120438. https://doi.org/10.1371/journal.pone.0120438 PMID: 25806805
24. Nassutt R, Wimmer MA, Morlock MM. The Influence of Resting Periods on Friction in the Artificial Hip. 2003; 127–138.
25. Morlock M, Nassutt R, Wimmer M, Schneider E. Influence of Resting Periods on Friction in Artificial Hip Joint Articulations. Bone. 2000; 6–16.
26. Morlock M, Schneider E, Bluhm A, Vollmer M, Bergmann G. Duration and frequency of every day activities in total hip patients. 2001; 34: 873–881.

27. Graichen F, Arnold R, Rohlmann A, Bergmann G. Implantable 9-channel telemetry system for in vivo load measurements with orthopedic implants. IEEE Trans Biomed Eng. 2007; 54: 253–61. https://doi.org/10.1109/TBME.2006.886857 PMID: 17278582

28. Graichen F, Bergmann G. Four-channel telemetry system for in vivo measurement of hip joint forces. J Biomed Eng. 1991; 13: 370–374. Available: http://www.ncbi.nlm.nih.gov/entrez/query.fcgi?cmd=Retrieve&db=PubMed&dopt=Citation&list_uids=1795503 PMID: 1795503

29. Wu G, Siegler S, Allard P, Kirtley C, Leardini A, Rosenbaum D, et al. ISB recommendation on definitions of joint coordinate system of various joints for the reporting of human motion—part I: ankle, hip, and spine. J Biomech. 2002; 35: 543–548. PMID: 11934426

30. Bergmann G, Bender A, Dymke J, Duda G, Damm P. Standardized Loads Acting in Hip Implants. PLoS One. 2016; 11: e0155612. https://doi.org/10.1371/journal.pone.0155612 PMID: 27195789

31. Bender A, Bergmann G. Determination of typical patterns from strongly varying signals. Comput Methods Biomech Biomed Engin. 2012; 15: 761–9. https://doi.org/10.1080/10255842.2011.560841 PMID: 21722048

32. Jalali-Vahid D, Jagatia M, Jin ZM, Dowson D. Prediction of lubricating film thickness in UHMWPE hip joint replacements. J Biomech. 2001; 34: 261–6. PMID: 11165292

33. Wang A, Essner A, Klein R. Effect of contact stress on friction and wear of ultra-high molecular weight polyethylene in total hip replacement. Proc Instn Mech Engrs. 2001; 215: 133–139.

34. Patil S, Bergula A, Chen PC, Colwell CW, D'Lima DD. Polyethylene Wear and Acetabular Component Orientation. J Bone Jt Surg. 2003; 85: 56–63. Available: http://jbjs.org/content/85/suppl_4/56.abstract

35. Adelaide:AOA. Australien Orthopaedic Association National Joint Replacement Registry. Annu Rep. 2013; 381: 1600–1602.

36. Bergmann G, Graichen F, Rohlmann A, Verdonschot N, van Lenthe GH. Frictional heating of total hip implants. Part 1: measurements in patients. J Biomech. 2001; 34: 421–8. PMID: 11266664

37. Bergmann G, Graichen F, Rohlmann A, Verdonschot N, van Lenthe GH. Frictional heating of total hip implants. Part 2: finite element study. J Biomech. 2001; 34: 429–35. PMID: 11266665

38. Collier JP, Surprenant VA, Jensen RE, Mayor MB, Surprenant HP. Corrosion between the components of modular femoral hip prostheses. J Bone Jt Surg. 1992; 74: 511–517.

39. Palmisano AC, Nathani A, Weber AE, Blaha JD. Femoral neck modularity: A bridge too far—Affirms. Semin Arthroplasty. 2014; 25: 93–98.

40. Weber AE, Blaha JD. Femoral neck modularity: A bridge too far. Semin Arthroplasty. 2013; 24: 71–75.

2.4. Einfluss von Kinematik und Belastung auf die Gelenkreibung

Der Anspruch an das Aufrechterhalten des Freizeitsports auch nach dem Gelenkersatz spielt für die Lebensqualität jüngerer Patienten eine immer größere Rolle. Dieser Umstand wird aktuell auch als ein potenzieller Risikofaktor für zukünftig höhere Versagensraten der Gleitpartner in dieser Patientengruppe diskutiert (Johnsen 2006). Die Ansichten darüber, welche Aktivitäten als kritisch bzw. unkritisch für die langfristige Funktion des künstlichen Gelenkersatzes einzuordnen sind, sind jedoch sehr unterschiedlich (W. L. Healy et al. 2008; Healy, Iorio, and Lemos 2001; Klein et al. 2007; Laursen et al. 2014; Swanson, Schmalzried, and Dorey 2009). Darüber hinaus ist die tatsächlich in vivo auftretende Gelenkreibung bei den so empfohlenen Aktivitäten bisher völlig unbekannt. Im Rahmen der folgenden Studie konnten wir zeigen, dass einbeinige und sportliche Aktivitäten mit hoher statischer Vorlast kritische Reibmomente für die Pfannenstabilität zur Folge haben können. Der nachfolgende Text entspricht dem Abstract der Arbeit *„Physical Activities that Cause High Friction Moments at the Cups of Hip Implants"*, welche im "Journal of Bone and Joint Surgery" 2018 veröffentlicht wurde:

"Background: High friction moments in hip implants contribute to the aseptic loosening of cementless cups in about 100,000 cases per year. Own findings and literature data suggested that sustained joint loading may cause such high moments. The most critical physical activities were identified in this study.

Methods: Friction moments in the cup were telemetrically measured 33,014 times in endoprostheses of nine subjects during 1,438 different activities. The highest moments were compared to the cup's fixation stability of approximately 4Nm.

Results: 124 different activities could cause friction moments above the critical limit, with a highest value of 11.5Nm. Most of them involved sustained high contact forces before or during the activity. The highest peak moments (11.5 to 6.3Nm) occurred when moving the contralateral leg during one-legged stance; during breaststroke swimming, muscle stretching or muscle contraction; during two-legged stance and during static one-legged stance. The median moments were highest (3.9 to 3.4Nm) for unstable one-legged stance, whole body vibration training, stance with an unexpected push at the upper body, one-legged stance plus exercises with the opposite leg and running after stance.

Conclusions: Frequent unloading plus simultaneous movement of the joint are required to maintain good joint lubrication and keep the friction moments low. Frequent, sustained high loads before or during an activity may cause or contribute to aseptic cup loosening. During the first postoperative months after hip arthroplasty, such activities should be avoided or reduced as much as possible. This especially applies for postoperative physiotherapy or when returning to sport after a hip replacement. Whether these guidelines also apply for subjects with knee implants or arthrotic hip or knee joints requires future investigation.

Clinical Relevance: Avoiding sustained loading of hip implants without joint movement reduces the risk of aseptic cup loosening."

Publikation: Physical Activities that Cause High Friction Moments at the Cups of Hip Implants

Bergmann G., Bender A., Dymke J., Duda N. G., Damm P.
Journal of Bone and Joint Surgery (JBJS), 2018; 100:1637-44
http://dx.doi.org/10.2106/JBJS.17.01298

2.5. Zusammenhang von Implantat-Orientierung und Gelenkreibung

Als weitere potentielle Versagensgründe werden neben der in vivo wirkenden Gelenkreibung (Damm, Bender, et al. 2017a; Damm, Jörn Dymke, et al. 2013; Damm, Bender, and Bergmann 2015b) und dem sich daraus ergebenden Abrieb insbesondere auch Fehlpositionierungen der Implantat-Komponenten diskutiert (Kennedy et al. 1998; Korduba et al. 2014; Nevelos et al. 2001; Wan et al. 2008). Aus technischer Perspektive ist die Reibung zwischen zwei Gleitpartnern zum einen abhängig von der verwendeten Gleitpaarung, zum anderen aber auch von der lasttragenden Kontaktfläche, also der individuellen Gelenküberdachung und somit von der individuellen Implantat-Orientierung (Kennedy et al. 1998; Korduba et al. 2014). Die intraoperative Positionierung innerhalb einer „Safe Zone“ soll das Risiko eine Gelenkluxation reduzieren, aber auch eine optimale und größtmögliche Gelenküberdachung im Alltag gewährleisten. So soll das Risiko von Randbelastungen reduziert und das reibungs- und belastungsinduzierte Revisionsrisiko des Gelenkersatzes minimiert werden (Kennedy et al. 1998; Korduba et al. 2014; Lewinnek et al. 1978; Nevelos et al. 2001; Wan et al. 2008). Allerdings zeigten retrospektive Versagensanalysen keinen Unterschied zwischen den Revisionsraten von Pfannen, die innerhalb bzw. außerhalb einer solchen „Safe Zone“ implantiert wurden (Abdel et al. 2016; Parratte et al. 2016). Weitere Studien zeigen darüber hinaus, dass der reibungsinduzierte Abrieb im künstlichen Gelenkersatzes wiederum direkt durch die individuelle Gelenküberdachung beeinflusst wird (Nevelos et al. 2001; Wan et al. 2008). Im Rahmen eines kombinierten Ansatzes aus retrospektiver Datenanalyse und prospektive geplanter in-vivo-Messung des reibungsinduzierten Temperaturanstieges beim kontinuierlichen Gehen auf dem Laufband bis zu 60 min, wurde der Einfluss der individuellen Gelenküberdachung auf die in vivo wirkende Gelenkreibung und den reibungsinduzierten Temperaturanstieg im Gelenk untersucht.

Es konnte gezeigt werden, dass der Summen-Anteversionswinkel (Pfanne + Schaft) die Gelenkreibung und darüber hinaus den reibungsinduzierten Temperaturanstieg im Gelenk signifikant beeinflusst. Mit anderen Worten, je zentraler die Lage der individuellen Belastungszone in der Pfanne bzw. umso größer die lasttragende Gelenkkontaktfläche, umso höher die in vivo gemessene Gelenkreibung und der sich daraus ergebende reibungsinduzierte Temperaturanstieg im Hüftgelenk.

Der nachfolgende Text entspricht dem Abstract der Arbeit *„ Surgical cup placement affects the heating up of total joint hip replacements"*, welche 2021 bei "Scientific Reports" veröffentlicht wurde:

"The long-term success of highly effective total hip arthroplasty (THA) is mainly restricted by aseptic loosening, which is widely associated with friction between the head and cup liner. However, knowledge of the in vivo joint friction and resulting temperature increase is limited. Employing a novel combination of in vivo and in silico technologies, we analyzed the hypothesis that the intraoperatively defined implant orientation defines the load carrying area, friction and its associated temperature increase. A total of 38,000 in vivo activity trials from a special group of 10 subjects with instrumented THA implants with an identical material combination were analyzed and showed a significant link between implant orientation, joint kinematics, load carrying area and friction-induced temperature increase but surprisingly not with acting joint contact force magnitude. This combined in vivo and in silico analysis revealed that cup placement in relation to the stem is key to the in vivo joint friction and heating-up of THA. Thus, intraoperative placement, and not only articulating materials, should be the focus of further improvements, especially for young and more active patients."

Publikation: Surgical cup placement affects the heating up of total joint hip replacements

Damm P., Bender A., Waldheim V., Winkler T., Duda G. N.

Scientific Reports, 2021, https://doi.org/10.1038/s41598-021-95387-8

3. Diskussion

Die rekonstruktive Hüftgelenkchirurgie ist heute eine der erfolgreichsten orthopädischen Verfahren (Learmonth et al. 2007), die es unzähligen Patienten ermöglicht, nach Arthrose oder Fraktur wieder ein schmerzfreies und aktives Leben zu führen. In den letzten Jahren ist jedoch das Patientenspektrum, welches mit einem solchen Gelenkersatz versorgt wird, immer jünger und auch aktiver geworden (Australian Orthopaedic Association National Joint Replacement Registriy (AOANJRR) 2019; Bashinskaya et al. 2012; Canadian Institute for Health Information 2019; Culliford et al. 2015; Danish Hip Arthroplasty Register 2020; Dutch Arthroplasty Register (LROI) 2019; Finnish Arthroplasty Register for National Institute of Health And Welfare 2020; Hepinstall et al. 2011; Koenen et al. 2014; Nemes et al. 2014; Norwegian National Advisory Unit Report on Arthoplasty and Hip Fractures 2019; Oehler, Schmidt, and Niemeier 2016; Pabinger and Geissler 2014; Pilz, Hanstein, and Skripitz 2018; Sloan, Premkumar, and Sheth 2018; Swedish Hip Arthroplasty Register 2019b; United Kingdom National Joint Registry 2019b). Der überwiegende Teil dieser Patienten möchte darüber hinaus bereits kurz nach der Operation wieder körperlich aktiv und insbesondere auch wieder sportlich aktiv sein (Abe et al. 2014; Arbuthnot et al. 2007; Batailler et al. 2019; Dubs, Gschwend, and U 1983; Ghomrawi et al. 2011; Hara et al. 2018; Hatterji et al. 2004; Hoorntje et al. 2018; Huch et al. 2005; Innmann et al. 2016; Jassim et al. 2019; Karampinas et al. 2017; Koenen et al. 2014; Lefevre et al. 2013; Mancuso et al. 2017; C. A. Mancuso et al. 2009; Meek et al. 2020; Mont et al. 1999; Ortmaier et al. 2019; Del Piccolo et al. 2016; Raguet, Pierson, and Pierson 2015; Schmidutz et al. 2012; Scott et al. 2012; Suckel and Best 2006). Die Ansichten darüber, welche Aktivitäten als kritisch bzw. unkritisch für die langfristige Funktion des künstlichen Gelenkersatzes sind, gehen jedoch weit auseinander und so werden Patienten oft sehr unterschiedliche Empfehlungen für die postoperative Rehabilitation gegeben, bzw. welche Sportarten für Endoprothesen-Patienten geeignet sind, ohne die individuelle Implantat-Stabilität und -Lebensdauer zu gefährden (Georg Bergmann et al. 2016; Bohannon 2007; Golant et al. 2010; W. L. Healy et al. 2008; Healy et al. 2001; Hernandez-Molina et al. 2009; Hoorntje et al. 2018; Klein et al. 2007; Koenen et al. 2014; Krismer 2017; Kuster 2002; Laursen et al. 2014; Oehler et al. 2016; Schneider et al. 2006; Swanson et al. 2009; Tudor-Locke et al. 2008; Widhalm et al. 1990).

In den vergangenen Dekaden war vor allen Dingen die aseptische Lockerung des Gelenkersatzes der häufigste Grund für die Notwendigkeit der Durchführung von Revisionsoperationen (Australian Orthopaedic Association National Joint Replacement Registriy (AOANJRR) 2019; Burke et al. 2019; United Kingdom National Joint Registry 2019b). Trotz enormer Anstrengungen in Forschung und Entwicklung ist jedoch die tatsächliche Ursache für ein solches Implantat-Versagen immer noch nicht eindeutig geklärt. Angesichts der aktuell wieder zu beobachtenden Zunahme von Revisionsfällen (Lee E. Bayliss et al. 2017b; Sean S Rajaee et al. 2018b) sind somit neue Perspektiven notwendig, um die individuellen Ursachen für das Versagen von Endoprothesen-Systemen differenzierter zu betrachten und biomechanisch einordnen zu können.

Während die Reibung zwischen den Gelenkkomponenten zwar seit langem als primärer Risikofaktor für das Überleben des Gelenkersatzes im Mittelpunkt der orthopädisch-biomechanischen Forschung steht, ist das Wissen über die tatsächlich in vivo wirkende Reibung hierzu immer noch sehr begrenzt. Unterschiedliche in-vitro- und ex-vivo-Ansätze konnten zwar wesentlich dazu beitragen, die technische Standzeit von Hüftgelenksprothesen signifikant zu verbessern, jedoch ist trotz dessen die aseptische Lockerung weiterhin einer der Hauptgründe für die Durchführung von Implantat Revisionen (Australian Orthopaedic Association National Joint Replacement Registry (AOANJRR) 2019; Bergen 2019; CJRR 2008; Grimberg et al. 2020; Leif I Havelin et al. 2009; Huch et al. 2005; NJR Editorial Board NJRSC 2019). Ein besseres und differenzierteres Verständnis der in-vivo-Bedingungen, welche die Gelenkreibung und den daraus resultierenden Gelenkabrieb verursachen, ist daher dringend erforderlich.

Für die systematische Erfassung der tatsächlich in vivo auftretenden Gelenkreibung, stellen instrumentierte Implantate, welche die wirkende Gelenkbelastung direkt in vivo messen, eine einzigartige technische Möglichkeit dar. Zu Beginn meiner wissenschaftlichen Arbeiten konnte ich am Julius Wolff Institut, gemeinsam mit der Arbeitsgruppe um Prof. Dr. Bergmann, ein instrumentiertes Hüftimplantat entwickeln, mit dem es weltweit erstmals möglich war, die in vivo auftretende Reibung im Hüftgelenkersatz direkt zu messen (Damm et al. 2010b). Nach umfangreichen mechanischen, biologischen und toxikologischen Prüfungen wurde dieses spezielle Implantat für die Anwendung am Menschen im Rahmen einer klinischen

Langzeitstudie zugelassen und zertifiziert. Im weiteren Verlauf des Projektes konnten so anschließend zehn besonders aktive Patienten mit symptomatischer Coxarthrose, welche für die Implantation eine Hüftendoprothese bereits indiziert waren, in die Studie eingeschlossen und mit diesem speziellen Mess-Implantat versorgt werden (DRKS-ID: DRKS00000563).

Mit allen Probanden wurden anschließend im postoperativen Verlauf von mehr als 10 Jahren, systematische in-vivo-Belastungsmessungen bei unterschiedlichsten Aktivitäten durchgeführt. So konnten seit Studienbeginn bereits mehr als 40.000 in-vivo-Belastungsdatensätze, bei insgesamt mehr als 1400 unterschiedlichsten Aktivitäten erhoben werden. Auf dieser Grundlage war es unter anderem möglich, erstmals systematische Daten zu den in vivo wirkenden Gelenkbelastungen bei Physiotherapie und Rehabilitation (Damm, Schwachmeyer, et al. 2013; Schwachmeyer et al. 2013) und alltäglichen Aktivitäten (Angelini et al. 2018; G. Bergmann et al. 2016; Damm et al. 2017, 2020), als auch bei sportlichen Aktivitäten (Bergmann, Kutzner, et al. 2018; Damm et al. 2017; Haffer et al. 2021; Palmowski et al. 2021) in internationalen Fachzeitschriften zu publizieren. Im Zuge weiterer biomechanischer Grundlagenforschungen konnte darüber hinaus der Einfluss des individuellen und intraoperativ gesetzten Muskelschadens auf die individuelle in vivo wirkende Gelenkbelastungen untersucht und beschrieben werden (Damm et al. 2018, 2019).

Im Rahmen weiterer unmittelbarer Forschungskooperationen, unter anderem mit dem Helmholtz-Institut für Biomedizinische Technik der RWTH Aachen, wurden die in vivo erhobenen Gelenkbelastungsdaten darüber hinaus für die Entwicklung bzw. Weiterentwicklung präoperativer Planungstools, als auch zur Evaluation von unterschiedlichen Mehrkörper-Simulationsmodellen für die numerischen Bestimmung der individuellen Gelenkbelastungen genutzt (Asseln et al. 2013; Fischer et al. 2018, 2021).

Um Orthopäden, Physiotherapeuten, Patienten und interessierten Laien, aber auch der Industrie und biomechanischen Forschung einen unmittelbaren Zugang zu den erhobenen Belastungsdaten zu ermöglichen, wurden und werden im Rahmen meiner wissenschaftlichen Arbeiten kontinuierlich ausgewählte Beispiele der in-vivo-Hüftgelenkbelastungen in der freien und öffentlich zugänglichen in-vivo-

Belastungsdatenbank OrthoLoad.com veröffentlicht. Diese können unter Auswahl des Implantat-Typs „Hip Joint III“ bzw. bei Verwendung der Zugangs-URL: https://orthoload.com/database/?implantId=2355 ausgewählt, online dargestellt aber auch direkt heruntergeladen werden.

Die vorliegende Habilitationsschrift ist eine Zusammenfassung meiner wissenschaftlichen Arbeiten zum Thema der in vivo wirkenden Reibung im endoprothetischen Hüftgelenkersatz. Diese weltweit einmaligen in-vivo-Belastungs- und Reibdaten haben gezeigt, dass die Gelenkreibung im künstlichen Gelenkersatz ein individueller und hochdynamischer Belastungsparameter ist (Damm, Joern Dymke, et al. 2013). Bereits die postoperativ zeitnah durchgeführten Messungen beim Gehen zeigten, dass das in vivo auftretende Reibmoment im Verlauf eines Schrittes nicht konstant ist, sondern sich stetig ändert. Mit Hilfe typischer Simulator-Versuche konnte dies hingegen bisher nur sehr eingeschränkt abgebildet werden. So wurde beispielsweise in einigen Studien das Gelenk ausschließlich in einer Ebene bewegt, wobei durch eine sinusförmige Pendelbewegung die Beugung und Streckung simuliert werden sollte (Brockett et al. 2006; Saikko 1992; Scholes, Unsworth, and Goldsmith 2000; Williams et al. 2006). Weitere Bewegungsachsen wurden hierbei jedoch vernachlässigt.

Die im Rahmen meiner wissenschaftlichen Arbeiten in vivo erhobenen Daten zeigten allerdings, dass die resultierende Gelenkreibung beim Gehen auch wesentlich durch Ab/Adduktionsbewegungen beeinflusst wird. So hat das durch diese Bewegungsrichtung wirkende Gelenkmoment (M_y) mit ca. 45% einen großen Anteil an der gesamten in vivo auftretenden Gelenkreibung (M_{res}) (Damm, Joern Dymke, et al. 2013). Es konnte außerdem gezeigt werden, dass das resultierende Moment M_{res} beim Gehen im Verlauf des Lastzyklus, beginnend beim ipsilateralen bis hin zum kontralateralen Fersenkontakt kontinuierlich ansteigt. In-vitro-Daten, erhoben im Rahmen typischer Simulator-Versuche, zeigen hingegen während der Belastungsphase ein deutliches Reibungsplateau (Brockett et al. 2006; Williams et al. 2006), was darauf hindeutet, dass die verwendeten Parameter die in-vivo-Situation nur eingeschränkt abbilden.

Ungeachtet dessen konnte jedoch auch gezeigt werden, dass die maximalen in vivo auftretenden Reibmomente beim Gehen, die als Torsionsbelastung in das Pfanne-Knochen-Interface übertragen werden, die in der Literatur als kritisch beschriebenen

Grenzwerte nicht überschreiten (Adler, Stuchin, and Kummer 1992; Curtis M. J. et al. 1992; Fehring et al. 2014; Goriainov et al. 2014; Shim et al. 2006; Small et al. 2013; Tabata et al. 2015). Es kann somit gefolgert werden, dass die beim Gehen in der frühen postoperatven Phase auftretende Gelenkreibung kein mechanisch induzierter Riskofaktor für die frühe Pfannenstabilität ist.

In einem weiteren Analyseschritt wurde auf Basis der erhobenen in-vivo-Belastungsdaten außerdem erstmals der dreidimensional im Gelenk auftretende Reibungskoeffizient (μ_{res}) über den gesamten Bewegungszyklus bestimmt, um so einen Eindruck über die tatsächlich in vivo vorherrschenden Reib- und Schmierbedingungen zu erhalten (Damm, Joern Dymke, et al. 2013). Es konnte gezeigt werden, dass der Reibungskoeffizient beim Gehen im Verlauf eines Belastungszyklus nicht konstant ist, sondern sich ebenfalls kontinuierlich ändert. Er steigt, beginnend beim ipsilateralen Fersenkontakt bis hin zum kontralateralen Fersenkontakt, bzw. zum Beginn der ipsilateralen Hüftflexion kontinuierlich an und erreicht sein Maximum zu Beginn der Schwungphase. Diese sich wiederholenden Änderungen im Verlauf eines jeden Lastzyklus können mit einer wiederkehrenden Änderung der in vivo vorherrschenden Schmierbedingungen im Gelenk erklärt werden (Bishop, Hothan, and Morlock 2012; Hall et al. 1997; Scholes and Unsworth 2000; Unsworth 1978).

Numerische Studien mit hart/hart-Paarungen zeigten, dass sich die Dicke des Schmierfilms im Verlauf eines Gangzyklus in Abhängigkeit der Lastphase und der wirkenden Gelenkkontaktkraft signifikant ändert (Meyer and Tichy 2003b; Williams et al. 2006). Daraus ergab sich, dass eine hohe Kontaktkraft während der Schwungphase die Neubildung des Schmierfilms in dieser Phase hemmte oder sogar verhinderte, welche jedoch die für eine optimale Gelenkschmierung in der nachfolgenden Lastphase erforderlich wäre. Der in vivo beobachtete deutliche Anstieg des Reibkoeffizienten zu Beginn der Hüftflexionsphase kann daher mit einen Zusammenbruch des Schmierfilms erklärt werden, der bereits durch einen kurzzeitige Unterbrechung der Gelenk-Relativbewegung verursacht wird, ähnlich wie es bereits bei in-vitro-Versuchen beobachtet wurde (Morlock et al. 2000). Unter der Voraussetzung, dass sich diese Beobachtungen teilweise auch auf hart/weich-Paarung übertragen lassen, deuten die in-vivo-Daten darauf hin, dass der Schmierfilm beim Gehen aus dem Gelenkspalt herausgepresst, beim Übergang von Hüftextension

zu -flexion zusammenbricht, und anschließend während der Schwungphase wieder zurück in den Gelenkspalt transportiert wird.

Auf der Basis weiterer postoperativer in-vivo-Belastungsmessungen konnte des Weiteren erstmals gezeigt werden, dass die Gelenkreibung in den ersten 12 Monaten in vivo kontinuierlich abnimmt, wenn auch mit hoher inter-individueller Variabilität (Damm, Bender, and Bergmann 2015a). Diese Änderung kann einerseits durch individuelle mechanisch-tribologisch induzierte "Einlaufeffekte" der Gelenkpartner erklärt werden, die wiederum abhängig vom Aktivitätsprofil der Patienten sind. Andererseits bieten aber auch die individuellen Fluideigenschaften der Synovia im Gelenkspalt bzw. deren individuelle Änderung im postoperativen Verlauf hier einen möglichen Erklärungsansatz (Fam et al. 2007).

Die Schmiereigenschaften eines Fluides, insbesondere bei einem nicht-Newtonschen Fluid, hängen primär von Gleitgeschwindigkeit und Kontaktkraft und somit von der Scherbeanspruchung des Fluides ab (Balazs 1974; Fam et al. 2007; Hall and Unsworth 1997; Scholes and Unsworth 2000). Ein potentielles strukturviskoses Verhalten des Fluides wird wiederum durch die Menge des individuell enthaltenen Hyaluronsäure-Anteils bestimmt (Chikama 1985; Fam et al. 2007; Gao et al. 2011; Jebens and Monk-Jones 1959; Mazzucco et al. 2002). Da die Gang- und somit die Gleitgeschwindigkeit im Gelenk zu den betrachteten Zeitpunkten (3 versus 12 Monate) aufgrund ähnlicher Ganggeschwindigkeiten zu beiden Untersuchungszeitpunkten vergleichbar waren, kann die beobachtete Abnahme der Reibbelastung jedoch ebenso auf zeitlich bzw. biologisch induzierte Änderungen der individuellen Fluidviskosität hindeuten.

Der Effekt der Änderung der Schmierparameter und -filmdicke unter dem Einfluss statischer Belastungen ist in der technischen Tribologie hinlänglich bekannt (Byerlee 1970; Chen 2014). Insbesondere der sich daraus ergebende Effekt der Anlaufreibung zu Beginn einer Bewegung unter Last, wurde bereits in der Literatur auf Basis von Simulator-Versuchen berichtet (Morlock et al. 2000; Nassutt et al. 2003). Im Rahmen weiterer in-vivo-Belastungsmessungen wurde der bereits in vitro beobachtete Effekt der Anlaufreibung und dessen potentielle Konsequenzen für die Gelenkreibung systematisch untersucht (Damm, Bender, et al. 2017b). So konnte gezeigt werden, dass bereits eine kurze Gangpause von nur wenigen Sekunden, bei Wiederaufnahme

der Bewegung eine im Vergleich zum kontinuierlichen Gehen um bis zu dreifach höhere Gelenkreibung bei vergleichbarer Gelenkkontaktkraft zur Folge hat.

Die hier beobachtete Änderung der Reibung im Verlauf der ersten Schritte kann daher nur mit einer Änderung der individuellen Schmierbedingungen im Gelenk erklärt werden (Gao et al. 2011; Meyer and Tichy 2003b; Unsworth 1991). So wird während der Ruhephase und unter statischer Belastung der Schmierfilm abhängig von Last und Fluid-Viskosität aus dem Gelenk herausgedrückt und bricht infolgedessen zusammen. Im Verlauf der ersten Schritte gleiten dann beide Partner ‚ungeschmiert' aufeinander, da aufgrund der kontinuierlich wirkenden Gelenkkontaktkraft bis zu Beginn der ersten Schwungphase kein Fluid in die Kontaktzone zurücktransportiert werden kann. Im Verlauf der folgenden Schritte kann dann wieder ein Schmierfilm durch die Relativbewegung der Gleitpartner zueinander aufgebaut werden, was indirekt durch die Abnahme bzw. ‚Normalisierung' der in vivo gemessenen Gelenkreibung beobachtet werden kann.

Die zu Beginn der Ganges deutlich erhöhte Reibung überschreitet zwar nicht die in der Literatur beschriebenen Grenzwerte der maximalen zulässigen Torsionsbelastung für das Pfanne-Knochen-Interface (Adler et al. 1992; Curtis M. J. et al. 1992; Fehring et al. 2014; Goriainov et al. 2014; Shim et al. 2006; Small et al. 2013; Tabata et al. 2015), kann jedoch die Primärstabilität des Pfannenersatzes insbesondere bei einer suboptimal implantierten Pfanne gefährden (Curtis M. J. et al. 1992; Tabata et al. 2015).

Die Versorgung mit einem totalen Hüftgelenkersatz betrifft heute nicht nur ausschließlich ältere, sondern vermehrt auch immer jüngere (Nemes et al. 2020; Pabinger and Geissler 2014) und aktivere Patienten (U. Chatterji et al. 2004; W. L. Healy et al. 2008; Huch et al. 2005; B. C. A. Mancuso et al. 2009). Diese haben, neben dem primären Ziel der Schmerzfreiheit vermehrt auch den Anspruch, bereits kurz nach der Implantation nicht nur wieder frei gehen zu können, sondern möchten auch wieder sportlich aktiv sein (Lee E Bayliss et al. 2017; Flugsrud et al. 2007; Malchau et al. 2000; Sean S Rajaee et al. 2018a).

Die Ansichten darüber, welche Aktivitäten als kritisch bzw. unkritisch für die langfristige Funktion des künstlichen Gelenkersatzes einzuordnen sind, gehen jedoch weit auseinander (Bender et al. 2022). Es werden Patienten daher oft sehr unterschiedliche

Empfehlungen gegeben (Golant et al. 2010; W. L. Healy et al. 2008; Healy et al. 2001; Hernandez-Molina et al. 2009; Klein et al. 2007; Krismer 2017; Kuster 2002; Laursen et al. 2014; Swanson et al. 2009; Widhalm et al. 1990). Der Fokus weiterführender wissenschaftlicher Analysen lag daher in der Gesamtbetrachtung der in vivo Reibbelastungen aller bis zu diesem Zeitpunkt erhobenen Aktivitäten (Physiotherapie, Alltag, Sport) mit dem Ziel, solche Aktivitäten zu identifizieren, welche ein potentielles reibungsinduziertes Risiko für den kurzfristigen als auch langfristigen Implantat-Erfolg darstellen könnten. Im Zuge dieser Untersuchungen konnten bei allen Patienten mehrfach Aktivitäten identifiziert werden, bei denen die aus der Literatur bekannten mechanischen Grenzwerte für die postoperative Pfannenstabilität deutlich überschritten wurden (Adler et al. 1992; Curtis M. J. et al. 1992; Fehring et al. 2014; Goriainov et al. 2014; Shim et al. 2006; Small et al. 2013; Tabata et al. 2015) und die somit als potentielle Risiko-Aktivitäten für die frühe als auch langfristige Stabilität des Pfanne-Knochen-Interfaces betrachtet werden müssen (Bergmann, Bender, et al. 2018).

Die Ergebnisse dieser systematischen Analysen zeigten, dass bei ca. 9% aller betrachten Aktivitäten kritische Reibbelastungen für die langfristige, aber insbesondere auch für die primäre Pfannenstabilität auftraten. Hierzu zählten vor allem Aktivitäten mit anhaltend hohen Gelenkkontaktkräften bzw. Aktivitäten ohne Entlastungsphasen im Verlauf der Aktivität (z.B. Vibrationstraining). Demgegenüber wurde außerdem beobachtet, dass bei Aktivitäten mit hohen Lasten und schnellen Lastwechseln (z.B. Joggen) niedrigere Reibbelastungen auftreten, als bei Aktivitäten mit vergleichsweise kleinen Lasten aber langsamen Lastwechseln (z.B. Gehen). Dieser Effekt kann wiederum mit einer geschwindigkeitsabhängigen Änderung der individuellen Schmierbedingungen im Gelenk erklärt werden (Gao et al. 2011; Meyer and Tichy 2003b; Unsworth 1991) und deutet so auf ein vorwiegend strukturviskoses Fluid-Verhalten der Gelenk-Synovia hin (Fam et al. 2007; Mazzucco et al. 2002). Je höher die Gleitgeschwindigkeit, umso größer ist die geschwindigkeitsabhängige Scherbelastung des Fluides und desto dünnflüssiger wird es bzw. umso größer wird dessen Fließfähigkeit (Abbildung 4).

Es kann somit gefolgert werden, dass im Verlauf eines Bewegungszyklus (z.B. Joggen) der Schmierfilm zunächst, aufgrund der auf die Gleitflächen wirkenden Kontaktkraft, aus dem Gelenkspalt herausgepresst wird. Im weiteren Verlauf, während

der Entlastungsphase, bei der im Gelenkspalt höhere Gleitgeschwindigkeiten bei kleineren Kontaktkräften auftreten, erfolgt dann der Rücktransport des Fluides in den Gelenkspalt und der Aufbau eines neuen Schmierfilms. In der frühen postoperativen Phase, während der Mobilisation sollten daher eher dynamische Aktivitäten mit niedrigen Gelenkkontaktkräften und gleichmäßigen Lastwechseln durchgeführt werden (z.B.: Fahrradergometer). Aktivitäten mit hohen Gelenkkontaktkräften, langsamen Lastwechseln und großen Bewegungsumfängen sollten hingegen vermieden werden, um insbesondere die Implantat-Osseointegration nicht zu gefährden. Hierzu gehören vor allem einbeinig durchgeführte Aktivitäten, aber auch Aktivitäten mit konstant hoher Gelenkkontaktkraft und schnellen Lastwechseln (z.B.: Vibrationstraining).

Durch die eigenen Arbeiten konnte gezeigt werden, dass die Reibung im Hüftgelenkersatz von den verwendeten Gleitpartnern, den individuellen Schmierbedingungen als auch den durchgeführten Aktivitäten beeinflusst wird. (Bergmann, Bender, et al. 2018; Damm, Bender, et al. 2017b; Damm, Joern Dymke, et al. 2013; Damm et al. 2015a) Dies findet sich auch in der Literatur bestätigt (Affatato et al. 2008; Brockett et al. 2006; Fisher and Dowson 2016; Hall et al. 1997; Morlock et al. 2000; Scholes, Unsworth, Hall, et al. 2000), (Jalali-Vahid et al. 2001; Mattei et al. 2010, 2011; Scholes, Unsworth, Hall, et al. 2000; Scholes and Unsworth 2000, 2006; Unsworth 1978; Williams et al. 2006).

Ein weiterer potenzieller Einflussparameter ist aus mechanischer Sicht jedoch auch die individuelle Gelenküberdachung bzw. die lasttragende Kontaktfläche im Gelenk, die durch die intraoperativ definierte Implantat-Orientierung von Schaft und Pfanne zueinander bestimmt wird. Klinisch wird eine solche ‚optimale' Gelenküberdachung primär vor dem Hintergrund der Minimierung des Luxationsrisikos bei alltäglichen Aktivitäten betrachtet (Kennedy et al. 1998; Korduba et al. 2014; Lewinnek et al. 1978; Nevelos et al. 2001; Wan et al. 2008) und weniger zur Minimierung der Gelenkreibung. Am bekanntesten ist die von Lewinnek (Lewinnek et al. 1978) postulierte „Safe Zone", welche eine maximale Gelenküberdachung im Alltag sicherstellen soll, um so ein langfristiges Überleben des Gelenkersatzes, insbesondere der Gelenkpfanne zu gewährleisten. Allerdings zeigten retrospektive Versagensanalysen keinen Unterschied zwischen den Revisionsraten von Pfannen, die innerhalb bzw. außerhalb der „Safe Zone" implantiert wurden (Abdel et al. 2016; Parratte et al. 2016).

Verschiedene Studien konnten bereits zeigen, dass der reibungsinduzierte Abrieb im Gelenk direkt durch die individuelle Gelenküberdachung beeinflusst wird (Nevelos et al. 2001; Wan et al. 2008).

Im Rahmen einer weiteren prospektiven Studie auf Basis der in-vivo-Belastungsdaten beim langen Gehen wurde daher untersucht, inwiefern die Implantat-Positionierung bzw. die individuelle Gelenküberdachung, aber auch die individuelle Gelenkkinematik die in vivo wirkende Gelenkreibung und den daraus resultierenden reibungsinduzierten Temperaturanstieg im Gelenkersatz beeinflusst (Damm et al. 2021). Die Ergebnisse dieser Studie zeigten, dass die Reibung und somit die reibungsinduzierte Temperaturerhöhung im Gelenk primär von der intraoperativ definierten Implantat-Orientierung bzw. der tragenden Gelenkkontaktfläche, als auch durch die Lage des Kontaktpfades in der acetabulären Gleitfläche beeinflusst wird.

Es konnte gezeigt werden, dass je zentraler die Lage des individuellen Kontaktpfades in der Pfanne bzw. je größer die lasttragende Gelenkkontaktfläche ist, desto höher ist die in vivo wirkende Gelenkreibung beim Gehen und der sich daraus ergebenen Temperaturanstieg im Hüftgelenk. Aus mechanischer Sicht bedeutet dies, je größer der Summen-Anteversionswinkel von Implantat-Schaft und -Pfanne, umso mehr verschiebt sich der Kontaktpfad zum Pfannenrand und umso kürzer ist der Weg für den Rücktransport der Synovia in die Lastzone. Dies wiederum bedeutet, je kürzer dieser Rücktransportweg, desto schneller und besser kann der Schmierfilm im Gelenk für die anschließende Lastphase aufgebaut werden und umso niedriger ist die dann auftretende Gelenkreibung. Insbesondere, weil durch jüngere bzw. auch sportlich aktivere Patienten, die heute einen totalen Gelenkersatz erhalten, die Anforderungen an Belastbarkeit und Lebensdauer der Implantate signifikant steigen, sollten etablierte „Safe Zonen“ vor dem Hintergrund der in vivo wirkenden Gelenkreibung neu bewertet und kritisch überarbeitet werden. Insbesondere die gezeigten tribologischen Einflussparameter sollten in diese Überarbeitungen mit einbezogen werden.

Limitationen

Im Rahmen der zugrundeliegenden klinischen Studie und meinen darauf aufbauenden wissenschaftlichen Arbeiten war es erstmals möglich einen weltweit einzigartigen Datensatz zu den in vivo wirkenden Gelenkbelastungen und der korrespondierenden

Gelenkreibung, mit einem außergewöhnlich langem Untersuchungszeitraum von mehr als 10 Jahren, zu erheben.

Diese in vivo Daten basieren jedoch ausschließlich auf einer kleinen Patientengruppe von 10 besonders jungen und aktiven Coxarthrose-Patienten, mit einem durchschnittlichen Implantationsalter von 52 Jahren. Da davon ausgegangen werden muss, dass sich die spezifischen Parameter der individuellen Synovia im Hüftgelenk bzw. der Pseudo-Synovia im künstlichen Gelenkersatz mit dem Alter ändern, können nur eingeschränkte Aussagen über die in vivo wirkenden Reibparameter in einer jüngeren bzw. älteren Patienten Kohorte getroffen werden.

Die Geschlechterverteilung innerhalb dies Probandengruppe ist mit acht Männern und zwei Frauen sehr ungleich verteilt. Um geschlechterspezifische Belastungs- und Reibanalysen durchführen zu können wäre eine entsprechende Rekrutierung von weiteren sechs weiblichen Probanden unerlässlich.

Das instrumentierte Hüftimplantat wurde im Rahmen der Studie ausschließlich mit einer Hart-Weich-Gleitpaarung, bestehend aus einer Al_2O_3 Keramik und einem Kopfdurchmesser von 32mm, sowie jeweils mit einem hochvernetztem UHMWPE Pfannen Inlay kombiniert. Es wurden keine weiteren Gleitpaarungen und Kopfdurchmesser implantiert. Entsprechende in vivo Vergleichsdaten für andere Gleitpaarungen wie beispielsweise weitere typische Hart/Hart Paarungen oder Hart/Weich Paarungen stehen daher nicht zur Verfügung.

Im Rahmen meiner wissenschaftlichen Arbeiten wurden bisher ausschließlich in vivo erhobenen Belastungsdaten analysiert und interpretiert. Zur Bestätigung der auf diesen Ergebnissen beruhenden Erkenntnisse sind systematische in-vitro Versuche notwendig. Insbesondere auch um spezifische Aussagen zu den individuellen Fluidparametern und den sich daraus in vivo vorherrschenden Schmierbedingungen im Gelenk machen zu können. Diese so gewonnenen Erkenntnisse können dann für weitere tribologische Optimierung der aktuellen Gleitpartner-Technologien, insbesondere aber auch für eine Evidenz basierte Auswahl der zu implantierenden Gleitpartner, genutzt werden. Ein solch kombinierter in-vivo/in-silico Ansatz würde dann eine detaillierte und systematische Analyse der wirkenden Reibung unter realistischeren Umgebungsbedingungen ermöglichen, mit dem Ziel das reibungsinduzierte Versagensrisiko und somit das individuelle Revisionsrisiko des

Gelenkersatzes, vor allem für die heute jüngeren und deutlich aktiven Patienten, zu reduzieren.

Zusammenfassung

Im Rahmen der durchgeführten Langzeituntersuchungen und den sich daraus ergebenden wissenschaftlichen Arbeiten war es weltweit erstmals möglich, die wirkende Reibung im totalen Hüftgelenkersatz direkt in vivo zu messen. So konnte unter anderem gezeigt werden, dass die Gelenkreibung in vivo ein hochdynamischer Belastungsparameter ist (Originalarbeit 2.1), welcher interindividuell stark variiert, dessen Höhe und Verlauf von der durchgeführten Aktivität, dem jeweiligen Aktivitätsablauf, als auch vom betrachteten postoperativen Zeitpunkt abhängt (Originalarbeit 2.2).

Es konnte darüber hinaus gezeigt werden, dass die Gelenkreibung nach und während langanhaltender Gelenkbelastung, ohne zwischenzeitliche Entlastung des Gelenkes, deutlich bis kritisch erhöht ist (Originalarbeit 2.3). Dieser Effekt wurde nach kurzen Gangpausen, aber auch bei mehr als 100 weiteren alltäglichen und sportlichen Aktivitäten beobachtet (Originalarbeit 2.4). Diese Beobachtungen können durch eine Änderung der individuellen Schmierbedingungen in Abhängigkeit der individuellen Gelenkkinematik erklärt werden. Diese deutlich erhöhten Reibbelastungen in der Gelenkgleitfläche werden unter anderem als Torsionsbelastung direkt in das Pfanne-Knochen-Interface übertragen und sind somit auch ein potentieller mechanischer Risikofaktor für die individuelle Implantat- und Pfannenstabilität.

Darüber hinaus zeigten die im Rahmen der Arbeiten durchgeführten Datenanalysen zur in vivo wirkenden Gelenkreibung auch, dass diese wesentlich von der intraoperativ definierten Implantat-Orientierung und somit von der Größe der lasttragenden Fläche, bzw. durch die Lage des Kontaktpfades in der Pfanne, bestimmt wird. Es konnte gezeigt werden, je kleiner der Summen-Anteversionswinkel zwischen Implantat-Schaft und –Pfanne ist, also desto größer die lasttragende Fläche, umso weiter ist der Kontaktpfad zur Mitte des Pfannenersatzes orientiert und desto höher ist die in vivo auftretende Gelenkreibung. Die in vivo wirkende Gelenkkontaktkraft spielt hierbei, im Vergleich zum Einfluss der individuellen Implantat-Orientierung, hingegen nur eine untergeordnete Rolle (Originalarbeit 2.5).

4. Literatur

Abdel, Matthew P., Philipp von Roth, Matthew T. Jennings, Arlen D. Hanssen, and Mark W. Pagnano. 2016. “What Safe Zone? The Vast Majority of Dislocated THAs Are Within the Lewinnek Safe Zone for Acetabular Component Position.” *Clinical Orthopaedics and Related Research* 474(2):386–91. doi: 10.1007/s11999-015-4432-5.

Abe, Hirohito, Takashi Sakai, Takashi Nishii, Masaki Takao, Nobuo Nakamura, and Nobuhiko Sugano. 2014. “Jogging after Total Hip Arthroplasty.” *American Journal of Sports Medicine* 42(1):131–37. doi: 10.1177/0363546513506866.

Abu-Amer, Yousef, Isra Darwech, and John C. Clohisy. 2007. “Aseptic Loosening of Total Joint Replacements: Mechanisms Underlying Osteolysis and Potential Therapies.” *Arthritis Research and Therapy* 9(SUPPL.1):1–7. doi: 10.1186/ar2170.

Adler, E., S. A. Stuchin, and F. J. Kummer. 1992. “Stability of Press-Fit Acetabular Cups.” *The Journal of Arthroplasty* 7(3):295–301. doi: 10.1016/0883-5403(92)90052-R.

Affatato, S., M. Spinelli, M. Zavalloni, C. Mazzega-Fabbro, and M. Viceconti. 2008. “Tribology and Total Hip Joint Replacement: Current Concepts in Mechanical Simulation.” *Medical Engineering & Physics* 30(10):1305–17. doi: 10.1016/j.medengphy.2008.07.006.

Angelini, L., P. Damm, T. Zander, R. Arshad, F. Di Puccio, and H. Schmidt. 2018. “Effect of Arm Swinging on Lumbar Spine and Hip Joint Forces.” *Journal of Biomechanics* 70. doi: 10.1016/j.jbiomech.2017.09.011.

Arbuthnot, Jamie Edmund, Michael J. McNicholas, Hassan Dashti, and William A. Hadden. 2007. “Total Hip Arthroplasty and the Golfer.” *The Journal of Arthroplasty* 22(4):549–52. doi: 10.1016/j.arth.2006.05.030.

Asseln, M., J. Eschweiler, P. Damm, G. Al Hares, G. Bergmann, M. Tingart, and K. Radermacher. 2013. “Evaluation of Biomechanical Models for the Planning of Total Hip Arthroplasty.” *Biomedical Engineering / Biomedizinische Technik* 58:10–11. doi: 10.1515/bmt-2013-4116.

Australian Orthopaedic Association National Joint Replacement Registriy (AOANJRR). 2019. *Hip, Knee & Shoulder Arthroplasty - Annual Report 2019*. Adelaide: AOA, 2019.

Australian Orthopaedic Association National Joint Replacement Registry

(AOANJRR). 2019. “Australian Orthopaedic Association National Joint Replacement Registry. Australian Orthopaedic Association National Joint Replacement Registry (AOANJRR). Hip, Knee & Shoulder Arthroplasty - Annual Report 2019.”

Babisch, Jürgen W., Frank Layher, and Louis Philippe Amiot. 2008. “The Rationale for Tilt-Adjusted Acetabular Cup Navigation.” *Journal of Bone and Joint Surgery - Series A* 90(2):357–65. doi: 10.2106/JBJS.F.00628.

Balazs, E. A. 1974. “The Physical Properties of Synovial Fluid and the Special Role of Hyaluronic Acid.” *Disorders of the Knee* 63–75.

Bart, Jan C. J., Emanuele Gucciardi, and Stefano Cavallaro. 2013. “Principles of Lubrication.” *Biolubricants* 10–23. doi: 10.1533/9780857096326.10.

Bashinskaya, Bronislava, Ryan M. Zimmerman, Brian P. Walcott, and Valentin Antoci. 2012. “Arthroplasty Utilization in the United States Is Predicted by Age-Specific Population Groups.” *ISRN Orthopedics* 2012:1–8. doi: 10.5402/2012/185938.

Batailler, Cécile, Anouk Rozinthe, Marcelle Mercier, Christopher Bankhead, Romain Gaillard, and Sébastien Lustig. 2019. “Return to Sport After Bilateral Single Stage Total Hip Arthroplasty Using the Direct Anterior Approach: A Case Control Study.” *Journal of Arthroplasty* 34(12):2972–77. doi: 10.1016/j.arth.2019.06.054.

Bayliss, Lee E, David Culliford, A. Paul Monk, Sion Glyn-jones, Daniel Prieto-alhambra, Andrew Judge, Cyrus Cooper, Andrew J. Carr, Nigel K. Arden, David J. Beard, and Andrew J. Price. 2017. “The Effect of Patient Age at Intervention on Risk of Implant Revision after Total Replacement of the Hip or Knee : A Population-Based Cohort Study.” *The Lancet* 389(10077):1424–30. doi: 10.1016/S0140-6736(17)30059-4.

Bayliss, Lee E., David Culliford, A. Paul Monk, Sion Glyn-Jones, Daniel Prieto-Alhambra, Andrew Judge, Cyrus Cooper, Andrew J. Carr, Nigel K. Arden, David J. Beard, and Andrew J. Price. 2017a. “The Effect of Patient Age at Intervention on Risk of Implant Revision after Total Replacement of the Hip or Knee: A Population-Based Cohort Study.” *The Lancet* 389(10077):1424–30. doi: 10.1016/S0140-6736(17)30059-4.

Bayliss, Lee E., David Culliford, A. Paul Monk, Sion Glyn-Jones, Daniel Prieto-Alhambra, Andrew Judge, Cyrus Cooper, Andrew J. Carr, Nigel K. Arden, David J. Beard, and Andrew J. Price. 2017b. “The Effect of Patient Age at Intervention

on Risk of Implant Revision after Total Replacement of the Hip or Knee: A Population-Based Cohort Study." *The Lancet* 389(10077):1424–30. doi: 10.1016/S0140-6736(17)30059-4.

Bender, Alwina, Philipp Damm, Hagen Hommel, and Georg N. Duda. 2022. "Overstretching Expectations May Endanger the Success of the ' Millennium Surgery ." *Frontiers in Bioengineering and Biotechnology* 10(February):1–14. doi: 10.3389/fbioe.2022.789629.

Bergen, Helse. 2010. *Annual Report 2010 - Norwegian Arthroplasty Register*.

Bergen, Helse. 2019. "Norwegian National Advisory Unit on Arthoplasty and Hip Fractures. Report 2019." 8906.

Bergmann, G., A. Bender, J. Dymke, G. Duda, and P. Damm. 2016. "Standardized Loads Acting in Hip Implants." *PLoS ONE* 11(5). doi: 10.1371/journal.pone.0155612.

Bergmann, Georg, Alwina Bender, Georg N. Duda, and Philipp Damm. 2018. "Physical Activities That Cause High Friction Moments at the Cup in Hip Implants." *The Journal of Bone and Joint Surgery* 100:1637–44.

Bergmann, Georg, Alwina Bender, Jörn Dymke, Georg Duda, and Philipp Damm. 2016. "Standardized Loads Acting in Hip Implants." *PloS One* 11(5):e0155612. doi: 10.1371/journal.pone.0155612.

Bergmann, Georg, Friedmar Graichen, Antonius Rohlmann, Peter Westerhoff, Bernd Heinlein, Alwina Bender, and Reinhald Ehrig. 2008. "Design and Calibration of Load Sensing Orthopaedic Implants." *Journal of Biomechanical Engineering* 130(2):021009. doi: 10.1115/1.2898831.

Bergmann, Georg, Ines Kutzner, Alwina Bender, Jörn Dymke, Adam Trepczynski, Georg N. Duda, Dieter Felsenberg, and Philipp Damm. 2018. "Loading of the Hip and Knee Joints during Whole Body Vibration Training." *PLoS ONE* 13(12):1–21. doi: 10.1371/journal.pone.0207014.

Bishop, Nicholas E., Arne Hothan, and Michael M. Morlock. 2012. "High Friction Moments in Large Hard-on-Hard Hip Replacement Bearings in Conditions of Poor Lubrication." *Journal of Orthopaedic Research* (October):1–7. doi: 10.1002/jor.22255.

Bohannon, R. W. 2007. "Number of Pedometer-Assessed Steps Taken Per Day by Adults: A Descriptive Meta-Analysis." *Physical Therapy* 87(12):1642–50. doi: 10.2522/ptj.20060037.

Bonnin, Michel P., Jean Charles Rollier, Jean Christophe Chatelet, Tarik Ait-Si-Selmi, Julien Chouteau, Laurent Jacquot, Gerjon Hannink, Mo Saffarini, and Michel Henri Fessy. 2018. “Can Patients Practice Strenuous Sports After Uncemented Ceramic-on-Ceramic Total Hip Arthroplasty?” *Orthopaedic Journal of Sports Medicine* 6(4):1–8. doi: 10.1177/2325967118763920.

Brockett, Claire, Sophie Williams, Zhongmin Jin, Graham Isaac, and John Fisher. 2006. “Friction of Total Hip Replacements With Different Bearings and Loading Conditions.” *Journal of Biomedical Materials Research* 508–15. doi: 10.1002/jbmb.

Burke, Neil G., John P. Gibbons, Adrian J. Cassar-Gheiti, Fionnuala M. Walsh, and James P. Cashman. 2019. “Total Hip Replacement—the Cause of Failure in Patients under 50 Years Old?” *Irish Journal of Medical Science (1971 -)* 188(3):879–83. doi: 10.1007/s11845-018-01956-8.

Byerlee, J. D. 1970. “The Mechanics of Stick-Slip.” *Tectonophysics* 9(5):475–86. doi: https://doi.org/10.1016/0040-1951(70)90059-4.

Canadian Institute for Health Information. 2019. *Hip and Knee Replacements in Canada - Canadian Joint Replacement Registry (CJRR) 2017-2019 Annual Report*.

Chatterji, U., M. J. Ashworth, P. L. Lewis, and P. J. Dobson. 2004. “Effect of Total Hip Arthroplasty on Recreational and Sporting Activity.” *ANZ Journal of Surgery* 74:446–49.

Chatterji, Urjit, Mark J. Ashworth, Peter L. Lewis, and Peter J. Dobson. 2004. “Effect of Total Hip Arthroplasty on Recreational and Sporting Activity.” *ANZ Journal of Surgery* 74(6):446–49. doi: 10.1111/j.1445-1433.2004.03028.x.

Chen, Gang B. T. Handbook of Friction-Vibration Interactions, ed. 2014. “3 - Fundamentals of Contact Mechanics and Friction.” Pp. 71–152 in. Woodhead Publishing.

Chikama, H. 1985. “The Role of Protein and Hyaluronic Acid in the Synovial Fluid in Animal Joint Lubrication.” *Nihon Seikeigeka Gakkai Zasshi.* (59(5)):559–72.

CJRR. 2008. *CJRR Report: Total Hip and Total Knee Replacements in Canada*.

Culliford, D., J. Maskell, A. Judge, C. Cooper, D. Prieto-Alhambra, and N. K. Arden. 2015. “Future Projections of Total Hip and Knee Arthroplasty in the UK: Results from the UK Clinical Practice Research Datalink.” *Osteoarthritis and Cartilage* 23(4):594–600. doi: 10.1016/j.joca.2014.12.022.

Curtis M. J., R. H. Jinnah, W. D. Valerie, and D. S. Hungerford. 1992. “The Initial Stability of Uncemented Acetabular Components.” *British Editorial Soviety of Bone and Joint Surgery* 74-B:372–76.

Curtis, M. J., R. H. Jinnah, V. D. Wilson, and D. S. Hungerford. 1992. “The Initial Stability of Uncemented Acetabular Components.” *Journal of Bone and Joint Surgery - Series B* 74(3):372–76. doi: 10.1302/0301-620x.74b3.1587880.

Cutler, David, Angus Deaton, and Adriana Lleras-Muney. 2006. “The Determinants of Mortality.” *Journal of Economic Perspectives* 20(3):97–120. doi: 10.1257/jep.20.3.97.

Damm, Philipp, Alwina Bender, and Georg Bergmann. 2015a. “Postoperative Changes in in Vivo Measured Friction in Total Hip Joint Prosthesis during Walking.” *PloS One* 10(3):e0120438. doi: 10.1371/journal.pone.0120438.

Damm, Philipp, Alwina Bender, and Georg Bergmann. 2015b. “Postoperative Changes in in Vivo Measured Friction in Total Hip Joint Prosthesis during Walking.” *PLoS ONE* 10(3). doi: 10.1371/journal.pone.0120438.

Damm, Philipp, Alwina Bender, Georg Duda, and Georg Bergmann. 2017a. “In Vivo Measured Joint Friction in Hip Implants during Walking after a Short Rest.” *PLoS ONE* 12(3). doi: 10.1371/journal.pone.0174788.

Damm, Philipp, Alwina Bender, Georg Duda, and Georg Bergmann. 2017b. “In Vivo Measured Joint Friction in Hip Implants during Walking after a Short Rest.” 1–14.

Damm, Philipp, Alwina Bender, Vivian Waldheim, Tobias Winkler, and Georg N. Duda. 2021. “Surgical Cup Placement Affects the Heating up of Total Joint Hip Replacements.” *Scientific Reports* 11(1):1–11. doi: 10.1038/s41598-021-95387-8.

Damm, Philipp, Sophie Brackertz, Florian Streitparth, Carsten Perka, Georg Bergmann, Georg N. Duda, and Tobias Winkler. 2019. “ESB Clinical Biomechanics Award 2018: Muscle Atrophy-Related Increased Joint Loading after Total Hip Arthroplasty and Their Postoperative Change from 3 to 50 months.” *Clinical Biomechanics* 65(February):105–9. doi: 10.1016/j.clinbiomech.2019.04.008.

Damm, Philipp, Joern Dymke, Robert Ackermann, Alwina Bender, Friedmar Graichen, Andreas Halder, Alexander Beier, and Georg Bergmann. 2013. “Friction in Total Hip Joint Prosthesis Measured in Vivo during Walking.” *PLoS ONE* 8(11):1–8. doi: 10.1371/journal.pone.0078373.

Damm, Philipp, Jörn Dymke, Robert Ackermann, Alwina Bender, Friedmar Graichen, Andreas Halder, Alexander Beier, and Georg Bergmann. 2013. “Friction in Total Hip Joint Prosthesis Measured in Vivo during Walking.” *PLoS ONE* 8(11). doi: 10.1371/journal.pone.0078373.

Damm, Philipp, Jörn Dymke, Alwina Bender, Georg Duda, and Georg Bergmann. 2017. “In Vivo Hip Joint Loads and Pedal Forces during Ergometer Cycling.” *Journal of Biomechanics* 60. doi: 10.1016/j.jbiomech.2017.06.047.

Damm, Philipp, Friedmar Graichen, Antonius Rohlmann, Alwina Bender, and Georg Bergmann. 2010a. “Total Hip Joint Prosthesis for in Vivo Measurement of Forces and Moments.” *Medical Engineering & Physics* 32(1):95–100.

Damm, Philipp, Friedmar Graichen, Antonius Rohlmann, Alwina Bender, and Georg Bergmann. 2010b. “Total Hip Joint Prosthesis for in Vivo Measurement of Forces and Moments.” *Medical Engineering & Physics* 32(1):95–100. doi: 10.1016/j.medengphy.2009.10.003.

Damm, Philipp, Ines Kutzner, Georg Bergmann, Antonius Rohlmann, and Hendrik Schmidt. 2017. “Comparison of in Vivo Measured Loads in Knee, Hip and Spinal Implants during Level Walking.” *Journal of Biomechanics* 51. doi: 10.1016/j.jbiomech.2016.11.060.

Damm, Philipp, Sandra Reitmaier, Sabine Hahn, Vivian Waldheim, Ali Firouzabadi, and Hendrik Schmidt. 2020. “In Vivo Hip and Lumbar Spine Implant Loads during Activities in Forward Bent Postures.” *Journal of Biomechanics* 102. doi: 10.1016/j.jbiomech.2019.109517.

Damm, Philipp, Verena Schwachmeyer, Jörn Dymke, Alwina Bender, and Georg Bergmann. 2013. “In Vivo Hip Joint Loads during Three Methods of Walking with Forearm Crutches.” *Clinical Biomechanics* 28(5). doi: 10.1016/j.clinbiomech.2012.12.003.

Damm, Philipp, Jip Zonneveld, Sophie Brackertz, Florian Streitparth, and Tobias Winkler. 2018. “Gluteal Muscle Damage Leads to Higher in Vivo Hip Joint Loads 3 Months after Total Hip Arthroplasty.” *PLOS ONE* 13(1):1–11. doi: 10.1371/journal.pone.0190626.

Danish Hip Arthroplasty Register. 2020. *The Danish Hip Arthroplasty Register (DHR), 2019 National Annual Report*.

David, Davidson, Stephen Graves, and Ann Tomkins. 2013. *Australien Orthopaedic Association National Joint Replacement Registry. Anual Report. Adelaide:AOA;*

2013.

Dubs, L., N. Gschwend, and Munzinger U. 1983. “Sport after Total Hip Arthoplasty.” *Archives of Orthopedic Trauma Surgery* 101(3):161–69.

Dutch Arthroplasty Register (LROI). 2019. *Online LROI Annual Report 2019*.

Fam, H., J. T. Bryant, and M. Kontopoulou. 2007. “Rheological Properties of Synovial Fluids.” *Biorheology* 44(2):59–74.

Fehring, Keith A., John R. Owen, Anton A. Kurdin, Jennifer S. Wayne, and William A. Jiranek. 2014. “Initial Stability of Press-Fit Acetabular Components under Rotational Forces.” *Journal of Arthroplasty* 29(5):1038–42. doi: 10.1016/j.arth.2013.10.009.

Fialho, Jorge C., Paulo R. Fernandes, Luis Eça, and João Folgado. 2007. “Computational Hip Joint Simulator for Wear and Heat Generation.” *Journal of Biomechanics* 40(11):2358–66.

Finnish Arthroplasty Register for National Institute of Health And Welfare. 2020. “Finnish Arthroplasty Register - ENDOnet.”

Fischer, M. C. M., J. Eschweiler, F. Schick, M. Asseln, P. Damm, and K. Radermacher. 2018. “Patient-Specific Musculoskeletal Modeling of the Hip Joint for Preoperative Planning of Total Hip Arthroplasty: A Validation Study Based on in Vivo Measurements.” *PLoS ONE* 13(4). doi: 10.1371/journal.pone.0195376.

Fischer, Maximilian C. M., Philipp Damm, Juliana Habor, and Klaus Radermacher. 2021. “Effect of the Underlying Cadaver Data and Patient-Specific Adaptation of the Femur and Pelvis on the Prediction of the Hip Joint Force Estimated Using Static Models.” *Journal of Biomechanics* (xxxx):110526. doi: 10.1016/j.jbiomech.2021.110526.

Fisher, J., and D. Dowson. 2016. “Tribology of Total Artificial Joints.” 205.

Flugsrud, G. B., L. Nordsletten, B. Espehaug, L. I. Havelin, and H. E. Meyer. 2007. “The Effect of Middle-Age Body Weight and Physical Activity on the Risk of Early Revision Hip Arthroplasty.” *Acta Orthopaedica* 78:99–107. doi: 10.1080/17453670610013493.

Gandhi, Rajiv, Herman Dhotar, J. Roderick Davey, and Nizar N. Mahomed. 2010. “Predicting the Longer-Term Outcomes of Total Hip Replacement.” *The Journal of Rheumatology* 37(12):2573–77. doi: 10.3899/jrheum.100149.

Gao, L., J. Fisher, and Z. Jin. 2011. “Effect of Walking Patterns on the Elastohydrodynamic Lubrication of Metal-on-Metal Total Hip Replacements.”

Proceedings of the Institution of Mechanical Engineers, Part J: Journal of Engineering Tribology 225(6):515–25. doi: 10.1177/1350650110396802.

Garellick, Goran, Johan Karrholm, Cecilia Rogmark, Ola Rolfson, and Peter Herberts. 2011. *Swedish Hip Arthroplasty Register - Annual Report 2011*.

Garllik, G., C. Rogemark, J. Kärrholm, and O. Rolfson. 2012. *Swedish Hip Arthroplasty Register 2012*.

Ghomrawi, Hassan M. K., Mark M. Dolan, John Rutledge, and Michael M. Alexiades. 2011. "Recovery Expectations of Hip Resurfacing Compared to Total Hip Arthroplasty: A Matched Pairs Study." *Arthritis Care and Research* 63(12):1753–57. doi: 10.1002/acr.20626.

Golant, Alexander, Dimitrios C. Christoforou, James D. Slover, and Joseph D. Zuckerman. 2010. "Athletic Participation After Hip and Knee Arthroplasty." *Bulletin of the NYU Hospital for Joint Diseases* 68(2):76–83.

Goriainov, Vitali, Andrew Jones, Adam Briscoe, Andrew New, and Douglas Dunlop. 2014. "Do the Cup Surface Properties Influence the Initial Stability?" *Journal of Arthroplasty* 29(4):757–62. doi: 10.1016/j.arth.2013.07.007.

Grimberg, Alexander, Volkmar Jansson, Jörg Lützner, Oliver Melsheimer, Michael Morlock, and Arnd Steinbrück. 2020. *Jahresbericht 2020 Mit Sicherheit Mehr Qualität*.

Haffer, Henryk, Srdan Popovic, Franziska Martin, Sebastian Hardt, Tobias Winkler, and Philipp Damm. 2021. "In Vivo Loading on the Hip Joint in Patients with Total Hip Replacement Performing Gymnastics and Aerobics Exercises." *Scientific Reports* 11(1):1–11. doi: 10.1038/s41598-021-92788-7.

Hall, R. M., and A. Unsworth. 1997. "Review Friction in Hip Prostheses." *Biomaterials* 18(15):1017–26.

Hall, R. M., A. Unsworth, B. M. Wroblewski, P. Siney, and N. J. Powell. 1997. "The Friction of Explanted Hip Prostheses." *British Journal of Rheumatology* 36(1):20–26.

Hara, Daisuke, Satoshi Hamai, Keisuke Komiyama, Goro Motomura, Kyohei Shiomoto, and Yasuharu Nakashima. 2018. "Sports Participation in Patients After Total Hip Arthroplasty vs Periacetabular Osteotomy: A Propensity Score-Matched Asian Cohort Study." *Journal of Arthroplasty* 33(2):423–30. doi: 10.1016/j.arth.2017.08.035.

Hatterji, U. Rjit C., M. A. R. K. J. A. Shworth, P. Eter L. L. Ewis, P. Eter J. D. Obson,

Urjit Chatterji, Mark J. Ashworth, Peter L. Lewis, and Peter J. Dobson. 2004. “Effect of Total Hip Arthroplasty on Recreational and Sporting Activity.” *ANZ Journal of Surgery* 74(6):446–49. doi: 10.1111/j.1445-1433.2004.03028.x.

Havelin, L. I., A. M. Fenstad, R. Salomonsson, F. Mehnert, O. Furnes, S. Overgaard, Al. B. Pedersen, P. Herberts, J. Kärrholm, and G. Garellick. 2009. “The Nordic Arthroplasty Register Association: A Unique Collaboration between 3 National Hip Arthroplasty Registries with 280,201 THRs.” *Acta Orthopaedica* 80(4):393–401. doi: 10.3109/17453670903039544.

Havelin, Leif I, Anne M. Fenstad, Roger Salomonsson, Frank Mehnert, Ove Furnes, Søren Overgaard, Alma B. Pedersen, Peter Herberts, Johan Kärrholm, and Göran Garellick. 2009. “The Nordic Arthroplasty Register Association: A Unique Collaboration between 3 National Hip Arthroplasty Registries with 280,201 THRs.” *Acta Orthopaedica* 80(4):393–401. doi: 10.3109/17453670903039544.

Healy, By William L., Sanjeev Sharma, Benjamin Schwartz, and Richard Iorio. 2008. “Athletic Activity After Total Joint Arthroplasty.” 2245–52. doi: 10.2106/JBJS.H.00274.

Healy, William L., Richard Iorio, and Mark J. Lemos. 2001. “Current Concepts Athletic Activity after Joint Replacement.” 29(3):377–88.

Healy, William L., Sanjeev Sharma, Benjamin Schwartz, and Richard Iorio. 2008. “Athletic Activity After Total Joint Arthroplasty.” *The Journal of Bone and Joint Surgery-American Volume* 90(10):2245–52. doi: 10.2106/JBJS.H.00274.

Hepinstall, Matthew S., John R. Rutledge, Lindsey J. Bornstein, Madhu Mazumdar, and Geoffrey H. Westrich. 2011. “Factors That Impact Expectations Before Total Knee Arthroplasty.” *The Journal of Arthroplasty* 26(6):870–76. doi: 10.1016/j.arth.2010.09.010.

Hernandez-Molina, G., Stephan Reichenbach, Bin Zhang, Michael LaValley, and David Felson. 2009. “Effect of Therapeutic Exercise for Hip Osteoarthritis Pain: Results of a Meta-Analysis.” *Arthritis Rheum* 59(9):1221–28. doi: 10.1002/art.24010.Effect.

Hoorntje, A., K. Y. Janssen, S. B. T. Bolder, K. L. M. Koenraadt, J. G. Daams, L. Blankevoort, Gmmj Kerkhoffs, and Ppfm Kuijer. 2018. “The Effect of Total Hip Arthroplasty on Sports and Work Participation: A Systematic Review and Meta-Analysis.” *Sports Med* 48(7):1695–1726. doi: 10.1007/s40279-018-0924-2.

Huch, K., K. A. C. Müller, T. Stürmer, H. Brenner, W. Puhl, and K. P. Günther. 2005.

"Sports Activities 5 Years after Total Knee or Hip Arthroplasty: The Ulm Osteoarthritis Study." *Annals of the Rheumatic Diseases* 64(2005):1715–20. doi: 10.1136/ard.2004.033266.

Innmann, M. M., S. Weiss, F. Andreas, C. Merle, and M. R. Streit. 2016. "Sports and Physical Activity after Cementless Total Hip Arthroplasty with a Minimum Follow-up of 10 Years." *Scand J Med Sci Sports* 26(5):550–56. doi: 10.1111/sms.12482.

Jalali-Vahid, D., M. Jagatia, Z. M. Jin, and D. Dowson. 2001. "Prediction of Lubricating Film Thickness in UHMWPE Hip Joint Replacements." *Journal of Biomechanics* 34(2):261–66.

Jassim, Shivan S., Jenni Tahmassebi, Fares S. Haddad, and Angus Robertson. 2019. "Return to Sport after Lower Limb Arthroplasty - Why Not for All?" *World Journal of Orthopedics* 10(2):90–100. doi: 10.5312/wjo.v10.i2.90.

Jebens, E. H., and M. E. Monk-Jones. 1959. "On the Viscosity and PH of Synovial Fluid and the PH of Blood." *The Journal of Bone and Joint Surgery. British Volume* 41 B(2):388–400. doi: 10.1302/0301-620x.41b2.388.

Jin, Z., M. Stone, E. Ingham, and J. Fisher. 2006. "(V) Biotribology." *Current Orthopaedics* 20(1):32–40. doi: 10.1016/j.cuor.2005.09.005.

Johnsen, S. P. 2006. "Patient-Related Predictors of Implant Failure after Primary Total Hip Replacement in the Initial, Short- and Long-Terms: A NATIONWIDE DANISH FOLLOW-UP STUDY INCLUDING 36 984 PATIENTS." *Journal of Bone and Joint Surgery - British Volume* 88-B(10):1303–8. doi: 10.1302/0301-620X.88B10.17399.

Kadoya, Y., A. Kobayashi, and H. Ohashi. 1998. "Wear and Osteolysis in Total Joint Replacements." *Acta Orthopaedica Scandinavica. Supplementum* 278:1–16.

Karampinas, Panagiotis K., Eustratios G. Papadelis, John A. Vlamis, Hlias Basiliadis, and Spiros G. Pneumaticos. 2017. "Comparing Return to Sport Activities after Short Metaphyseal Femoral Arthroplasty with Resurfacing and Big Femoral Head Arthroplasties." *European Journal of Orthopaedic Surgery and Traumatology* 27(5):617–22. doi: 10.1007/s00590-016-1897-1.

Kennedy, J. G., W. B. Rogers, K. E. Soffe, R. J. Sullivan, D. G. Griffen, and L. J. Sheehan. 1998. "Effect of Acetabular Component Orientation on Recurrent Dislocation, Pelvic Osteolysis, Polyethylene Wear, and Component Migration." *Journal of Arthroplasty* 13(5):530–34. doi: 10.1016/S0883-5403(98)90052-3.

Klein, Gregg R., Brett R. Levine, William J. Hozack, Eric J. Strauss, James a

D'Antonio, William Macaulay, and Paul E. Di Cesare. 2007. "Return to Athletic Activity after Total Hip Arthroplasty. Consensus Guidelines Based on a Survey of the Hip Society and American Association of Hip and Knee Surgeons." *The Journal of Arthroplasty* 22(2):171–75. doi: 10.1016/j.arth.2006.09.001.

Koenen, Paola, Holger Bäthis, Marco M. Schneider, Matthias Fröhlich, Bertil Bouillon, and Sven Shafizadeh. 2014. "How Do We Face Patients' Expectations in Joint Arthroplasty?" *Archives of Orthopaedic and Trauma Surgery* 134(7):925–31. doi: 10.1007/s00402-014-2012-x.

Korduba, L. A., A. Essner, R. Pivec, P. Lancin, M. A. Mont, A. Wang, and R. E. Delanois. 2014. "Effect of Acetabular Cup Abduction Angle on Wear of Ultrahigh-Molecular-Weight Polyethylene in Hip Simulator Testing." *Am J Orthop (Belle Mead NJ)* 43(10):466–71.

Krismer, Martin. 2017. "Sports Activities after Total Hip Arthroplasty." *EFORT Open Reviews* 2(5):189–94. doi: 10.1302/2058-5241.2.160059.

Kuijpers, Martijn F. L., Gerjon Hannink, Liza N. van Steenbergen, and B. Willem Schreurs. 2020. "Outcome of Revision Hip Arthroplasty in Patients Younger than 55 Years: An Analysis of 1,037 Revisions in the Dutch Arthroplasty Register." *Acta Orthopaedica* 3674:1–6. doi: 10.1080/17453674.2019.1708655.

Kuster, Markus S. 2002. "Total Joint Replacement A Review of the Current Literature and Proposal of Scientifically Based Guidelines." *Sports Med* 32(7):433–45.

Laursen, Mia K., Jakob B. Andersen, Mikkel M. Andersen, Ole H. Simonsen, and Mogens B. Laursen. 2014. "Danish Surgeons Allow the Most Athletic Activities after Total Hip and Knee Replacement." *European Journal of Orthopaedic Surgery and Traumatology* 24(8):1571–77. doi: 10.1007/s00590-014-1442-z.

Learmonth, Ian D., Claire Young, and Cecil Rorabeck. 2007. "The Operation of the Century: Total Hip Replacement." *Lancet* 370(9597):1508–19. doi: 10.1016/S0140-6736(07)60457-7.

Lefevre, Nicolas, Didier Rousseau, Yoann Bohu, Shahnaz Klouche, and Serge Herman. 2013. "Return to Judo after Joint Replacement." *Knee Surgery, Sports Traumatology, Arthroscopy* 21(12):2889–94. doi: 10.1007/s00167-012-2064-9.

Lewinnek, GE, JL Lewis, R. Tarr, CL Compere, and JR Zimmerman. 1978. "Dislocations after Total Hip-Replacement Arthroplasties." *J Bone Joint Surg Am* 60(2):217–20.

Liao, Y. 2003. "The Effect of Frictional Heating and Forced Cooling on the Serum

Lubricant and Wear of UHMW Polyethylene Cups against Cobalt–Chromium and Zirconia Balls." *Biomaterials* 24(18):3047–59. doi: 10.1016/S0142-9612(03)00148-0.

Lübbeke, Anne, Jeffrey N. Katz, Thomas V. Perneger, and Pierre Hoffmeyer. 2007. "Primary and Revision Hip Arthroplasty: 5-Year Outcomes and Influence of Age and Comorbidity." *The Journal of Rheumatology* 34(2):394–400. doi: 06/13/127 [pii].

Malchau, H., P. Herberts, P. Söderman, and A. Odén. 2000. "Prognosis of Total Hip Replacement." *The Swedish National Hip Arthroplasty Registry*.

Mancuso, By Carol A., Jennifer Jout, Eduardo A. Salvati, and Thomas P. Sculco. 2009. "Fulfillment of Patients' Expectations for Total Hip Arthroplasty." 2073–78. doi: 10.2106/JBJS.H.01802.

Mancuso, Carol A., Jennifer Jout, Eduardo A. Salvati, and Thomas P. Sculco. 2009. "Fulfillment of Patients' Expectations for Total Hip Arthroplasty." *Journal of Bone and Joint Surgery - Series A* 91(9):2073–78. doi: 10.2106/JBJS.H.01802.

Mancuso, Carol A., Catherine H. Wentzel, Hassan M. K. Ghomrawi, and Bryan T. Kelly. 2017. "Hip Preservation Surgery Expectations Survey: A New Method to Measure Patients' Preoperative Expectations." *Arthroscopy - Journal of Arthroscopic and Related Surgery* 33(5):959–68. doi: 10.1016/j.arthro.2016.11.012.

Marshall, Amanda, Michael D. Ries, and Wayne Paprosky. 2008. "How Prevalent Are Implant Wear and Osteolysis, and How Has the Scope of Osteolysis Changed since 2000?" *JAAOS - Journal of the American Academy of Orthopaedic Surgeons* 16.

Mattei, L., F. Di Puccio, B. Piccigallo, and E. Ciulli. 2010. "Lubrication and Wear Modelling of Artificial Hip Joints: A Review." *Tribology International* 44(5):532–49. doi: 10.1016/j.triboint.2010.06.010.

Mattei, L., F. Di Puccio, B. Piccigallo, and E. Ciulli. 2011. "Lubrication and Wear Modelling of Artificial Hip Joints: A Review." *Tribology International* 44(5):532–49. doi: 10.1016/j.triboint.2010.06.010.

Mazzucco, Dan, Gareth Mckinley, Richard D. Scott, and Myron Spector. 2002. "Rheology of Joint Fluid in Total Knee Arthroplasty Patients." 20.

Meek, R. M. D., R. Treacy, A. Manktelow, J. A. Timperley, and F. S. Haddad. 2020. "Sport after Total Hip Arthroplasty: Undoubted Progress but Still Some

Unknowns.” *Bone and Joint Journal* 102(6):661–63. doi: 10.1302/0301-620X.102B6.BJJ-2020-0208.

Meyer, Donna M., and John A. Tichy. 2003a. “3-D Model of a Total Hip Replacement In Vivo Providing Hydrodynamic Pressure and Film Thickness for Walking and Bicycling.” *Journal of Biomechanical Engineering* 125(6):777–84. doi: 10.1115/1.1631585.

Meyer, Donna M., and John A. Tichy. 2003b. “3-D Model of a Total Hip Replacement In Vivo Providing Hydrodynamic Pressure and Film Thickness for Walking and Bicycling.” *Journal of Biomechanical Engineering* 125(6):777. doi: 10.1115/1.1631585.

Mjöberg, B., L. I. Hansson, and G. Selvik. 1984. “Instability of Total Hip Prostheses at Rotational Stress.” *Acta Orthop Scand* 55:504–6.

Mont, Michael A., Dawn M. Laporte, Tarun Mullick, Charles E. Silberstein, and David S. Hungerford. 1999. “Tennis After Total Hip Arthroplasty.” *The American Journal of Sports Medicine* 27(1):60–64. doi: 10.1177/03635465990270011801.

Morlock, M., R. Nassutt, M. Wimmer, and E. Schneider. 2000. “Influence of Resting Periods on Friction in Artificial Hip Joint Articulations.” *Bone* 6–16.

Naal, Florian-D., Nicola a Maffiuletti, Urs Munzinger, and Otmar Hersche. 2007. “Sports after Hip Resurfacing Arthroplasty.” *The American Journal of Sports Medicine* 35(5):705–11. doi: 10.1177/0363546506296606.

Nassutt, Roman, Markus A. Wimmer, and Michael M. Morlock. 2003. “The Influence of Resting Periods on Friction in the Artificial Hip.” (407):127–38. doi: 10.1097/01.blo.0000048133.30533.13.

Nemes, Szilárd, Max Gordon, Cecilia Rogmark, and Ola Rolfson. 2014. “Projections of Total Hip Replacement in Sweden from 2013 to 2030.” *Acta Orthopaedica* 85(3):238–43. doi: 10.3109/17453674.2014.913224.

Nemes, Szilárd, Max Gordon, Cecilia Rogmark, and Ola Rolfson. 2020. “Projections of Total Hip Replacement in Sweden from 2013 to 2030.” 85(3):238–43. doi: 10.3109/17453674.2014.913224.

Nevelos, J. E., E. Ingham, C. Doyle, A. B. Nevelos, and J. Fisher. 2001. “The Influence of Acetabular Cup Angle on the Wear of ‘BIOLOX Forte’ Alumina Ceramic Bearing Couples in a Hip Joint Simulator.” *Journal of Materials Science: Materials in Medicine* 12(2):141–44. doi: 10.1023/A:1008970027306.

NJR Editorial Board NJRSC. 2019. “United Kingdom National Joint Registry. 2019

16th Annual Report." (December 2018).

Norwegian National Advisory Unit Report on Arthoplasty and Hip Fractures. 2019. *Norwegian National Advisory Unit Report on Arthoplasty and Hip Fractures 2019*. Vol. 8906.

Oehler, N., T. Schmidt, and A. Niemeier. 2016. "Endoprothetischer Gelenkersatz Und Sport." *Sportverletzung · Sportschaden* 30(04):195–203. doi: 10.1055/s-0042-119109.

Ortmaier, Reinhold, Hannes Pichler, Wolfgang Hitzl, Katja Emmanuel, Georg Mattiassich, Fabian Plachel, and Josef Hochreiter. 2019. "Return to Sport After Short-Stem Total Hip Arthroplasty." *Clinical Journal of Sport Medicine* 29(6):451–58. doi: 10.1097/JSM.0000000000000532.

Pabinger, C., and A. Geissler. 2014. "Utilization Rates of Hip Arthroplasty in OECD Countries." *Osteoarthritis and Cartilage* 22(6):734–41. doi: 10.1016/j.joca.2014.04.009.

Palmowski, Yannick, Srdan Popovic, Simone G. Schuster, Sebastian Hardt, and Philipp Damm. 2021. "In Vivo Analysis of Hip Joint Loading on Nordic Walking Novices." *Journal of Orthopaedic Surgery and Research* 16(1):1–10. doi: 10.1186/s13018-021-02741-7.

Parratte, Sebastien, Matthieu Ollivier, Alexandre Lunebourg, Xavier Flecher, and Jean Noel A. Argenson. 2016. "No Benefit After THA Performed With Computer-Assisted Cup Placement: 10-Year Results of a Randomized Controlled Study." *Clinical Orthopaedics and Related Research* 474(10):2085–93. doi: 10.1007/s11999-016-4863-7.

Philippot, R., J. Wegrzyn, F. Farizon, and M. H. Fessy. 2009. "Pelvic Balance in Sagittal and Lewinnek Reference Planes in the Standing, Supine and Sitting Positions." *Orthopaedics and Traumatology: Surgery and Research* 95(1):70–76. doi: 10.1016/j.otsr.2008.01.001.

Del Piccolo, N., C. Carubbi, A. Mazzotta, G. Sabbioni, M. Filanti, C. Stagni, and D. Dallari. 2016. "Return to Sports Activity with Short Stems or Standard Stems in Total Hip Arthroplasty in Patients Less than 50 Years Old." *Hip Int* 26 Suppl 1:48–51. doi: 10.5301/hipint.5000404.

Pierrepont, J. W., H. Feyen, B. P. Miles, D. A. Young, J. V. Baré, and A. J. Shimmin. 2016. "Functional Orientation of the Acetabular Component in Ceramic-on-Ceramic Total Hip Arthroplasty and Its Relevance to Squeaking." *The Bone &*

Joint Journal 98-B(7):910–16. doi: 10.1302/0301-620X.98B7.37062.

Pilz, Veronika, Tim Hanstein, and Ralf Skripitz. 2018. “Projections of Primary Hip Arthroplasty in Germany until 2040.” *Acta Orthopaedica* 89(3):308–13. doi: 10.1080/17453674.2018.1446463.

Raguet, M., C. Pierson, and A. Pierson. 2015. “Is Ultrarunning Possible with a Total Hip Arthroplasty?” *Journal de Traumatologie Du Sport* 32(1):3–14. doi: 10.1016/j.jts.2015.01.005.

Rajaee, Sean S, Joshua C. Campbell, James Mirocha, and Guy D. Paiement. 2018a. “Increasing Burden of Total Hip Arthroplasty.” 449–58.

Rajaee, Sean S., Joshua C. Campbell, James Mirocha, and Guy D. Paiement. 2018. “Increasing Burden of Total Hip Arthroplasty Revisions in Patients Between 45 and 64 Years of Age.” *Journal of Bone and Joint Surgery* 100(6):449–58. doi: 10.2106/JBJS.17.00470.

Rajaee, Sean S, Joshua C. Campbell, James Mirocha, and Guy D. Paiement. 2018b. “Increasing Burden of Total Hip Arthroplasty Revisions in Patients Between 45 and 64 Years of Age.” *Journal of Bone and Joint Surgery* 100(6):449–58. doi: 10.2106/JBJS.17.00470.

Roser, Max. 2019. “Life Expectancy.” *Published Online at OurWorldInData.Org*.

Saikko, V. 1992. “A Simulator Study of Friction in Total Replacement Hip Joints.” *Proceedings of the Institution of Mechanical Engineers Part H Journal of Engineering in Medicine* 206(4):201–11.

Schäfer, R., U. Soltész, and P. F. Bernard. 1998. “Friction in Hip-Joint Prostheses and Its Influence on the Fixation of the Artificial Head.” *Journal of Materials Science: Materials in Medicine* 9(12):687–90.

Schmidutz, Florian, Stefan Grote, Matthias Pietschmann, Patrick Weber, Farhad Mazoochian, Andreas Fottner, and Volkmar Jansson. 2012. “Sports Activity after Short-Stem Hip Arthroplasty.” *American Journal of Sports Medicine* 40(2):425–32. doi: 10.1177/0363546511424386.

Schneider, Patrick L., David R. Bassett, Dixie L. Thompson, Nicolaas P. Pronk, and Kenneth M. Bielak. 2006. “Effects of a 10,000 Steps per Day Goal in Overweight Adults.” *American Journal of Health Promotion* 21(2):85–89. doi: 10.4278/0890-1171-21.2.85.

Scholes, S. C., and A. Unsworth. 2000. “Comparison of Friction and Lubrication of Different Hip Prostheses.” *Proceedings of the Institution of Mechanical*

Engineers Part H Journal of Engineering in Medicine 214(1):49–57.

Scholes, S. C., and A. Unsworth. 2006. “The Effects of Proteins on the Friction and Lubrication of Artificial Joints.” *Proceedings of the Institution of Mechanical Engineers Part H Journal of Engineering in Medicine* 220(6):687–93.

Scholes, S. C., A. Unsworth, and A. A. J. Goldsmith. 2000. “A Frictional Study of Total Hip Joint Replacements.” *Physics in Medicine and Biology* 45(12):3721–35.

Scholes, S. C., A. Unsworth, R. M. Hall, and R. Scott. 2000. “The Effects of Material Combination and Lubricant on the Friction of Total Hip Prostheses.” *Wear* 241(2):209–13. doi: 10.1016/S0043-1648(00)00377-X.

Schwachmeyer, Verena, Philipp Damm, Alwina Bender, Jörn Dymke, Friedmar Graichen, and Georg Bergmann. 2013. “In Vivo Hip Joint Loading during Post-Operative Physiotherapeutic Exercises.” *PloS One* 8(10):e77807. doi: 10.1371/journal.pone.0077807.

Scott, C. E. H., K. E. Bugler, N. D. Clement, D. MacDonald, C. R. Howie, and L. C. Biant. 2012. “Patient Expectations of Arthroplasty of the Hip and Knee.” *The Journal of Bone and Joint Surgery. British Volume* 94-B(7):974–81. doi: 10.1302/0301-620X.94B7.28219.

Shim, V. P. W., L. M. Yang, J. F. Liu, and V. S. Lee. 2006. “Characterisation of the Dynamic Compressive Mechanical Properties of Cancellous Bone from the Human Cervical Spine.” *International Journal of Impact Engineering* 32(1–4):525–40. doi: 10.1016/j.ijimpeng.2005.03.006.

Sloan, Matthew, Ajay Premkumar, and Neil P. Sheth. 2018. “Projected Volume of Primary Total Joint Arthroplasty in the u.s., 2014 to 2030.” *Journal of Bone and Joint Surgery - American Volume* 100(17):1455–60. doi: 10.2106/JBJS.17.01617.

Small, Scott R., Michael E. Berend, Leah A. Howard, Renee D. Rogge, Christine A. Buckley, and Merrill A. Ritter. 2013. “High Initial Stability in Porous Titanium Acetabular Cups: A Biomechanical Study.” *Journal of Arthroplasty* 28(3):510–16. doi: 10.1016/j.arth.2012.07.035.

Suckel, A., and R. Best. 2006. “Der Golfsport Mit Hüft- Und Knietotalendoprothesen.” *Sportverletzung-Sportschaden* 20(3):127–31. doi: 10.1055/s-2006-926996.

Swanson, Eli a, Thomas P. Schmalzried, and Frederick J. Dorey. 2009. “Activity Recommendations after Total Hip and Knee Arthroplasty: A Survey of the

American Association for Hip and Knee Surgeons." *The Journal of Arthroplasty* 24(6 Suppl):120–26. doi: 10.1016/j.arth.2009.05.014.

Swedish Hip Arthroplasty Register. 2019a. *Swedish Hip Arthroplasty Register Annual Report 2018*.

Swedish Hip Arthroplasty Register. 2019b. *Swedish Hip Arthroplasty Register Annual Report 2018*.

Tabata, Tomonori, Nobuhiro Kaku, Katsutoshi Hara, and Hiroshi Tsumura. 2015. "Initial Stability of Cementless Acetabular Cups: Press-Fit and Screw Fixation Interaction--an in Vitro Biomechanical Study." *European Journal of Orthopaedic Surgery & Traumatology : Orthopédie Traumatologie* 25(3):497–502. doi: 10.1007/s00590-014-1571-4.

Tudor-Locke, Catrine, Yoshiro Hatano, Robert P. Pangrazi, and Minsoo Kang. 2008. "Revisiting 'How Many Steps Are Enough?'" *Medicine & Science in Sports & Exercise* 40(Supplement):S537–43. doi: 10.1249/MSS.0b013e31817c7133.

United Kingdom National Joint Registry. 2019a. *2019 16th Annual Report*.

United Kingdom National Joint Registry. 2019b. *National Joint Registry for England, Wales, Northern Ireland and the Isle of Man - 2019 16th Annual Report*.

Unsworth, A. 1978. "The Effects of Lubrication in Hip Joint Prostheses." *Physics in Medicine and Biology* 23(2):253–68.

Unsworth, A. 1991. "Tribology of Human and Artificial Joints." *Proceeding of the Institution of Mechanical Engnieers, Part H: Journal of Engineering in Medicine* 205:163–72.

Wan, Zhinian, Myriam Boutary, and Lawrence D. Dorr. 2008. "The Influence of Acetabular Component Position on Wear in Total Hip Arthroplasty." *Journal of Arthroplasty* 23(1):51–56. doi: 10.1016/j.arth.2007.06.008.

Wang, W-z, Z. M. Jin, D. Dowson, and Y. Z. Hu. 2008. "A Study of the Effect of Model Geometry and Lubricant Rheology upon the Elastohydrodynamic Lubrication Performance of Metal-on-Metal Hip Joints." *J Engineering Tribology* 222:493–501. doi: 10.1243/13506501JET363.

Wang, Yansong, and Q. Jane Wang. 2013. "Stribeck Curves." Pp. 3365–70 in *Encyclopedia of Tribology*, edited by Q. J. Wang and Y.-W. Chung. Boston, MA: Springer US.

Wäsche, Rolf, and Mathias Woydt. 2014. "Stribeck Curve." Pp. 1998–2005 in *Encyclopedia of Lubricants and Lubrication*, edited by T. Mang. Berlin,

Heidelberg: Springer Berlin Heidelberg.

Widhalm, R., G. Höfer, J. Krugluger, and L. Bartalsky. 1990. “Ist Die Gefahr Der Sportverletzung Oder Die Gefahr Der Inaktivitätsosteoporose Beim Hüftprothesenträger Grösser? Folgerungen Auf Die Dauerhaftigkeit von Prothesenverankerungen.” *Z Orthop* 128:139–43.

Williams, Sophie, Davood Jalali-Vahid, Claire Brockett, Zhongmin Jin, Martin H. Stone, Eileen Ingham, and John Fisher. 2006. “Effect of Swing Phase Load on Metal-on-Metal Hip Lubrication, Friction and Wear.” *Journal of Biomechanics* 39(12):2274–81. doi: 10.1016/j.jbiomech.2005.07.011.

Wright, JG G., S. Rudicel, and AR R. Feinstein. 1994. “Ask Patients What They Want. Evaluation of Individual Complaints before Total Hip Replacement.” *The Journal of Bone and Joint Surgery. British Volume* 76-B(2):229–34. doi: 10.1302/0301-620X.76B2.8113282.

Xiong, D., and S. Ge. 2001. “Friction and Wear Properties of UHMWPE/Al2O3 Ceramic under Different Lubricating Conditions.” *Wear* 250:242–45.

Zhu, Jinjun, Zhinian Wan, and Lawrence D. Dorr. 2010. “Quantification of Pelvic Tilt in Total Hip Arthroplasty.” *Clinical Orthopaedics and Related Research* 468(2):571–75. doi: 10.1007/s11999-009-1064-7.

Danksagung

Zu allererst möchte ich allen herzlich danken, die mich bei der Durchführung und Auswertung der sehr umfangreichen in-vivo-Belastungsmessungen und den anschließenden Datenanalysen unterstützt haben. Es hat mir große Freude bereitet, in diesem einzigartigen wissenschaftlichen Umfeld zu arbeiten.

Ein ganz besonderer Dank geht insbesondere auch an alle Studienpatienten, die immer hochmotiviert an den vielen und teils sehr umfangreichen in-vivo-Belastungsmessungen über einen Zeitraum von mehr als 10 Jahren teilgenommen haben. Ohne ihren Enthusiasmus und ihre Bereitschaft zur Teilnahme an dieser Studie wäre diese Arbeit nicht möglich gewesen.

Darüber hinaus möchte ich mich bei Prof. Georg N. Duda und Prof. Georg Bergmann bedanken, die mir mit ihrer konstruktiven Kritik und ihren Ratschlägen immer beratend und wohlwollend zur Seite standen und mir so während meiner gesamten bisherigen wissenschaftlichen Laufbahn großartige Mentoren gewesen sind.

Mein besonderer Dank gilt aber auch dem gesamten Team des Julius-Wolff-Instituts und allen Studierenden, die in den vergangenen Jahren aktiv an der Durchführung der Messungen mitgewirkt und erst durch ihren besonderen Fleiß die sehr umfangreichen Datenanalysen möglich gemacht haben.

Mein besonderer Dank gilt außerdem Jörn Dymke für seine große Unterstützung während der Messungen und Dr.-Ing. Friedmar Graichen für seine Hilfe bei der Implantatherstellung und vor allem auch seiner moralischen Unterstützung. Ebenso gilt mein Dank auch Dr. Alwina Bender für ihre immer wieder sehr konstruktive und fundierte Unterstützung in meiner bisherigen wissenschaftlichen Laufbahn.

„Last but not least“ möchte ich insbesondere aber auch meiner Familie und ganz besonders meiner Frau Grit, sowie meinen Töchtern Elisa und Johanna danken. Ich konnte mich jederzeit auf euch verlassen und ihr habt mich immer aktiv unterstützt, auch wenn ich meine Arbeit wiederholt mit „nach Hause“ gebracht habe.

Erklärung

§ 4 Abs. 3 (k) der HabOMed der Charité

Hiermit erkläre ich, dass

- weder früher noch gleichzeitig ein Habilitationsverfahren durchgeführt oder angemeldet wurde,
- die vorgelegte Habilitationsschrift ohne fremde Hilfe verfasst, die beschriebenen Ergebnisse selbst gewonnen sowie die verwendeten Hilfsmittel, die Zusammenarbeit mit anderen Wissenschaftlern/Wissenschaftlerinnen und mit technischen Hilfskräften sowie die verwendete Literatur vollständig in der Habilitationsschrift angegeben wurden,
- mir die geltende Habilitationsordnung bekannt ist.

Ich erkläre ferner, dass mir die Satzung der Charité – Universitätsmedizin Berlin zur Sicherung Guter Wissenschaftlicher Praxis bekannt ist und ich mich zur Einhaltung dieser Satzung verpflichte.

_____ _____